

TNO

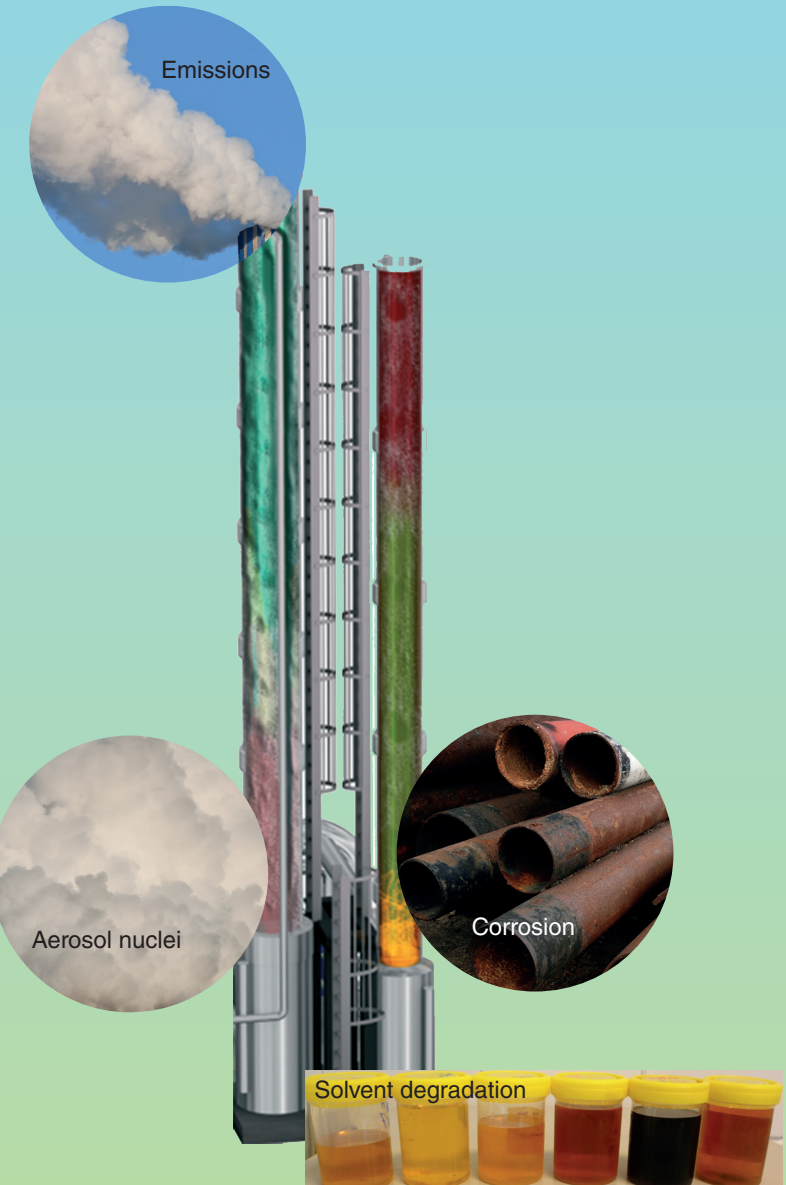
The TU Delft logo consists of a stylized flame icon above the letters "TU Delft".

Delft
University of
Technology

ISBN 978-94-6259-566-8

Aerosol-based Emission, Solvent Degradation, and Corrosion in Post Combustion CO₂ Capture

Aerosol-based Emission, Solvent Degradation, and Corrosion in Post Combustion CO₂ Capture



Purvil Khakharia

Invitation

You are cordially invited to the
public defense of my doctoral
thesis entitled:

“Aerosol-based Emission, Solvent Degradation, and Corrosion in Post Combustion CO₂ Capture”

On Monday, March 2nd, 2015
at 3:00 pm at the
Senaatszaal, Aula Congress
Centre, Delft University of
Technology, Mekelweg 5,
2628 CC, Delft.

Prior to the defense a short presentation on my research will be given at 2:30 pm.

You are also invited to the reception following the graduation ceremony.

Purvil Khakharia

purvilkh@gmail.com

Aerosol-based Emission, Solvent Degradation, and Corrosion in Post Combustion CO₂ Capture

Purvil Khakharia

Aerosol-based Emission, Solvent Degradation, and Corrosion in Post Combustion CO₂ Capture

Proefschrift

ter verkrijging van de graad van doctor
aan de Technische Universiteit Delft,
op gezag van de Rector Magnificus Prof. ir. K.C.A.M. Luyben,
voorzitter van het College voor Promoties,
in het openbaar te verdedigen op 2 Maart 2015 om 15:00 uur

door

Purvil Khakharia

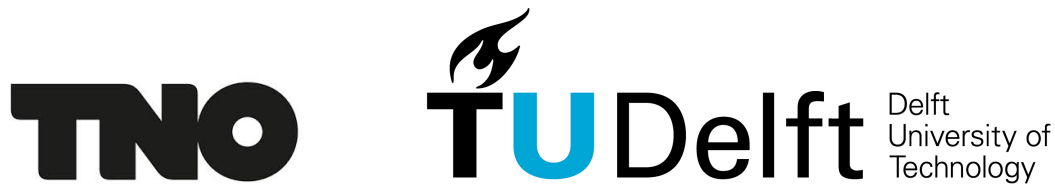
Master of Science in Chemical Engineering
Technische Universiteit Delft, the Netherlands
Geboren te Mumbai, India

Dit proefschrift is goedgekeurd door de promotor:
Prof.dr.ir. T.J.H. Vlugt

Samenstelling promotiecommissie:

Rector Magnificus,	voorzitter
Prof.dr.ir. T.J.H. Vlugt	Technische Universiteit Delft
Prof.dr. C. Secuianu	Politehnica U-Bucharest
Prof.dr.ir. A.B. de Haan	Technische Universiteit Delft
Prof.dr.ir. M.C. Kroon	TU Eindhoven
Prof.dr.ir. B.J. Boersma	Technische Universiteit Delft
Prof.dr.ir. J.T.F. Keurentjes	TU Eindhoven
Dr.ir. E.L.V. Goetheer	TNO

This work has been financially supported by TNO (Nederlandse Organisatie voor Toegepast Natuurwetenschappelijk Onderzoek). The research topics presented in this work have been an integral part of the Dutch national CCS project, CATO-2, and the European FP7 project, OCTAVIUS.



Copyright © 2015 Purvil Khakharia
ISBN 978-94-6259-566-8

An electronic version of this thesis can be downloaded from:
<http://repository.tudelft.nl/>

Contents

1	Introduction	9
1.1	Atmospheric CO ₂ reduction for mitigation of climate change	10
1.2	CO ₂ capture from power sector	10
1.2.1	Post Combustion CO ₂ capture	11
1.2.2	Pre Combustion CO ₂ capture	11
1.2.3	Oxyfuel combustion	12
1.3	Post Combustion CO ₂ capture	12
1.3.1	Solvents	13
1.3.2	Novel materials for CO ₂ capture	14
1.4	Solvent management in absorption based PCCC processes	14
1.4.1	Solvent degradation	14
1.4.2	Corrosion	15
1.4.3	Treated flue gas emission	16
1.5	CCS in the Netherlands and its status worldwide	16
1.6	Scope and structure of the thesis	17
2	Solvent degradation and corrosion in long term pilot plant tests	19
2.1	Introduction	21
2.2	Test equipment and methodology	22
2.2.1	CO ₂ capture pilot plant	22
2.2.2	Corrosion monitoring	23
2.2.3	Fourier Transform Infrared (FTIR) Spectroscopy	24
2.2.4	ICP-MS	24
2.3	Results and discussion	25
2.3.1	Overview of campaigns	25
2.3.2	General trends in online corrosion measurements	27
2.3.3	Inter-relation of corrosion, solvent degradation and ammonia emission	32
2.4	Conclusions	34
3	Acid wash scrubbing as a countermeasure for ammonia emissions from a post combustion CO₂ capture plant	37
3.1	Introduction	38
3.2	Test Equipment, method and model	39
3.2.1	CO ₂ capture pilot plant	39
3.2.2	Fourier Transform Infrared (FTIR) Spectroscopy	44
3.2.3	Ammonium ion analyses	45
3.2.4	Acid wash model in Aspen Plus	45
3.3	Results and discussion	46
3.3.1	Campaign overview	46

3.3.2	Parametric study for NH ₃	47
3.3.3	Parametric study for MEA	53
3.4	Scale up and cost estimation of an acid wash for a full scale CO ₂ capture plant	55
3.4.1	Sizing of full scale acid wash	55
3.4.2	Cost estimation	56
3.5	Conclusions	56
4	Investigation of aerosol-based emissions of MEA due to sulphuric acid aerosol and soot in a post combustion CO₂ capture process	59
4.1	Introduction	60
4.2	Test Equipment	61
4.2.1	Aerosol generator setup	61
4.2.2	CO ₂ Capture plant	62
4.2.3	FTIR	62
4.2.4	CPC and dilution system	62
4.3	Results and discussion	64
4.3.1	Typical CO ₂ capture plant operating conditions	64
4.3.2	Effect of Soot	66
4.3.3	Effect of H ₂ SO ₄ aerosols	67
4.3.4	Effect of particle number concentration on MEA emission	70
4.3.5	Effect of capture plant parameters on MEA emissions	70
4.4	Conclusions	72
5	Understanding aerosol-based emissions in a post combustion CO₂ capture process: parameter testing and mechanisms	75
5.1	Introduction	76
5.2	Saturation and aerosol growth	77
5.3	Test equipment and methods	78
5.3.1	Pilot plant for aerosol generation	78
5.3.2	CO ₂ capture mini-plant	79
5.3.3	FTIR	79
5.3.4	CPC and dilution system	79
5.4	Results and discussion	79
5.4.1	The lean solvent temperature	81
5.4.2	AMP-Pz as the CO ₂ capture solvent	82
5.4.3	The pH of the lean solvent	84
5.4.4	CO ₂ concentration in the flue gas	86
5.4.5	AMP-KTau as CO ₂ capture solvent	90
5.5	Mechanisms	91
5.5.1	Particle number concentration	91
5.5.2	Supersaturation	91
5.5.3	Reactivity of the amine	92
5.6	Overall hypothesis	95

5.7	Conclusions	96
6	Field study of a Brownian Demister Unit to reduce aerosol-based emission from a post combustion CO₂ capture plant	99
6.1	Introduction	100
6.2	Test equipment and methods	101
6.2.1	TNO's CO ₂ capture pilot plant	101
6.2.2	Operating conditions of the CO ₂ capture plant	101
6.2.3	Brownian Demister Unit (BDU) and its working	103
6.2.4	Gas sampling	103
6.2.5	Liquid analysis	104
6.3	Results and discussion	104
6.3.1	MEA emissions	104
6.3.2	Nitrosamines and nitramines	109
6.3.3	NH ₃ emissions	110
6.3.4	Application of a BDU for a full scale CO ₂ capture plant	112
6.4	Conclusions	113
7	Predicting aerosol-based emissions in a Post Combustion CO₂ Capture process using an Aspen Plus model	115
7.1	Introduction	116
7.2	Modelling approach and assumptions	117
7.2.1	Methodology	117
7.2.2	Implementation in Aspen Plus	117
7.2.3	Assumptions	121
7.3	Results and discussion	122
7.3.1	Base case	123
7.3.2	Effect of the change in inlet flue gas CO ₂ concentration	124
7.3.3	Effect of the lean solvent temperature	126
7.3.4	Effect of the lean solvent loading	128
7.4	Conclusions	131
Appendix		133
References		139
Summary		155
Samenvatting		159
Curriculum vitae		163
Publications and presentations		165
Acknowledgments		167

Chapter 1

Introduction

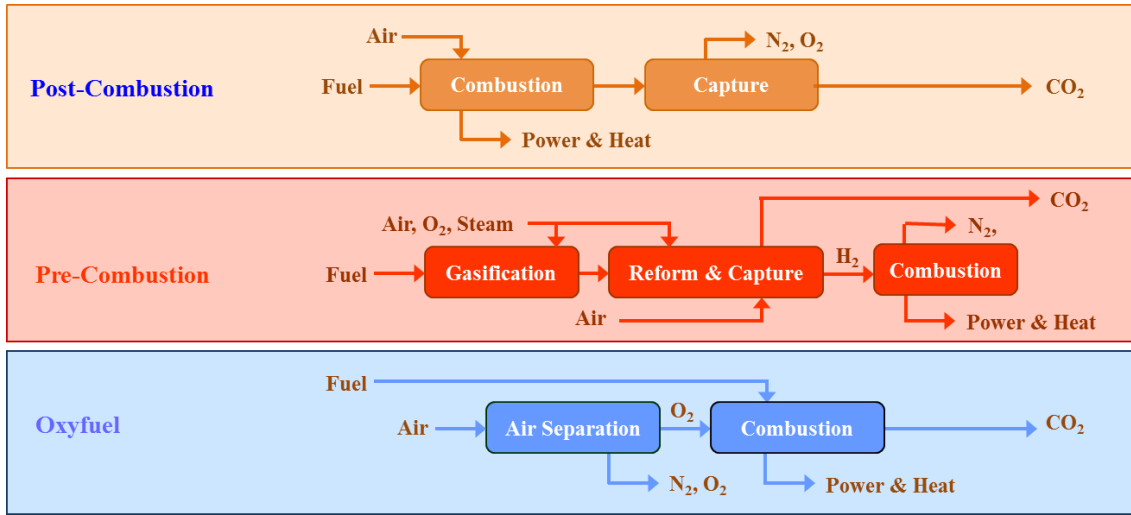


Figure 1.1. Different options for capturing CO₂ from combustion of fossil fuels. The capture of CO₂ after the combustion of a fuel is known as the Post combustion route, while CO₂ separation prior to combustion is termed as the Pre combustion route. The combustion of fuel in presence of high oxygen content and subsequent capture from a CO₂ rich stream is termed as CO₂ capture from oxyfuel combustion.

1.1 Atmospheric CO₂ reduction for mitigation of climate change

As per the fifth assessment report of the Intergovernmental Panel on Climate Change (IPCC), the climate system is changing rapidly, especially since the 1950's and it will have an everlasting impact. The change in the climate system refers to the warming of atmosphere and ocean, diminishing of snow and ice, increase of the sea level and an increase in the concentration of greenhouse gases. The increase of surface temperature, termed as positive radiative forcing, is largely due to the increase in atmospheric concentration of CO₂ since 1750. Specifically, the increase in anthropogenic CO₂ emissions has led to an increase in the average temperature of the climate system, commonly known as global warming¹.

1.2 CO₂ capture from power sector

Mitigation of climate change by means of reduction in CO₂ emissions is necessary to reduce the impact of climate change on future generations. The major source of anthropogenic CO₂ emissions is the use of fossil fuels. The use of fossil fuels accounted for ca. 82 % of the global primary energy consumption in 2011². The electricity and heat generation accounted for 42 % of the global CO₂ emissions in 2011, which was the largest contribution by any sector to global CO₂ emissions³. Carbon Capture and Storage (CCS) is one of the most important means to reduce the CO₂ emissions to lower the global average temperatures. The different possible ways of capturing the CO₂ produced from the combustion of fuel are as shown in Figure 1.1 and further explained in this section.

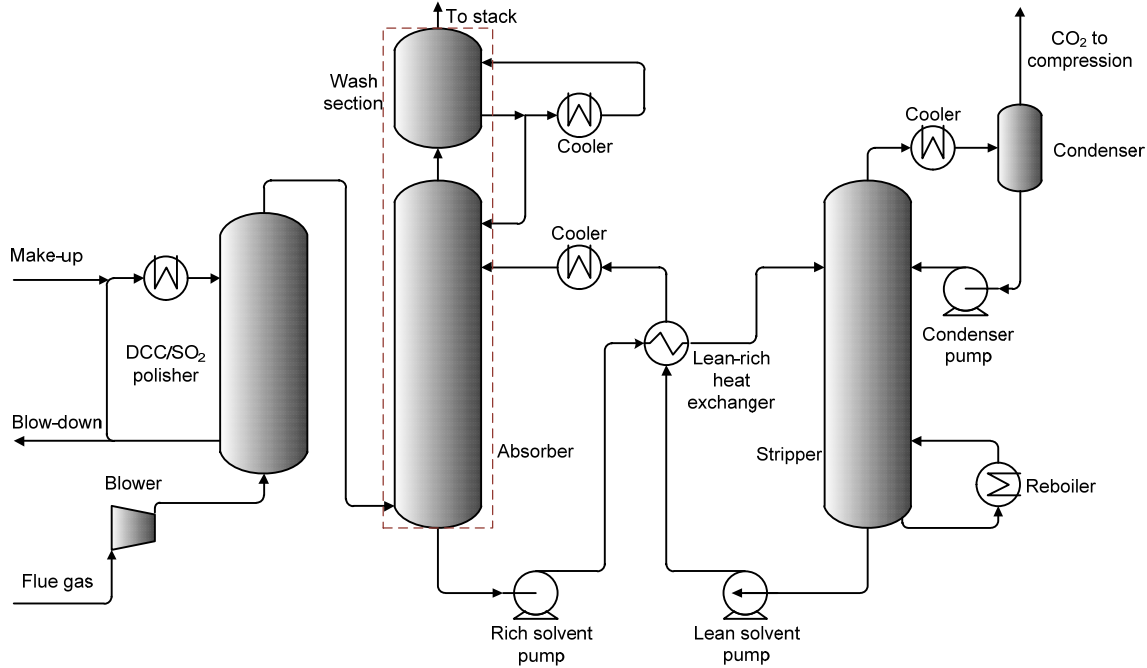


Figure 1.2. Typical configuration of an absorption-desorption based CO₂ capture process. There are three columns; (a) Direct contact cooler DCC/SO₂ polisher for cooling the flue gas and reducing SO₂ levels in the flue gas, (b) Absorption column to capture the CO₂ and (c) Stripper to thermally regenerate the solvent. The treated flue gas leaves the absorption column whereas a CO₂ rich stream is obtained from the stripper. The solvent recycles between the absorber and stripper columns. The water wash is integrally mounted in the absorption tower but is shown as a separate unit here. Moreover, the DCC is combined with a SO₂ polishing step in a single column.

1.2.1 Post Combustion CO₂ capture

The flue gas generated from the combustion of various fuels such as coal, gas or biomass contains N₂, CO₂, O₂, and other impurities such as NO_x and SO_x. The capture of CO₂ as an end-of-pipe solution is referred to as Post Combustion CO₂ capture (PCCC). The flue gas is at atmospheric pressures and contains CO₂ in the range of 3-15 vol.% ^{4,5}. The CO₂ partial pressure in the gas stream is comparatively low resulting in a lower driving force for CO₂ separation and therefore higher specific energy requirements. However, CO₂ capture from industrial flue gas streams has been widely used in the industry and can be considered a mature technology. Absorption processes are widely used, while other technologies such as adsorption, membranes and solid sorbents are being developed and used for niche applications. The main advantage of PCCC over other processes is that it can be retrofitted to existing plants without significant modifications in a short duration of time ⁶.

1.2.2 Pre Combustion CO₂ capture

In this type of CO₂ capture, the fuel is converted such that the CO₂ can be separated prior to its combustion. The fuel is converted to syngas, a mixture of carbon monoxide

and hydrogen, in the presence of oxygen or air and/or steam. The syngas is then converted by means of water gas shift step to make it hydrogen rich, while the carbon monoxide is converted to CO₂. The CO₂ is separated from this stream and the hydrogen rich stream is then used for producing electricity. The stream containing CO₂ is at pressures of 20-70 bar and the CO₂ content is in the range of 8-20 vol. %. Therefore, the driving force for CO₂ capture is relatively higher, resulting in a lower specific energy requirement. The technology options suited for pre-combustion CO₂ capture are pressure swing adsorption and physical solvent based absorption processes ⁷⁻⁹. The individual technologies such as the water-gas shift conversion and CO₂ absorption have been extensively used in the chemical industry. However, its application to power plants such as an Integrated Gasification Combined Cycle (IGCC) is not trivial due to the larger scale and more complex operation ¹⁰.

1.2.3 Oxyfuel combustion

In oxyfuel combustion, stream containing mainly oxygen is used as the oxidizing medium instead of air. This results in a flue gas stream containing mainly CO₂ and H₂O. A part of the flue gas is recycled in order to reduce the temperature in the combustion chamber. The flue gas is cooled to remove water vapour resulting in a stream of ca. 80-98 % CO₂ depending on the fuel and operation mode of oxy-fuel combustion. Alternatively, a metal oxide can be used as the oxygen carrier for combustion. This method is known as chemical looping combustion ¹¹. The principle of chemical looping combustion is to use metal oxides for the exothermic oxidation of the fuel, while the reduced metal is regenerated by the endothermic reaction with air. The resulting stream from endothermic reaction step with air contains mainly CO₂ and water ¹²⁻¹⁴.

1.3 Post Combustion CO₂ capture

Absorption based CO₂ capture processes have been widely used in the industry, specifically for natural gas treatment since several decades ¹⁵⁻¹⁷. Reactive absorption is the preferred technology for large scale capture of CO₂ from flue gases due to the low partial pressure of CO₂ in the gas stream, and therefore, is the focus of this study ¹⁸. A typical process flowsheet of an absorption-desorption based PCCC process is shown in Figure 1.2.

The flue gas from the power plant is firstly cooled to ca. 40°C, for improved absorption performance. The presence of SO₂ leads to degradation of the solvent and is therefore, removed to levels below 10 ppmv. Both steps can be performed in an absorption column with a pump around of caustic soda as the solvent (pH~6-7) and a heat exchanger to cool the solvent. Alternatively, these two steps can also be performed in separate absorption columns. A blower provides the gas with the required energy to overcome the pressure drop in the absorption column. The CO₂ from the flue gas is selectively captured by the “lean” solvent typically an amine, in the absorption column.

Table 1.1. Criteria for an ideal solvent and its direct impact on a PCCC process.

Criteria	Direct Impact
High CO ₂ capacity	Lower amount of required solvent
Fast reaction kinetics	Shorter absorption column
Resistance to degradation	Reduced solvent make-up
Resistance to corrosion	Increased lifetime of the plant
Health, Safety and Environmental	Easy to handle and dispose
Cost and procurement	Lower operating costs and easy availability

It is referred to as the lean solvent as it has a lower CO₂ content as it has been regenerated in the stripper. Typically, a packed bed is used to provide an improved contacting of the solvent and the flue gas. The CO₂ lean flue gas from the absorption column is hot. A water wash cools the flue gas to maintain a water balance in the system and capture the volatile amine prior to its emission. A conventional water wash is a pump around system with cooling and a purge stream to avoid accumulation of absorbed components in the system. The purge of the water wash can be either returned to the absorber or stripper section. Advanced configuration includes an additional water wash section with pH control in the wash loop and/or using pure water stream for enhanced capture of amines. The solvent, “rich” in CO₂ is then thermally regenerated in a stripper. The stripper column is a packed column, too with a reboiler to heat the solvent to ca. 120°C. The vapour stream from the stripper is condensed to recover water vapour and other volatile components, while the product CO₂ stream can be sent for compression or further use. The hot lean solvent transfers its heat to the rich solvent by a lean-rich heat exchanger and is further cooled to ca. 40°C by a lean cooler prior to its next cycle of absorption-desorption.

Advanced process configuration includes absorption inter-cooling, lean vapour compression, split-flow, etc. can have an improved energy performance. The reader is referred to literature for further description and benefits of these options ¹⁹⁻²¹.

1.3.1 Solvents

Traditionally, physical solvents such as dimethyl ethers of polyethylene glycol (DEPG), methanol and chemical solvents such as N-methyldiethanolamine (MDEA), monoethanolamine (MEA), diethanolamine (DEA) are used for gas purification ^{18,22,23}. Solvent development in PCCC is aimed towards matching the criteria mentioned in Table 1.1 ^{24,25}. Several solvents have been developed which either use novel amine components, blends of known components or additives specifically aimed at reducing degradation, corrosion, etc. The active component of the solvent includes ammonia, amines and amino acid salts. Components such as piperazine (Pz), which is known to have fast reaction kinetics with CO₂, can be used in combination with amines such as MDEA, 2-amino-2-methyl-1-propanol (AMP) which have high capacity for CO₂. Typically, additives in the form of inhibitors such as Ethylenediaminetetraacetic acid

(EDTA) and vanadium salts are used to suppress degradation which further reduces the extent of corrosion^{26,27}.

Second generation solvents for PCCC includes solvents which lead to a phase change on CO₂ absorption. The phase change can be either solids formation or two distinct liquid layers. The phase change solvents can be better in terms of CO₂ capacity, lower steam reboiler duty, higher CO₂ pressure from the stripper, etc. The use of such solvent systems requires specific process configuration and therefore, are not preferred as drop-in solvents. The reader is referred to literature for recent developments in phase change solvents^{19,28-30}.

1.3.2 Novel materials for CO₂ capture

Recently, several new materials have been studied for their use in CO₂ capture. The reader is referred to literature for further information³¹⁻³³. They can be broadly classified into: (a) physisorbents such as zeolites, activated carbon, clays, and (b) chemisorbents such as metal oxides and amine functionalised sorbents³¹. These materials have advantages such as significantly higher capacity for CO₂, ease of regeneration and improved thermal and chemical stability. More advanced materials such as Metal-organic frameworks (MOFs) and zeolitic imidazolate frameworks (ZIFs) are also being extensively studied due to their unique structural properties^{34,35}. Ionic Liquids (ILs) are known to be customisable and therefore, can be modified to enhance its CO₂ solubility³⁶. Although promising, these materials are not well suited for CO₂ capture from flue gases because of intolerance to water, high cost, difficulty of handling, requirement of specialised equipment, etc.

1.4 Solvent management in absorption based PCCC processes

The solvent is the working horse of a PCCC process. Therefore, its appropriate management is necessary for long term steady state operation. The different aspects of solvent management are: (i) degradation, (ii) corrosion, (iii) emission and (iv) foaming. The objective of solvent management is not only to maintain its performance but also, to consider other aspects like minimising wastage, avoiding environmental hazard, maintain the health of the plant, etc. It is important for the plant operator to understand the different aspects of solvent management and the inter-connection between them, in order to take the necessary remedial action such as solvent reclaiming when required. In this section, the first three different aspects of solvent management are briefly described. Foaming of solvent is beyond the scope of this thesis^{37,38}.

1.4.1 Solvent degradation

Typically, solvents are aqueous solutions of amines, alkanolamines, amino acid salts, etc. or their blends. In the presence of other components and/or temperature the solvent can react further, reducing the active component concentration and therefore,

its degradation. In PCCC, solvent degradation can occur by the following routes; (i) oxidative degradation, (ii) thermal degradation, and (iii) reaction with impurities in the flue gas such as SO_x, NO_x, etc. ^{38,39}.

Flue gas contains oxygen which is dissolved in to the solvent in the absorber column. In the presence of metal ions, oxygen can react with the amine to form degradation products. The compounds formed as a result of oxidative degradation can be classified into primary and secondary degradation products. The primary products are formed by the reaction of oxygen with the solvent component forming aldehydes, carboxylic acids and ammonia. These components can act as an intermediate for further reactions with the solvent component, itself or other primary degradation products. Examples of secondary degradation products include amides and imidazoles ⁴⁰. Oxidative degradation has been found to be the dominating route for solvent degradation in PCCC ^{38,40,41}.

Thermal degradation refers to the degradation of the solvent component at high temperature in the presence of CO₂. This leads to formation of large polymeric products by means of carbamate polymerisation.

Flue gases contain impurities in the form of NO_x, SO_x, fly ash, etc. ⁴² These components can enter the solvent loop and enhance the oxidative and/or thermal degradation of the solvent. Sulphite, sulphate and thiosulphate ions are present in the solvent in the presence of SO₂ in the flue gas ⁴³. The presence of SO₂ increases the degradation rate of MEA and loss in CO₂ capacity, mainly due to the formation of Heat stable salts (HSS) ⁴⁴⁻⁴⁶. SO₂ can also act as an inhibitor of oxidative degradation of MEA, by means of scavenging the active oxide which otherwise would have led to degradation of MEA ⁴⁷.

NO_x is a representation for the family of species, NO, NO₂, N₂O₃, N₂O₄ and HNO₂ some of which are present in flue gases. NO_x can react with amines to form nitrosamines and nitramines ^{39,48-50}. These compounds are known to be carcinogenic and, thus their emissions must be limited ⁵¹. Nitrosamines have been identified in plants using amines as the solvent ^{38,52}. The reader is referred to section 6.3.2 and literature for further information ⁵³⁻⁵⁵.

Fly ash enhances the oxidative degradation of MEA and can lead to a threefold increase in the loss of MEA as shown in a laboratory test setup ⁵⁶. Fly ash are known to contain metal ions which can catalyse the oxidative degradation of MEA. However, fly ash did not impact the thermal degradation rate of MEA ⁵⁷.

1.4.2 Corrosion

Corrosion in gas treating applications, specifically using amines is a well-known phenomenon ¹⁷. Corrosion in gas treating plants is due to wet acid gas and amine solution ⁵⁸. Wet acid gas corrosion refers to local condensation with acid gases dissolved in it which results in an extremely corrosive environment. The amines on their own are not known to be corrosive, however their degradation products causes corrosion ⁵⁹⁻⁶¹.

The presence of oxygen in the flue gas and the higher CO₂ content in the lean solvent are the two main differences from the perspective of corrosion as compared to other gas treating applications. It is important to control corrosion in the plant in order to reduce maintenance costs, increase the lifetime of the plant, and avoid further degradation of the solvent.

1.4.3 Treated flue gas emission

The treated flue gas stream from the absorber tower is emitted to the atmosphere by means of a stack. Although, emission of certain components such as SO_x and NO₂ can be lower from a power plant with CCS, the presence of amine and its degradation products in the treated flue gas stream can increase the environmental burden ⁶²⁻⁶⁵. Amines being volatile, are present in the flue gas leaving the CO₂ capture absorption column in the order of 10-100's of mg per m³ STP (STP; 0°C and 101.325 kPa), depending on the operating conditions and activity of the amine ⁶⁶⁻⁶⁹. Ammonia being the major degradation product of amines is also present in the treated flue gas stream and its concentration can increase over time due to severe solvent degradation ^{70,71}. Conventional counter-measures such as a water wash and an acid wash are effective in reducing the amine and ammonia emissions, respectively to few mg per m³ STP ^{68,72,73}. Out of all the degradation products of amines, the emissions of nitrosamines and nitramines are of great concern as they are known to be carcinogenic ^{38,49}. Recently, aerosol-based emissions have been pointed out from PCCC facilities ^{72,74}. This can lead to emissions in the order of several hundreds of mg per m³ STP and therefore, can lead to increased operation costs and environmental hazard. The emitted components can be further transformed, both physically and chemically, in the atmosphere to form components which can be even more hazardous ⁷⁵.

1.5 CCS in the Netherlands and its status worldwide

CATO (CO₂ Afvang Transport en Opslag) is the national research program of the Netherlands relating to CCS. Spanning over a period of 10 years (2005-2014) and across a wide range of research fields, it has been instrumental in increasing the knowledge position of the Netherlands in the field of CCS. Such a knowledge position is essential if demonstration projects such as ROAD (Rotterdam Opslag and Afvang Demonstratie) and subsequent commercial scale CCS has to be a success. ROAD, a joint venture of E.ON and GDF-Suez ⁷⁶, has been the only CCS demonstration project remaining under consideration in Europe from an initial list of over 6-7 projects. Currently, the Boundary Dam project ⁷⁷ in Saskatchewan, Canada, is the only commercial scale PCCC project reaching the commissioning stage.

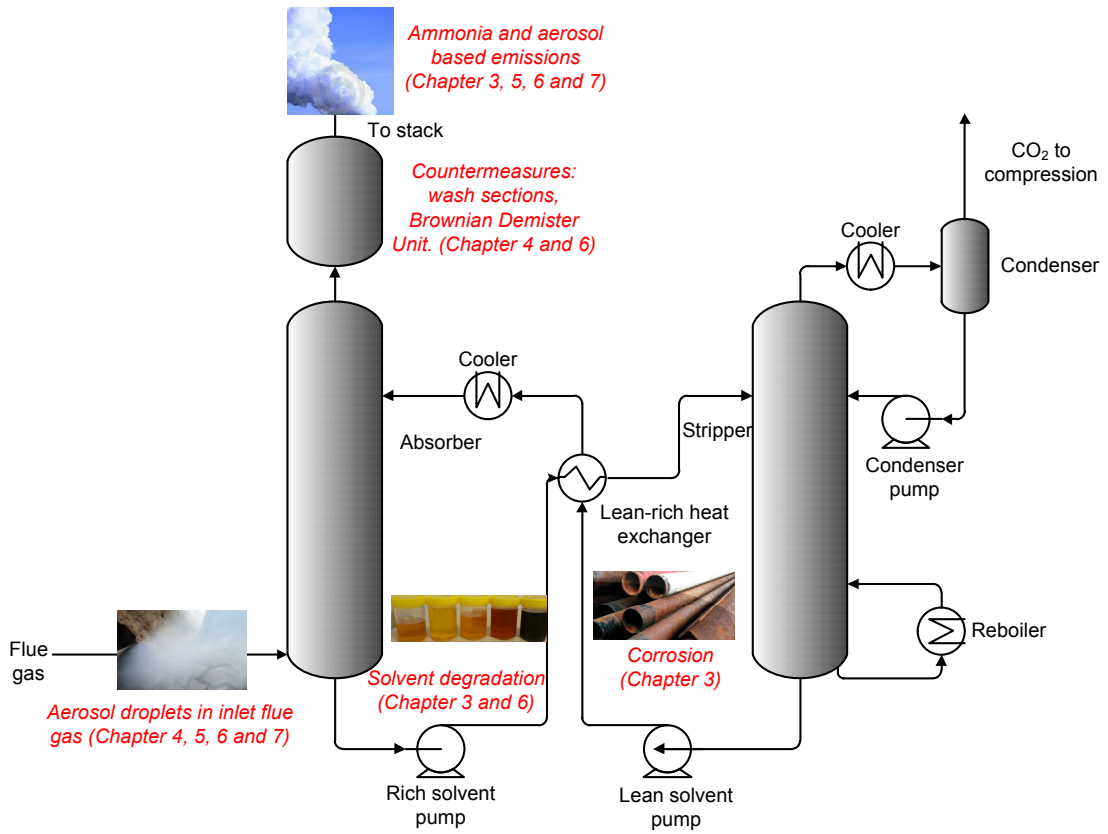


Figure 1.3. Schematic representation of a typical PCCC flowsheet with pictures representing the topics studied in this thesis.

1.6 Scope and structure of the thesis

The goal of this thesis is to understand the key operating issues pertaining to the solvent in a PCCC process. This has been achieved by using a pilot plant using real flue gas and thereby, making it a highly representative test environment. Figure 1.3 aids in understanding the scope of this thesis by depicting the key operating issues and countermeasures considered here.

In Chapter 2, the aspect of solvent degradation and ageing is studied over two pilot plant campaigns using MEA 30 wt.%, each lasting at least 1500 operating hours. The impact of solvent degradation on corrosion and emissions was evaluated using online monitoring devices. For the first time, a direct and instantaneous relation between the solvent degradation, corrosion and emissions was proven. Moreover, an autocatalytic solvent chemistry was observed resulting in iron concentration and ammonia emissions, above 500 mg/kg and 150 mg/m³ STP, respectively. Emissions of ammonia are inevitable when the solvent is highly degraded. In Chapter 3, an acid wash scrubber is tested as a countermeasure for ammonia emissions. Several parametric tests including high ammonia concentrations (~150 mg/m³ STP) proved that an acid wash scrubber is an effective solution for reducing ammonia emissions. The results are compared with a model made in Aspen Plus ⁷⁸.

Aerosol-based emissions have been recently observed in PCCC plants. In Chapter 4, the cause of these aerosol-based emissions has been investigated using an aerosol generator and mobile CO₂ capture mini-plant. Soot and sulphuric acid aerosol droplets were generated and their number concentration was found to be the cause of aerosol-based solvent emissions. It was confirmed that high level of emissions, in the order of grams per m³ STP, can be found when the particle number concentration is in the range of 10⁷-10⁸ per cm³.

In Chapter 5, the aspect of aerosol-based emissions was further investigated experimentally. The influence of the various operating conditions such as the temperature of the lean solvent, the pH of the lean solvent and the CO₂ concentration in the flue gas, on aerosol-based emissions was studied. Moreover, different solvent systems such as AMP-Pz and AMP-potassium taurate were evaluated for their potential for aerosol-based emissions. These tests led to a deeper understanding of the mechanisms involved in aerosol-based emissions in a PCCC process. Along with supersaturation and the particle number concentration, the reactivity of the amine was also found to play an important role.

In Chapter 6, a Brownian Demister Unit (BDU) was tested as a potential countermeasure for aerosol-based emissions. In this pilot plant campaign, nitrosamines and nitramines were measured both in the liquid and gas phase. Moreover, offline impinger based emission measurement was compared with online FTIR based emission measurement. The BDU was found to be an effective countermeasure for reducing aerosol-based emissions, below 1 mg/m³ STP. However, the design of the BDU used here led to a high pressure drop, in the order of 50 mbar.

To understand aerosol-based emissions, a methodology and a model are presented in Chapter 7. The methodology involves separate interaction of the aerosol-gas phases and the gas-liquid phases. Such a methodology is adopted to lower the complexity and implement in commercially available simulators such as Aspen Plus. The model developed in Aspen Plus V8.0 predicts the trends in MEA emissions in good agreement with experimental results presented in Chapter 4 and 5, at various operating conditions. Moreover, additional information such as supersaturation profile and amine content in the aerosol phase can be obtained.

Chapter 2

Solvent degradation and corrosion in long term pilot plant tests.

This chapter is based on the following manuscript in preparation:

Khakharia, P., Mertens, J., Huizinga, A., De Vroey, S., Sanchez Fernandez, E., Srinivasan, S., Vlugt, T.J.H., Goetheer, E., “Online corrosion monitoring in a Post Combustion CO₂ capture pilot plant and its relation to solvent degradation and ammonia emissions.”

2.1 Introduction

An absorption-desorption based process for acid gas removal has been widely used in applications such as natural gas treatment, refineries, etc.¹⁷ Typically, alkanolamines such as monoethanolamine (MEA), diethanolamine (DEA), methyldiethanolamine (MDEA), 2-amino-2-methyl-1-propanol (AMP), and other amines such as piperazine and their blends are used for acid gas removal^{16,17}. A reactive absorption based process is considered to be the first choice for a Postcombustion CO₂ Capture (PCCC) plant^{6,18,79,80}. The application of amine treatment in a PCCC plant needs further attention as compared to existing acid gas removal applications due to the following differences; (a) CO₂ partial pressure in the range of 0.03-0.15 bar as compared to 8-80 bar, (b) presence of oxygen (6-10 vol.%) as compared to almost no O₂ (<0.5 vol.%), and (c) higher CO₂ content in the lean stream leaving the stripper (e.g. 0.2 as compared to 0.1 mol CO₂/mol amine)^{60,80}. These differences can potentially lead to increased corrosion.

Corrosion of amine plants has been widely reported based on practical experience⁸¹. The different types of corrosion observed in CO₂ capture applications are general corrosion, stress corrosion cracking, hydrogen damage, crevice corrosion, pitting corrosion, erosion-corrosion, etc.^{59,82} Monoethanolamine (MEA), 30 wt. % aq., is one of the most widely used amine for CO₂ capture and therefore, the focus of this study. MEA, like other amines, is not an intrinsically corrosive solvent, however, when it absorbs acid gases such as CO₂ and H₂S it can become corrosive⁵⁹. The presence of oxygen and flue gas impurities such as fly ash, SO_x, and NO_x can degrade the amine and form degradation products, which are corrosive^{45,47,83-85}. Solvent degradation can occur by two routes, namely; oxidative degradation, caused by the dissolved oxygen in the solvent, and thermal degradation, caused by the high temperature in the stripper in the presence of CO₂^{17,38}. The different parameters that have been studied for their impact on the extent and rate of solvent degradation are oxygen partial pressures, temperature, CO₂ loading, concentration of amines, presence of metals, etc.^{45,86-92} Oxidative degradation of the solvent forms products such as oxalic, glycolic, formic, and acetic acid, which are in a salt form. These salts cannot be regenerated thermally and are thus, called Heat Stable Salts (HSS)⁹³. Oxidative degradation of MEA produces ammonia, amongst other degradation products. This has been well understood from lab scale experiments and has also been observed in pilot plant studies^{38,69,86,94-96}. Being extremely volatile, ammonia is emitted into the atmosphere in the treated flue gas stream.

Many of the degradation products of amines are known to be corrosive^{26,90,97}. Several corrosion studies have been performed at laboratory and pilot plant scale with different solvents and materials. The laboratory scale studies used electrochemical measurements at different temperatures, CO₂ loadings, oxygen content, and gas phase impurities such as SO₂ and NO₂^{27,98-100}. Corrosion has also been evaluated at several pilot plants using MEA and other solvents^{61,83,101,102}. The process equipment that are typically vulnerable

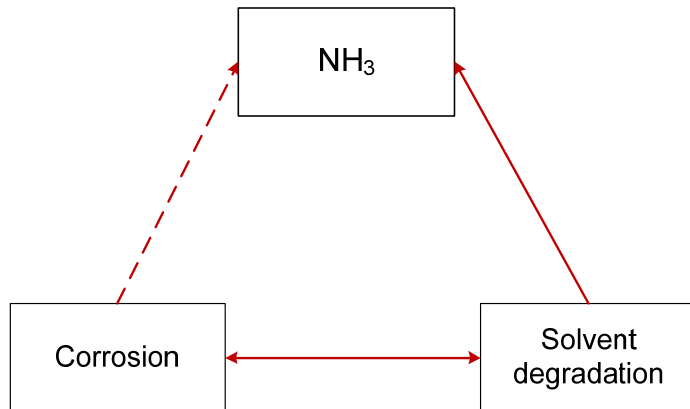


Figure 2.1. Inter-relation of corrosion, solvent degradation and ammonia emission. Solid lines indicate proven correlation. Solvent degradation causes corrosion which leads to further degradation of the solvent. Therefore, they are linked by a double-headed arrow. Solvent degradation leads to the formation of ammonia, and not vice-versa. Therefore, their relation is linked by a single-headed one-directional arrow. The dashed line between corrosion and ammonia indicate no experimental evidence of a direct relation.

to corrosion include, columns (absorber and stripper), amine heat exchanger, regenerator and reclainer⁸⁴. Typically, coupons are installed at different locations in the pilot plant and their weight loss is translated into corrosion rate as per standard norms, such as ISO 8407 and ASTM G1-03. The different materials that are used in a process equipment include carbon steel, stainless steel 304L, stainless steel 316L, polymers such as polypropylene, polyvinylidene fluoride (PVDF), ethylene propylene diene monomer (EPDM) rubbers and composites such as fibre reinforced polymers (FRP). These materials are tested for their susceptibility to corrosion. Corrosion of equipment can lead to downtime, cost of repair and maintenance, structural modifications, etc. Therefore, corrosion should be kept to a minimum to keep the plant in stable operation for long periods of time.

An inter-dependence between solvent degradation, corrosion and NH₃ emissions is expected as shown in Figure 2.1. However, no information is available in the literature about the existence and nature of this inter-dependence. There exists a direct relation between solvent degradation and ammonia emissions, as well as, solvent degradation and corrosion. Although intuitive, no experimental evidence exists of a direct correlation of corrosion with ammonia emissions in real-time. Recently, an auto-catalytic behaviour of solvent in terms of the ammonia emission and solvent metal content has been pointed out from long term operation of a pilot plant using 30 wt. % MEA as the amine solvent without a reclainer⁷². This behaviour can be expected based on the chemistry but, has never been observed in any lab scale experiments. This implies, either the lab scale experiments are not representative enough of a typical PCCC process or the duration of experiments were too short to observe this effect. Moreover, based on classical corrosion coupon technique, the corrosion behaviour is known only towards the end of a test and no information exists about the corrosion behaviour during operation.

The objective of this study is to verify the inter-relation between the three parameters; solvent degradation, corrosion and NH₃ emissions from pilot plant tests. Furthermore, an on-line tool for corrosion monitoring is presented. The results presented here are part of 2 pilot plant campaigns conducted over successive years: 2011 (Campaign 1) and 2012 (Campaign 2). For both the pilot plant campaigns, MEA (30 wt. %) was used as the CO₂ capture solvent.

2.2 Test equipment and methodology

2.2.1 CO₂ capture pilot plant

Tests were performed at TNO's Post-combustion CO₂ capture pilot plant at Maasvlakte, The Netherlands. It receives part of the flue gas stream from E.ON's coal fired power plant. The pilot plant can handle a maximum of 1210 m³ STP/h (STP; 0°C and 101.325 kPa) flue gas and captures a maximum of 6 tons CO₂ per day. A schematic representation of the pilot plant is shown in Figure 2.2.

The flue gas undergoes pre-treatment to remove SO_x from the flue gas stream by scrubbing the gas with soda (aqueous sodium carbonate) and is also cooled to ca. 40°C. After pre-treatment, the flue gas enters the CO₂ absorption tower which has a total height of 23 m and a diameter of 0.65 m and includes (1) four absorption beds (each 2 m high) with random packing of IMTP 50, (2) water wash section (2 m) with structured packing of Mellapak 250 Y, and (3) demister to remove entrained droplets bigger than 10 µm. The stripper tower is ca. 15 m high, with two beds each of 4 m with random packing of IMTP 50. In the desorber, the reboiler heats up the absorption liquid to strip CO₂ typically at a temperature of 120°C and pressure of 1.9 bar.

It is important to note that there was no reclaiming section in the pilot plant. The total solvent inventory during operation was ca. 2500 l and varies according to the water balance in the system. The water balance was maintained by varying the temperature of the treated flue gas leaving the water wash and addition of demineralised water in the stripper sump. Typically, pure MEA was added periodically to achieve the required solvent strength. However, no solvent bleed was performed.

The principal materials of the pilot plant are austenitic stainless steel (304L and 316L). The total surface area of the pilot plant in contact with liquid is ca. 1255 m², mainly from the packing surface.

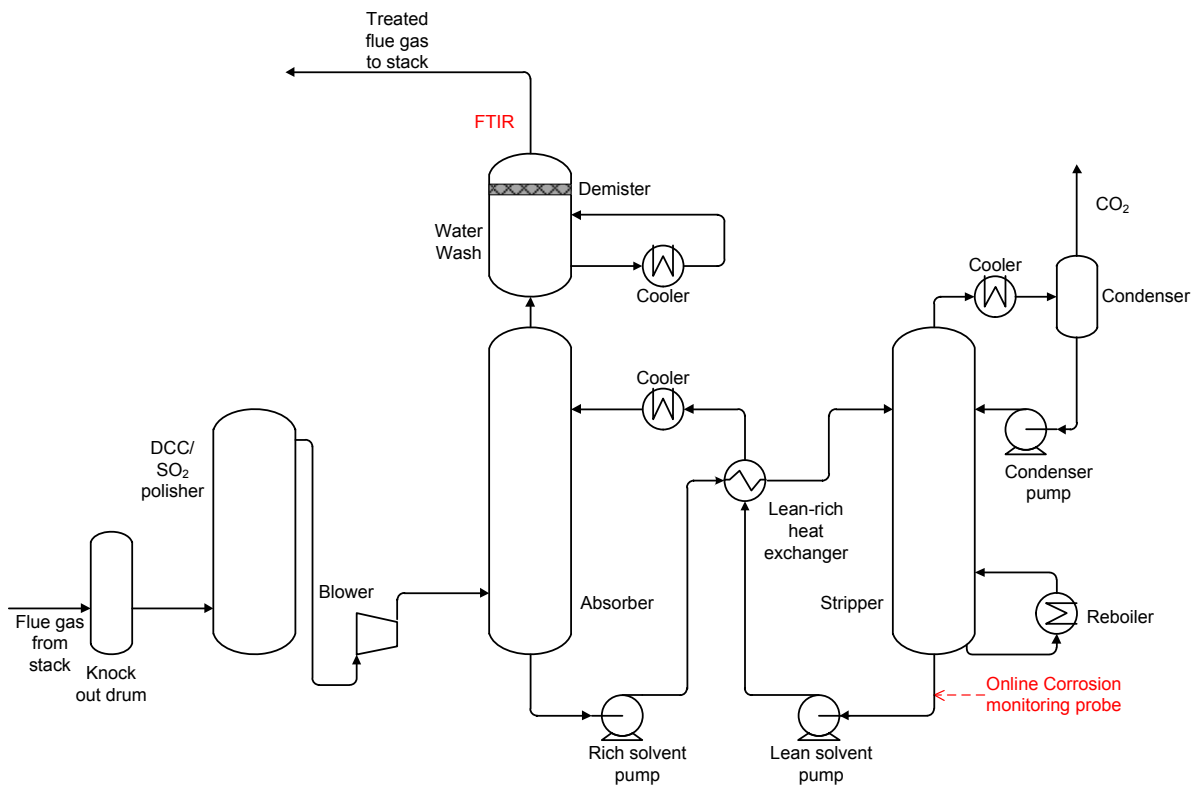


Figure 2.2. Schematic representation of the CO₂ capture pilot plant indicating the measurement locations of the FTIR analyser for the on-line monitoring of NH₃ and the online corrosion monitoring probe. The water wash section is within the absorber tower but, shown as a separate unit for better visualisation.

2.2.2 Corrosion monitoring

2.2.2.1 Online corrosion monitoring

Real-time online corrosion monitoring was achieved through Honeywell's SmartCET® real-time measurement system ¹⁰³. SmartCET uses electrochemical measurements in order to characterize the corrosion behaviour. Electrochemical methods provide a sensitive and rapid means of assessing corrosion behaviour of metallic materials ¹⁰⁴. The corrosion rate is obtained from electrochemical measurements designed to evaluate the corrosion current originating from the oxidation of the metal. The nature of the measurements requires an ionically conducting medium such as water or a molten salt, between the electrodes.

SmartCET is designed to operate with three identical electrodes as the electrochemical sensor array. These three electrodes can be of various geometries and sizes depending on the particular application. They are incorporated into a corrosion "probe", which performs the functions of providing mechanical support, electrically insulates the electrodes from each other and the probe body, and allows access into process fluids which may be at elevated temperatures and pressures. The three electrodes perform different functions, and are designated as the Working, Reference



Figure 2.3. Finger probe configuration of the SmartCET sensor used in the test. (Honeywell Smart CET 5000). Depending on the type of the probe, its length can be in the range of 15-30 cm.

and Auxiliary electrode. A finger probe type SmartCET sensor configuration as shown in Figure 2.3 was used in the test. The current flow is measured and analysed using several different techniques: linear polarisation resistance, electrochemical noise, and superficial capacitance measurements. This yields the following four output variables:

- General corrosion rate ($\mu\text{m/year}$) of the electrode material in the tested conditions
- B-value or Stern Geary Constant, measured in mV
- Pitting factor; a dimensionless quantity indicating the occurrence of localized corrosion and the overall stability of the corrosion process¹⁰⁵.
- Corrosion Mechanism Indicator ($\mu\text{F/cm}^2$); a qualitative indicator to identify the presence and type of surface films.

One of the most susceptible part to corrosion is the hot lean zone which is the outlet of the stripper and thus, the coupon and the probe were installed at the outlet of the stripper (see Figure 2.2)^{81,84}.

2.2.2.2 Offline corrosion monitoring

During both test campaigns, a corrosion coupon was installed in parallel to the on-line corrosion monitoring at the same location to validate the results of online corrosion monitoring. The corrosion rate and mechanisms were evaluated by visual examination and by weight loss measurements (according to ISO 8407 and ASTM G1-03).

2.2.3 Fourier Transform Infrared (FTIR) Spectroscopy

A FTIR analyser (GASMET CX 4000) was used to analyse the gas phase components. A trace heated line at 180°C is used to sample the gas. Further detailed information on the FTIR and its application in PCCC plants can be found in literature^{69,95,106,107}.

2.2.4 ICP-MS

ICP-MS (Inductively Coupled Plasma Mass Spectrometry) was used for determining the solvent metal content of elements such as Fe, Ni, Cr, Mn, etc.

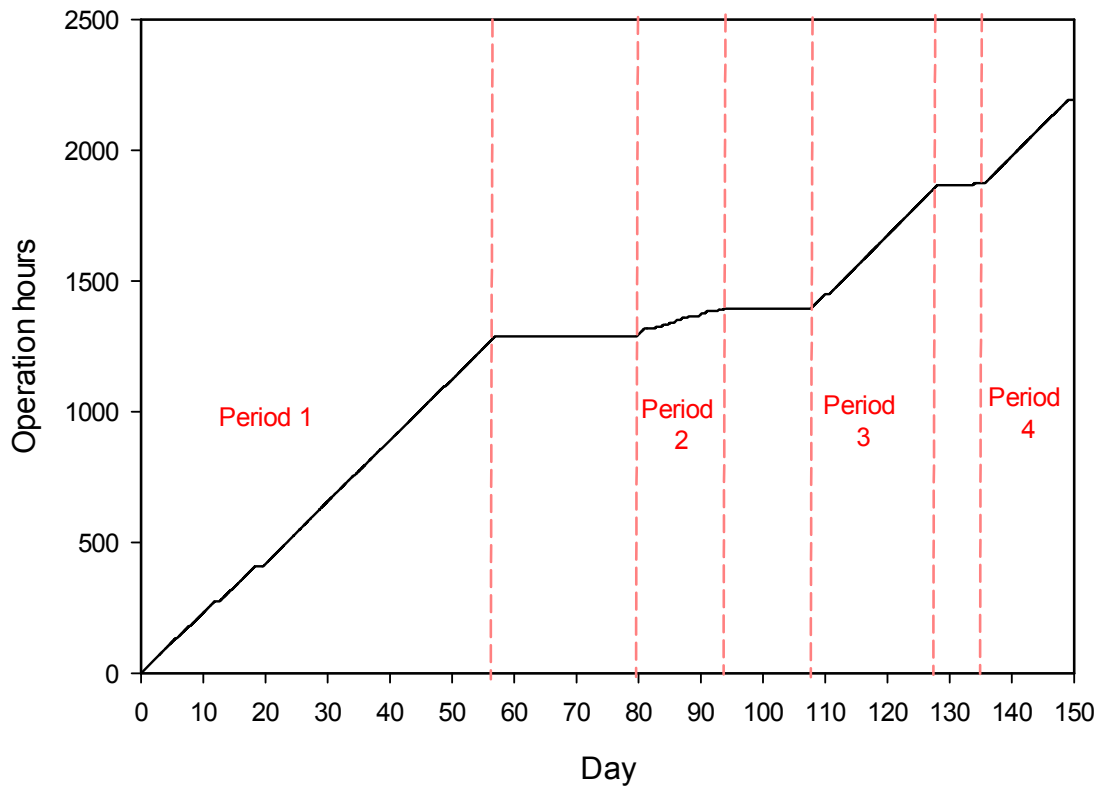


Figure 2.4. Operation hours during campaign 1 indicating the three periods of continuous operation.

2.3 Results and discussion

The main events and process parameters are discussed for both campaigns. The trends in online corrosion monitoring i.e. general corrosion rate, CMI and pitting factor and their relation to specific events are discussed for Campaign 1 and 2. The online corrosion monitoring is then compared with the offline corrosion coupons results. Finally, the inter-dependence of corrosion, solvent degradation and ammonia emissions is presented.

2.3.1 Overview of campaigns

In order to understand the state of the solvent and the pilot plant, it is important to have an overview of the operating conditions and events during a campaign. In this section, the events during the campaigns are discussed in detail and will aid in the discussion of the results. The operating hours are defined as the time during which there was flow of both flue gas and the solvent.

The duration of pilot plant campaign 1 was ca. 149 days and a total of ca. 2200 operating hours as shown in Figure 2.4. Several tests were carried out and the entire campaign can be divided into 4 continuous operation runs; Period 1 from day 0 to day 57, Period 2 from day 79 to day 94, Period 3 from day 108 to day 128, and Period 4

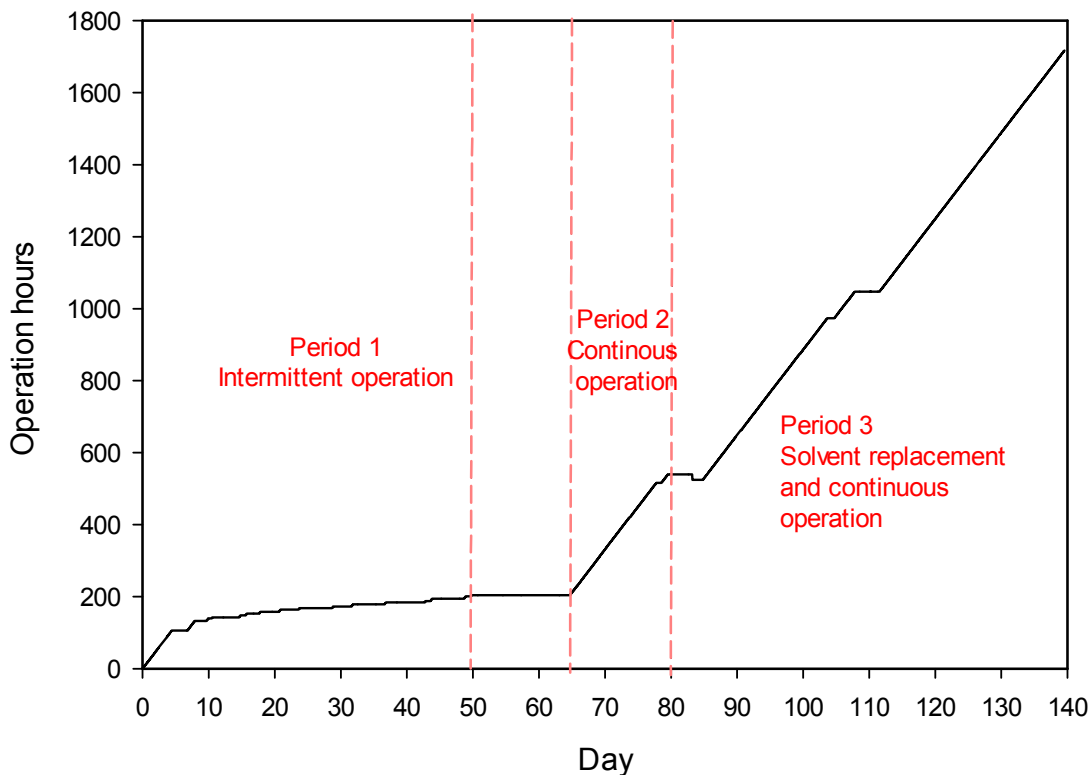


Figure 2.5. Operation hours during campaign 2 indicating the three periods of operation and its nature.

from day 135 to day 149. The pilot plant was not in operation in between the continuous operation periods. During shutdowns, the solvent was stored in the pilot plant itself (absorber and stripper sump) in the absence of any additional inert gas blanketing. During the 1st, 3rd and 4th operational period, the CO₂ and O₂ content in the flue gas was ca. 13 vol.% and 7 vol.%, respectively. The flue gas contained 4 vol.% and 17 vol.% of CO₂ and O₂ during period 2. The flue gas composition was altered in order to mimic natural gas combustion derived flue gas by mixing the flue gas with ambient air. It is important to note that the resulting gas would be under saturated with water. Corrosion monitoring was performed for period 3 and 4. It is important to mention that the same solvent was used from day 0 until day 128 after which, the entire solvent inventory was completely replaced.

The duration of Campaign 2 was for ca. 140 days and a total of ca. 1700 operation hours as shown in Figure 2.5. Several tests were carried out and the entire campaign can be divided into 3 operational periods; Period 1 from day 0 to day 50, Period 2 from day 65 to day 80 and Period 3 from day 85 to day 140. During period 1, the pilot plant was operated intermittently. This was followed by a shutdown of 2 weeks. The solvent was stored in the pilot plant during the intermittent operation period and shutdown. During period 2, the pilot plant was in continuous operation for 2 weeks. The solvent was completely replaced thereafter, and from day 85 onwards, during period 3, the pilot plant was in continuous operation till the end of the campaign. The typical CO₂ and O₂

content in the flue gas was ca. 13 vol.% and 7 vol.%. Corrosion monitoring was performed for the entire time period of the campaign.

2.3.2 General trends in online corrosion measurements

The measured general corrosion rate, CMI and pitting factor during period 3 and 4 of campaign 1 were as shown in Figure 2.6, Figure 2.7 and Figure 2.8 respectively. During days 94 to 108, stagnant used solvent from previous operation periods (1 and 2) was in the plant. The low corrosion rate and CMI factor during this period indicate the characteristic of a “passive” system as shown in Figure 2.6 and Figure 2.7. The corrosion rate increases as the operation of the pilot plant is started on day 108. The start of the pilot plant operation induces a change from a “passive” to an “active” corrosion mode. This gives rise to an increase in the CMI to values greater than $0.02\mu\text{F}/\text{cm}^2$. On day 110, on further operation the corrosion rate and CMI increase rapidly and reach a maximum value of ca. $800 \mu\text{m}/\text{y}$ and $1\mu\text{F}/\text{cm}^2$, respectively. On day 115, pure MEA is added into the pilot plant which temporarily reduces the corrosion rate and CMI. This effect is expected as the total volume increases which leads to dilution of the corrosive products. However, on further operation of the plant, the corrosion rate and CMI keep increasing further. The average corrosion rate reaches a maximum of $600 \mu\text{m}/\text{y}$, while the maximum average CMI value is $0.7\mu\text{F}/\text{cm}^2$. The pilot plant was cleaned and replaced with fresh solvent on day 128. Thereafter, the corrosion rate then reduces back to the initial values to below $20 \mu\text{m}/\text{y}$, with temporary peaks on few days. However, the CMI value remains in the range of $0.3\text{--}0.5 \mu\text{F}/\text{cm}^2$.

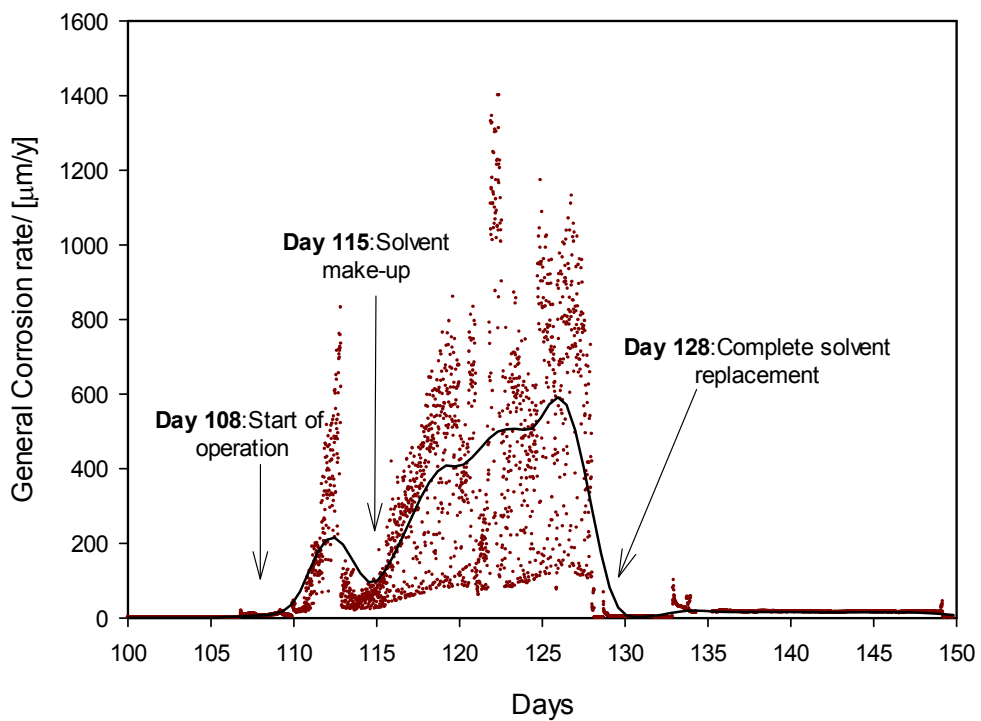


Figure 2.6. Corrosion rate during the pilot plant Campaign 1, specifically period 3 and 4. The solid line represents the trend in the measurements.

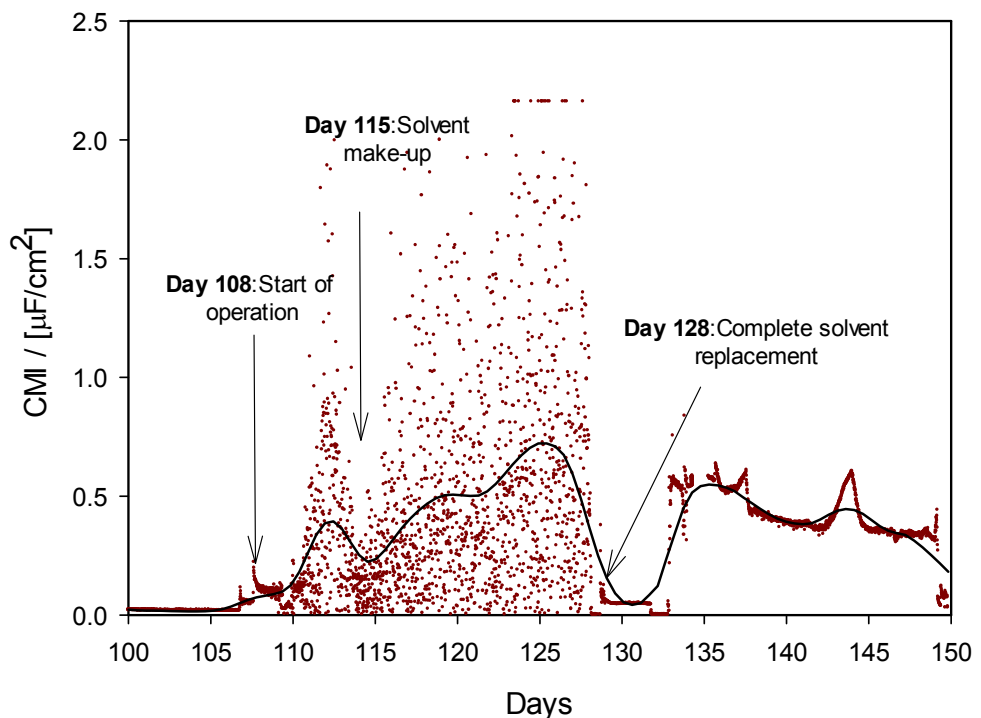


Figure 2.7. CMI during the pilot plant Campaign 1, specifically period 3 and 4. The solid line represents the trend in the measurements.

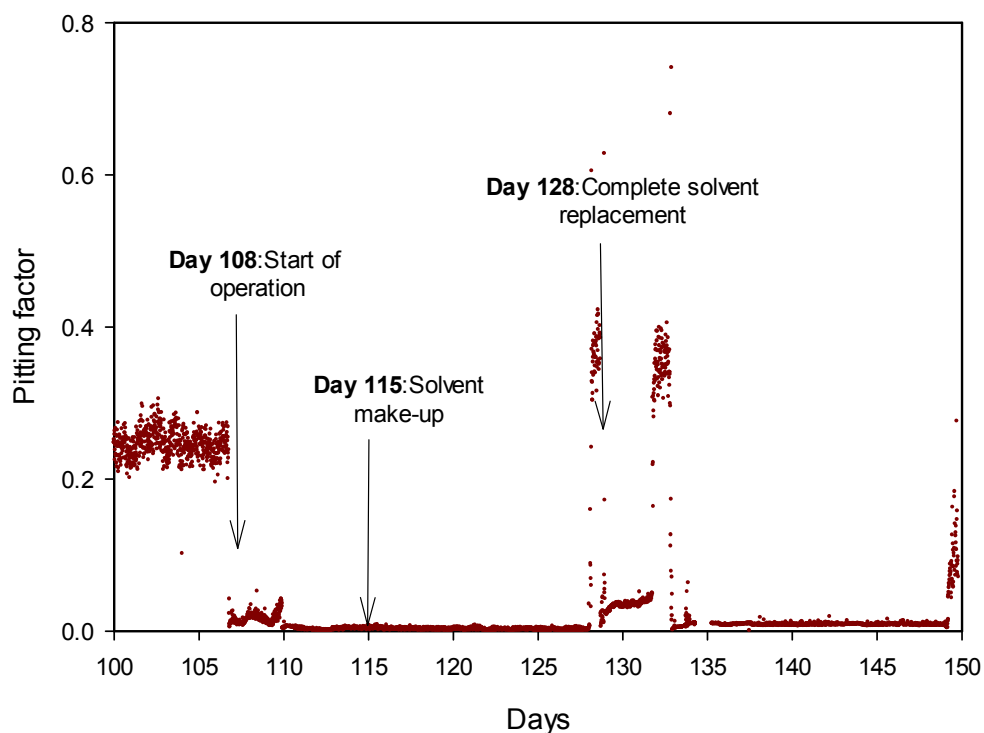


Figure 2.8. Pitting factor during the pilot plant Campaign 1, specifically period 3 and 4. Pitting factor is lower when the pilot plant is in operation.

The pitting factor remains low when the pilot plant is in operation and increases when the pilot plant is not in operation. The corrosion mechanism is expected to be general corrosion. The average corrosion rate measured during Campaign 1 was ca. 0.13 mm/y. The associated corrosion resistance belongs to the “good” category (i.e. 0.1-0.5 mm/y)¹⁰⁵. The corrosion resistance after solvent replacement (~day 123) belongs to the “outstanding” category (i.e. <25 µm/y)¹⁰⁵. The corrosion coupon placed at the hot lean solvent stream was lost and thus, the corrosion rate could not be calculated. This is likely due to the improper installation of the coupon holder.

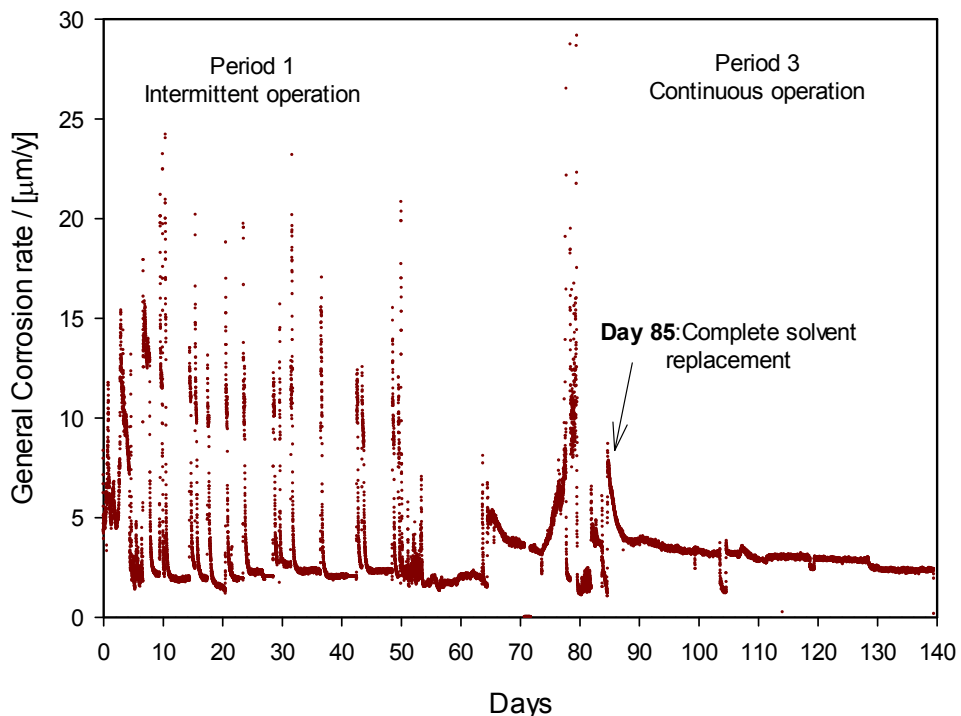


Figure 2.9. Corrosion rate during the pilot plant Campaign 2. The pilot plant was operated intermittently in period 1, while it was operated continuously during period 3.

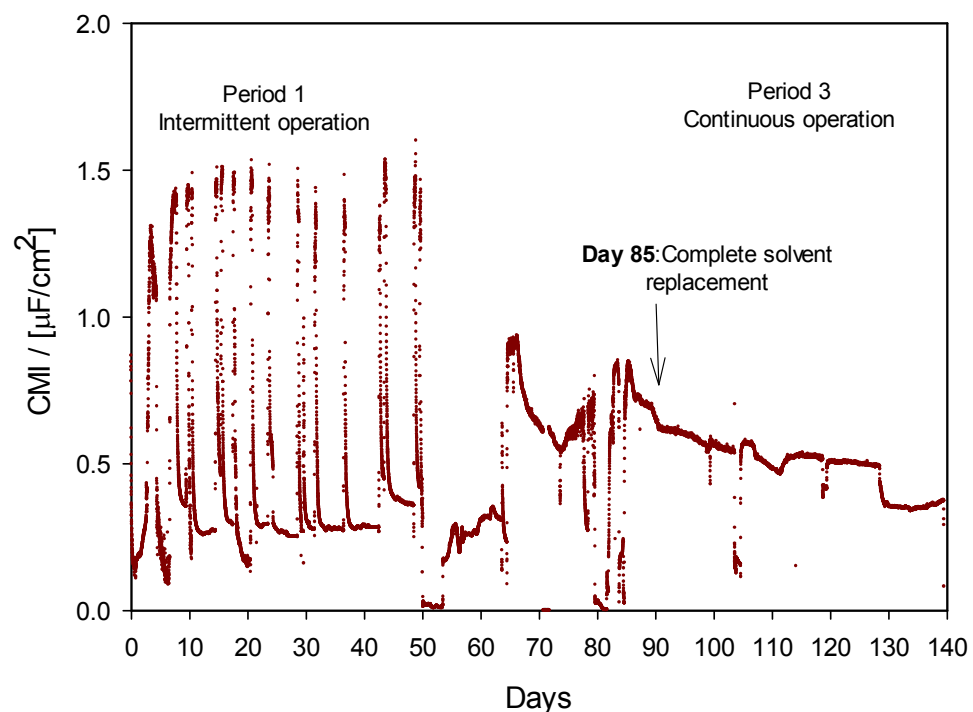


Figure 2.10. CMI during the pilot plant Campaign 2. The pilot plant was operated intermittently in period 1, while it was operated continuously during period 3.

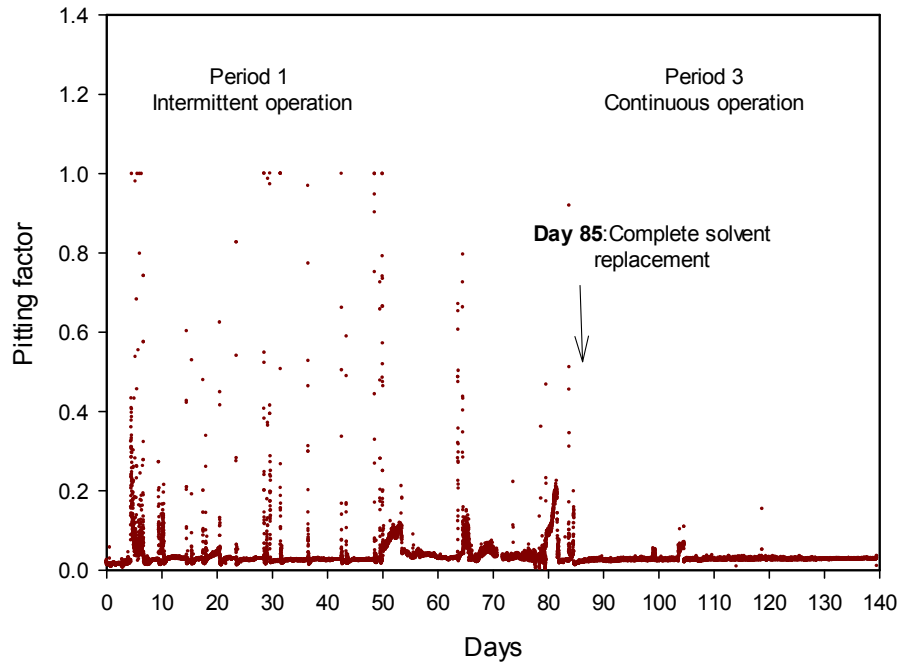


Figure 2.11. Pitting factor during the pilot plant Campaign 2. The pilot plant was operated intermittently in period 1, while it was operated continuously during period 3.

The measured general corrosion rate, CMI and pitting factor during campaign 2 were shown in Figure 2.9, Figure 2.10 and Figure 2.11, respectively. The corrosion rate and CMI increases when the pilot plant is in operation during the intermittent operation of period 1. The corrosion rate is in the range of 10-25 $\mu\text{m}/\text{y}$, while the CMI is in the range of 1.3-1.5 $\mu\text{F}/\text{cm}^2$. When the pilot plant is started on day 65 for continuous operation period 2, a peak in both the corrosion rate and CMI is observed and continues to decrease in time until day 74. From day 74 till day 80, when the pilot plant is stopped, both the parameters shows a rapid increase in both the corrosion rate and CMI. Once the solvent is replaced, both the parameters continue to decrease in time on continuous operation until the end of the campaign.

The change in corrosion mode could not be clearly identified but, is probably due to solvent state modifications associated with intermittent operation and/or solvent/demin water additions. The general corrosion rate and the pitting factor are globally stable and constant during the entire campaign, with the exception of two stops of the pilot plant. During those stops, the corrosion rate is lower than the normal operation, while the pitting factor is higher (the pitting factor is by definition inversely proportional to the general corrosion rate). The measured general corrosion rate is ca. 4 $\mu\text{m}/\text{y}$ which corresponds to an outstanding corrosion resistance ($<25\mu\text{m}/\text{y}$) ¹⁰⁵. The calculated corrosion rate based on the coupon is 0.3 $\mu\text{m}/\text{y}$. This value is within the order of the minimum detection limit and therefore, cannot be interpreted quantitatively. However, it can be concluded that the corrosion rates measured by both methods are similar and correspond to outstanding corrosion resistance.

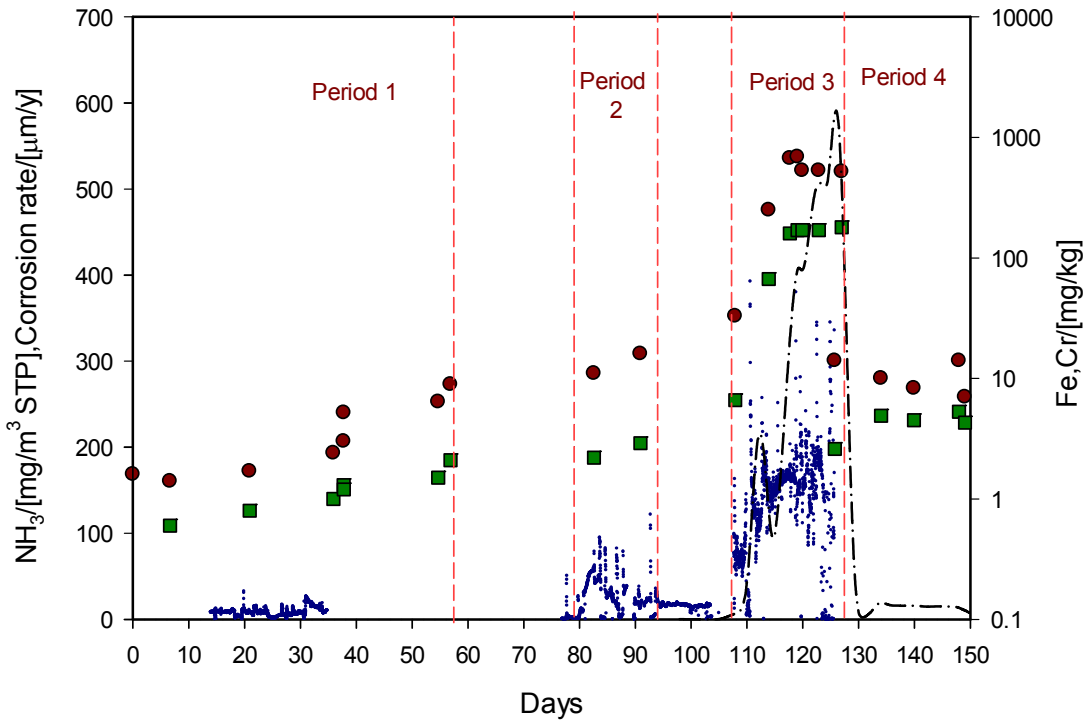


Figure 2.12 Ammonia emissions (\circ), average corrosion rate ($- \cdot -$) and solvent metal content (here: Fe (\bullet), Cr (\blacksquare)) as measured during the campaign 1. The oxygen content in the flue gas in period 2 was ca. 17 vol.%. At the start of period 4, the solvent was replaced.

2.3.3 Inter-relation of corrosion, solvent degradation and ammonia emission

Figure 2.12 shows the measured average general corrosion rate, ammonia emissions and the solvent metal content during Campaign 1. Here, Fe and Cr are shown as representative of metals in the solvent but, other metals such as Ni and Mn, which are typically present in stainless steel, also show a similar trend. The solvent metal content increases throughout the campaign and specifically, shows a rapid increase during the continuous operation period from day 108 till day 128. The solvent metal content increases to values larger than 500 mg/kg at the end of the campaign. It is important to note that the method for metal content is calibrated only up to 500 mg/kg. The ammonia emission remains fairly constant, in the range of 10-20 mg/m³ STP, with some temporary peaks, until day 108. This is a typical value of ammonia emissions from a post combustion capture plant ^{72,95}. In the continuous operation period from day 108 till day 128, all three parameters, i.e. the corrosion rate, ammonia emissions and solvent metal content, increases rapidly. The maximum ammonia emissions reaches almost 300 mg/m³ STP while, the maximum average corrosion rate is ca. 600 µm/y. The solvent was completely replaced on day 125 and subsequently, all three parameters are close to the initial values.

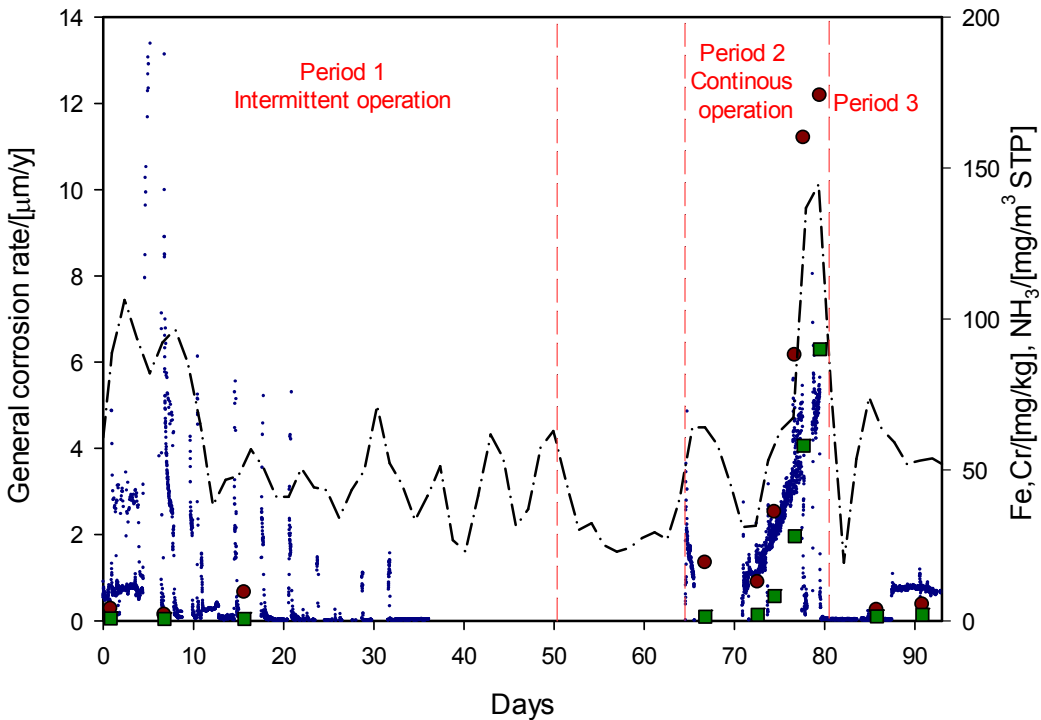


Figure 2.13 Ammonia emission (○), average corrosion rate (— · —) and solvent metal content (here: Fe (●), Cr (■)) as measured during the campaign 2. At the start of period 3, the solvent was replaced.

There is a clear correlation between the corrosion rate, the metal content and the emitted NH_3 during the entire campaign. Metal ions, and in particular Cr, Ni and Fe ions, are known to have a catalytic effect on oxidative solvent degradation²⁶. Moreover, the oxidative degradation of MEA renders the solvent more corrosive, leading to an increase of the metal ions concentration. The degradation of the solvent eventually produces NH_3 which is present in the treated flue gas stream. Thus, the general trend of the inter-dependence can be explained on the basis of existing knowledge on this topic. Moreover, it is known that the degraded solvent leads to further corrosion after which the autocatalytic cycle continues, eventually leading to an out of control solvent chemistry. However, there is no experimental evidence yet, either lab-scale or pilot plant scale, of a direct correlation of these three parameters in the literature.

One hypothesis for the sudden rapid increase in solvent degradation is that the high oxygen content (~17 vol.%) during the period of day 80 to day 94, increased the solvent degradation rate tremendously. It is well known that increasing the oxygen content increases the rate of solvent degradation. During the subsequent continuous operation period (day 108 onwards) a critical metal concentration would have reached, which led to autocatalytic chemistry in the solvent and increased metal content and ammonia emissions.

Figure 2.13 shows the measured average general corrosion rate, ammonia emissions and the solvent metal content during campaign 2. During period 1 of intermittent operation, the solvent metal content is ca. 1 mg/kg while, the corrosion rate is in the range of 2-8 $\mu\text{m}/\text{y}$. The corresponding ammonia emissions is in the range of 10-50 mg/m^3 STP, with temporary peaks during start-up and shutdown of the pilot plant. A sudden and rapid increase in the three parameters is seen when the pilot plant was in continuous operation, specifically, from day 72 to 80. The solvent metal content and the NH_3 emissions reach a maximum of 70 mg/kg and 80 mg/m^3 STP, respectively. On solvent replacement, all the three parameters are back to their initial values.

The solvent seems to be less degraded during campaign 2 than campaign 1, which is confirmed by the lower solvent metal content, corrosion rate and ammonia emission. Operation hours during campaign 1 were significantly more than during campaign 2. Moreover, during certain periods, the solvent was exposed to higher concentration of oxygen in the flue gas during campaign 1. Both these reasons explain the increased degradation observed in campaign 1 as compared to campaign 2.

For both the campaigns, there is a time period during which a rapid increase in all the three parameters is seen. This rapid increase indicated an auto-catalytic reaction. However, the exact cause and time at which the rapid increase in degradation occurs, are not known either from this pilot plant campaign or from laboratory studies. The common characteristic before the onset of rapid degradation for both the campaigns, is the restart-up of the pilot plant after an extended period of shutdown. During campaign 1 and campaign 2, the pilot plant was shut down for a period of two weeks, between periods 1 and 2, before further continuous operation. This indicates the degradation of the solvent and corrosion continues even during shut down of the pilot plant but, the mechanism of degradation is likely to be different than during the operation of the pilot plant. The increased amount of degradation products thus formed during the shutdown period, subsequently increases the corrosion significantly, which further degrades the solvent and leads to ammonia emissions. In order to understand this mechanism further, experiments at laboratory and pilot plant scale must be designed in a representative manner to observe the same effects as observed during operation.

2.4 Conclusions

Corrosion in amine based gas treating process is a major concern for proper functioning and continuous operation of the plant. It is expected that for Postcombustion CO_2 capture plants, corrosion is a bigger issue, mainly because of the presence of high concentrations of oxygen in the flue gas. An online, real-time corrosion monitoring system has been presented which provides online information on the corrosion rate and indirectly, the state of the solvent. The general corrosion rate was ca. 0.13 mm/y for campaign 1 while, for campaign 2 it was 4 $\mu\text{m}/\text{y}$. The higher corrosion rate during campaign 1 was surmised to be due to the longer operation hours and exposure to flue

gas containing higher content of oxygen, i.e. 17 vol.% instead of 7 vol.%. Addition of fresh MEA in order to make up the solvent strength, reduced the corrosion rate and solvent degradation, only temporarily. For the first time, the impact of corrosion on ammonia emission has been highlighted and a direct relation with corrosion rate and dissolved metal content has been presented for a typical pilot plant scale Postcombustion CO₂ Capture process. In the absence of solvent-reclaiming, an autocatalytic solvent degradation behaviour was observed for both the campaigns during which all the three parameters: corrosion rate, solvent metal content and ammonia emissions, reach alarmingly high values. A common chain of events, i.e. extended shutdown periods followed by restart of the pilot plant was observed at the onset of the rapid solvent degradation during both the campaigns. This observation will assist in the design of representative experiments to understand the relevant mechanism either on a laboratory or a pilot plant scale. A complete replacement of solvent was seen as necessary in order to obtain the baseline values of corrosion rate, solvent metal content and ammonia emissions. The presented results can also be used to make a strategy for the extent and timing of solvent feed and bleed and/or reclaiming during continuous operation of a full scale Postcombustion CO₂ capture process.

Based on the observed correlations, online corrosion monitoring has been demonstrated to be an effective tool to detect early signs of solvent degradation and increased emissions. In the same way, online NH₃ emission measurements were seen to be a good indicator of the state of the solvent and the extent of corrosion to the equipment.

Chapter 3

Acid wash scrubbing as a countermeasure for ammonia emissions from a post combustion CO₂ capture plant.

This chapter is based on the following publication:

Khakharia, P., Huizinga, A., Jurado Lopez, C., Sanchez Sanchez, C., de Miguel Mercader, F., Vlugt, T.J.H., Goetheer, E., Acid wash scrubbing as a countermeasure for ammonia emissions from a Postcombustion CO₂ capture plant, *Ind. Eng. Chem. Res.*, 53, 13195–13204, 2014.

3.1 Introduction

Solvent degradation and emissions of solvent components and degradation products are important points of concern in amine based CO₂ capture processes ⁷². Oxygen present in the flue gas reacts with amines in the solution, leading to oxidative degradation ³⁸. Several intermediates and reaction pathways have been identified for the oxidative degradation of amines. The exact degradation mechanism is not yet fully understood, although ammonia is known to be a major oxidative degradation product of amines ^{70,86,89,108}. As ammonia is highly volatile, it is emitted to the atmosphere in the treated flue gas stream. The release of ammonia can not only cause a severe environmental burden, but it is also hazardous to human health ^{109,110}. The design limit of ammonia emissions is expected to be ca. 5 mg/m³ STP (STP; 0°C and 101.325 kPa); however, no permit has been set for ammonia emissions from a CO₂ capture plant ^{71,111,112}. Typical ammonia concentrations during the operation of a CO₂ capture plant in a treated flue gas stream using MEA are expected to be higher than 5 mg/m³ STP.

Treatment of the flue gas containing ammonia from the absorption column is necessary before its emission to air ^{113,114}. Several abatement techniques to treat off-gases containing ammonia, such as thermal oxidation, catalytic combustion, catalytic decomposition, condensation, membrane separation, scrubbing, adsorption, and biofiltration, have been widely studied and used ^{115,116}. The advantages of acid scrubbing over other techniques are its suitability for deep removal of ammonia, its removal of other amine based components, its ease of operation, and the formation of valuable byproducts such as ammonium sulphate (which can be used as a fertilizer upon further purification), among others.

Limited information is available on the use of acid wash scrubbing in PCCC plants. The main objective of this study was to assess the efficiency of an acid wash scrubber for reducing the amine and ammonia content in the treated flue gas stream of a pilot plant scale PCCC process. The efficiency of the acid wash was evaluated in terms of the removal of ammonia and MEA from the treated flue gas stream. High amounts of ammonia (>50 mg/m³ STP) in the treated flue gas can be expected after long-term operation (in the order of 1000-1500 operating hours, i.e., several months of operation) as the solvent is increasingly degraded. To test the robustness and efficiency of the acid wash even under extreme conditions, additional ammonia was injected into the flue gas prior to the acid wash to an ammonia concentration of ca. 150 mg/m³ STP in the flue gas (a so-called spiking experiment). Parametric tests included changes in the pH of acid wash, the temperature of the flue gas and the flow rate of the acid liquid. A model was developed in Aspen Plus V8.0 to closely resemble the acid wash column ⁷⁸. The results of the parametric studies were then compared with results from the model. Finally, an economic evaluation was performed to assess the applicability of acid wash scrubbing for amine and ammonia removal in a full scale CO₂ capture plant.

3.2 Test Equipment, method and model

3.2.1 CO₂ capture pilot plant

The test campaign was conducted at TNO's CO₂ capture plant at Maasvlakte, The Netherlands. The CO₂ capture plant receives flue gas from Unit 2 of a coal-fired power station (E.ON). It is designed for the capture of 6 metric tonnes of CO₂ per day. A schematic representation of the CO₂ capture plant is shown in Figure 3.1. In the next subsections, a detailed description of the CO₂ capture pilot plant is provided.

3.2.1.1 SO₂ Polisher/Direct Contact Cooler (DCC)

The SO₂ removal step is combined with the cooling of the flue gas. This is done by means of counter-current scrubbing by a wash liquid in a packed column with dimensions listed in Table S1 of the Appendix. The pH of the washing liquid is maintained between 6.3 and 6.7, and the temperature of the flue gas leaving the SO₂ polisher is maintained at 40°C. The flue gas enters a blower that provides the necessary increase in pressure to overcome the pressure drop across the subsequent equipment.

3.2.1.2 Brownian Demister Unit (BDU)

In previous pilot plant campaigns at TNO's CO₂ capture pilot plant, it was observed that a significant loss of solvent can occur through aerosol-based emissions under certain operating conditions. Thus, under such conditions, continuous steady-state operation of the pilot plant is not possible because of issues such as environmental regulations, excessive solvent makeup and unsteady water balance. A BDU is made up of a polypropylene filter which removes particles larger than 1-2 µm by a combination of impingement and diffusion mechanisms. The BDU was installed in front of the absorber as shown in Figure 3.1 for this campaign, thus enabling the operation of the pilot plant at steady state in a continuous manner. A picture of the BDU is shown in Figure 3.2.

3.2.1.3 Absorber Tower

CO₂ capture occurs by means of counter-current absorption by a solvent in the absorption tower. Aqueous MEA (30 wt.%) was used as the capture solvent. The CO₂ absorption section consists of four packed beds with liquid distributors installed between the packed sections. The column and the packing specifications are summarized in Table S2 of the Appendix.

A water wash section lies above the packed beds in the absorption tower. The water wash section minimizes solvent losses and condenses water vapour to maintain the water balance. This is achieved by means of cooling and recirculating water over the packed bed. The temperature and the circulation rate of the wash liquid are

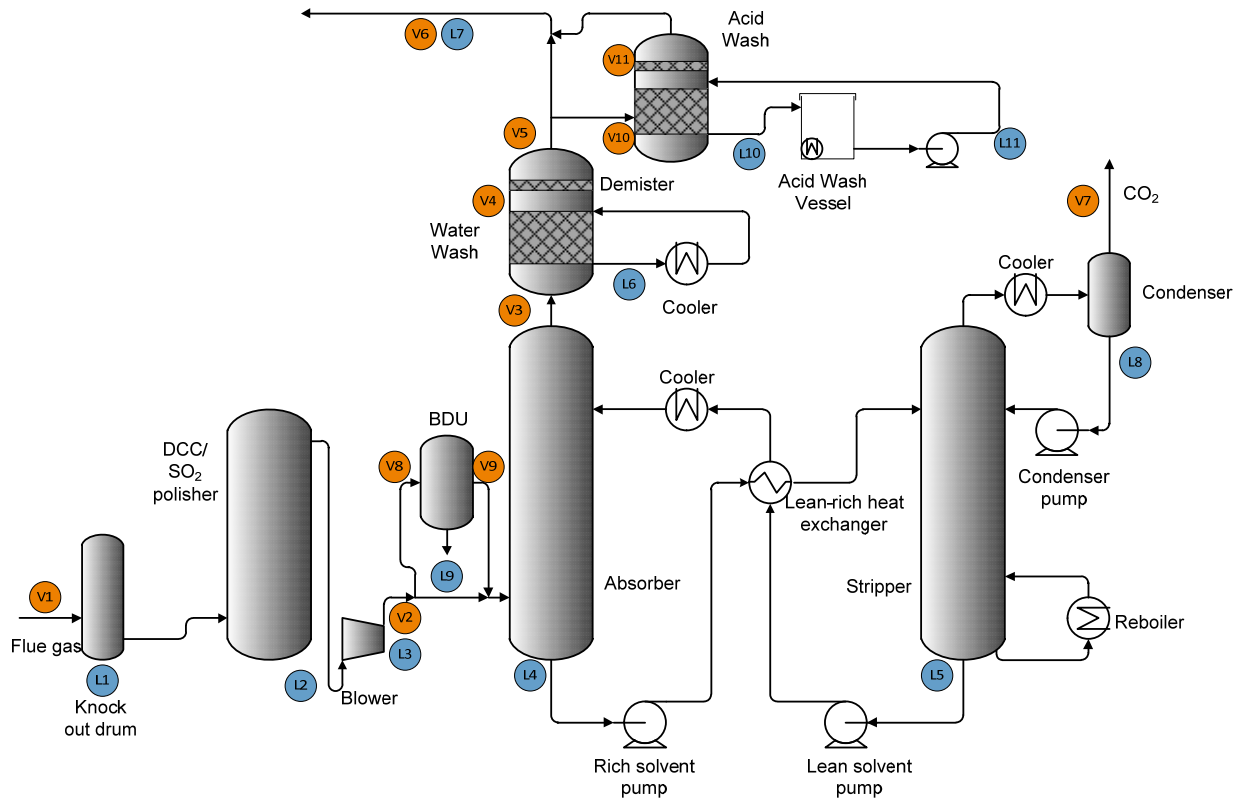


Figure 3.1. Schematic of TNO's CO₂ capture pilot plant at Maasvlakte, The Netherlands. The water wash section is integrally mounted in the absorber tower and is shown as a separate unit for clarity of representation. The sampling locations are denoted by; L for liquid sampling ports, and V for vapour sampling ports.

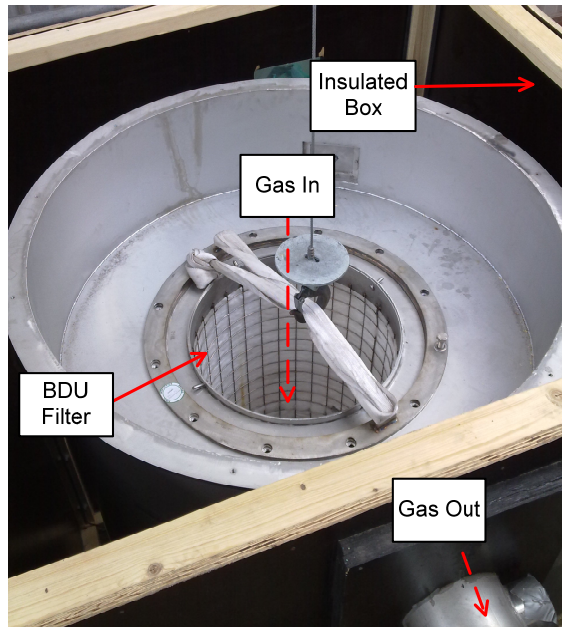


Figure 3.2. BDU used at the CO₂ capture pilot plant for the removal of nuclei from the flue gas to minimize aerosol-based emissions. Dashed red lines indicate the path of gas flow. The BDU filter is 1 m long with an internal diameter of ca. 50 cm and a thickness of ca. 5 cm.

controlled to maintain the water balance in the system. The specifications of the water wash section are shown in Table S3 of the Appendix.

After the water wash section, the treated flue gas passes through a conventional demister to minimize solvent carryover. The demister is a knitted pad that causes the droplets to coalesce at the wire surfaces as a result their inertia 117,118. Droplets larger than 10 μm are removed.

3.2.1.4 Acid Wash Scrubber

The acid wash is located downstream of the water wash as a separate column. The acid wash consists of an acid wash column and a buffer tank. Acid scrubbing occurs by means of counter-current contact of the flue gas with an acid. An aqueous solution of sulphuric acid (H_2SO_4) was used as the acid liquid. Sulphuric acid was used here because it is the most commonly used acid.

Figure 3.3 shows a 3-D representation of the acid wash column along with the dimensions, and Figure 3.4 shows the type of packing, Mellapak 250 (Sulzer Chemtech), used for the acid wash column. This packing consists of six layers of packing, each of 222 mm, adding up to a total packed height of 1.26 m. The distribution of the liquid over the packing has to be uniform to avoid any channelling of liquid. A VKG (Sulzer Chemtech) type of liquid distributor was used. It consists of branches off the main pipe with holes for dripping of liquid as shown in Figure 3.5. The orifice size is 7.1 mm and there are 50 holes in total. The distributor is designed for a flow rate of 4.09–5.45 $\text{m}^3 \text{STP/h}$, corresponding to a turndown ratio of 90–120%. A demister is necessary to prevent carryover of droplets. A general purpose demister, KnitMesh (Sulzer Chemtech) mist eliminator, was installed in the column, as shown in Figure 3.6. It consists of a bed of knitted mesh that presents a tortuous path and a large surface area to the droplets entrained in the gas stream.

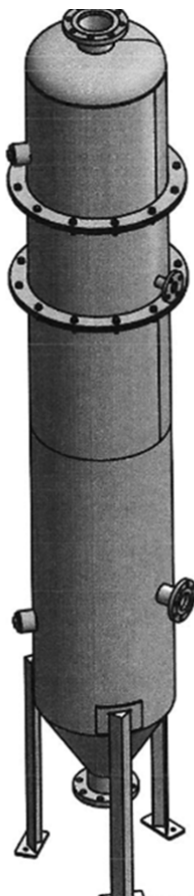


Figure 3.3. Three dimensional representation of the acid wash column. The total height of the column is 4.7 m from the base to the top.

The liquid is separated from the gas stream by means of impingement on, and capture by, the filaments of the mesh, where the droplets coalesce and drain. It is capable of removing droplets of 2 µm with an efficiency of 96.4 %, whereas droplets above 10 µm are removed with a 100 % efficiency. The specifications of the acid wash column are summarised in Table S4 of the Appendix. The total height of the column, from the base to the top, is ca. 4.7 m. The total height includes internals, ports for gas sampling, and legs for support. The column diameter was fixed at 0.65 m to have the same column hydrodynamics as the absorber tower.

A vessel of 300 l was used as a holdup tank for the acid liquid. Both demineralised water and acid can be dosed into this tank. A provision was made for a port to measure the pH of the acid in the vessel. A heater was placed at the bottom to heat the liquid if necessary.

Sensors for measuring temperature, pressure, flow rate and pH were placed in the necessary gas and liquid lines to obtain essential process information and facilitate steady-state operation. All pipelines, for both gas and liquid, were insulated. For steady state operation of the acid wash system, an appropriate control strategy was implemented which required minimum operator interference. The two main parameters



Figure 3.4. Structured packing (Mellapak 250 Y) for the acid wash column with a diameter of 0.65 m and a height of 0.22 m for each layer.



Figure 3.5. Liquid distributor over the structured packing in the acid wash column. It has a diameter of 0.65 m and the total number of orifices are 50, each with a diameter of 7.1 mm.



Figure 3.6. Conventional knit mesh demister for droplet removal with a diameter of 0.65 m and a height of ca. 10 cm.

that were controlled were the pH of the acid liquid and the temperature of the flue gas leaving the acid wash column. Specifically, over a period of time, the pH of the acid liquid will increase due to the accumulation of basic components (ammonia, MEA, etc.). Thus, the pH of the acid liquid was maintained by adding fresh sulphuric acid to the acid wash buffer tank. The acid was dosed using a syringe pump from a fresh sulphuric acid stock solution. In addition, the temperature of the flue gas leaving the acid wash column was maintained slightly higher (0.5-1.5°C) than its inlet temperature to avoid condensation in the column. This was achieved by heating the acid liquid in the buffer tank. The set point for the temperature was based on a fixed offset on the temperature of the flue gas entering the acid wash column.

3.2.1.5 Stripper Tower

The solvent that is loaded with CO₂ (rich solvent) is sent to the stripper tower through the lean-rich heat exchanger. The rich solution is further heated in a reboiler to strip the CO₂. The stripping of CO₂ occurs by counter-current contact of the steam generated in the stripper with the rich solution flowing to the stripper sump. At the top of the stripper tower, a conventional demister minimizes the solvent carryover. The desorbed CO₂ exits the stripper tower and enters the product cooler and a knockout drum, where the relatively pure CO₂ stream is condensed. The condensate from the knockout drum is returned to the top of the stripper to minimize the loss of steam and maintain the water balance. The lean solvent (solvent stripped of CO₂) accumulates in the stripper sump and is pumped to the absorber tower for next cycle of absorption-desorption via the lean-rich heat exchanger. The heat from the lean solvent preheats the rich solvent. Heat integration by means of preheating the rich solution minimizes the reboiler duty. Table S5 of the Appendix lists the stripper tower specifications. The CO₂ exiting the stripper is combined with the treated flue gas from the absorber and is returned to the power plant's flue gas stack.

3.2.2 Fourier Transform Infrared (FTIR) Spectroscopy

An FTIR analyser (GASMET CX 4000) was used to analyse the flue gas. The FTIR spectrometer was specifically calibrated for the following components: water, CO₂, NH₃, MEA and oxygen as shown in Table S6 of the Appendix. For the components mentioned here, the FTIR spectrometer was calibrated to an accuracy of 2 %. For NH₃, additional spectra were added from literature up to a range of 400 mg/m³ STP with an accuracy within 5 %. Additional information about the FTIR can be found in literature⁶⁹.

The gas is sampled by means of a heated probe. A long heated line (180°C) carries the gas from the sampling probe to the FTIR analyser. Two sampling probes were used; one before the acid wash column and the other after the acid wash column, to obtain the gas concentrations before and after the acid wash scrubber, respectively. A multiplexer was used to alternate the sampling of gas between these two positions.

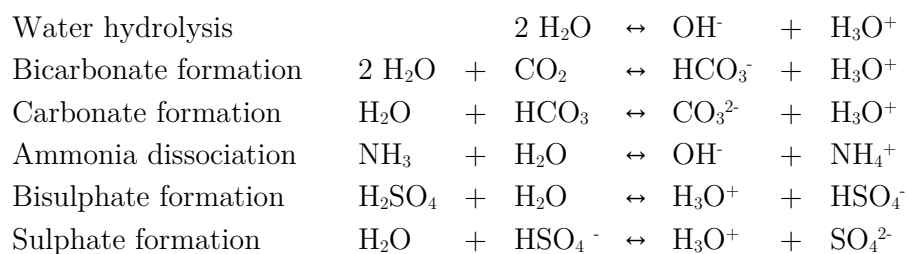
3.2.3 Ammonium ion analyses

The liquid samples for ammonium ion analyses were diluted in an ammonia-free sodium carbonate buffer to reach a pH in the range of 7–10. These dilutions were added with an internal standard (ammonium-¹⁵N-d₄) before being derivatised with dansyl chloride. The derivates of ammonia and its internal standard were then analysed on an Agilent 1290 Infinity LC system (Ascentis Express C18 reverse phase column) for chromatographic separation, using an Agilent 6490 triple quadrupole (MS–MS) instrument as a detector.

3.2.4 Acid wash model in Aspen Plus

An acid wash model was developed in Aspen Plus V8.0 for comparison with the experiments. The calculation type was chosen to be rate-based in a RadFrac column. Based on in-house experience with absorption column modelling three stages with no condenser or reboiler were considered, given the column height and the packing type. The number of stages were fixed to three, as increasing the number of stages did not change the predicted values of ammonia emissions. The column was considered to be at atmospheric pressure and it was assumed that there was no pressure drop in the column. The liquid phase was considered to be well-mixed whereas the gas phase was considered to have a plug flow behaviour. The reader is referred to the literature for further information on rate-based modelling in Aspen Plus ¹¹⁹. The dimensions of the acid wash model were based on the actual acid wash design at the pilot plant scale. The thermodynamic model chosen was ENRTL-RK. The interfacial area factor was assumed to be 0.7, which is considered to be typical for such a packing type ^{120,121}.

The reactions included in the model based on reaction set “NH₃ REA” as available in Aspen Plus, are as follows:



The RadFrac column approach in Aspen Plus does not support salt formation. The salt formation of ammonium sulphate was not considered, as the amount of ammonium sulphate formed would be very low and ammonium sulphate is highly soluble in water. The equilibrium constants were calculated based on expressions available in the literature ¹²². The ammonia concentration and the composition of the flue gas in the model were fixed based on the measurements from the FTIR spectrometer from each experiment. An example is shown in Table S7 of the Appendix.

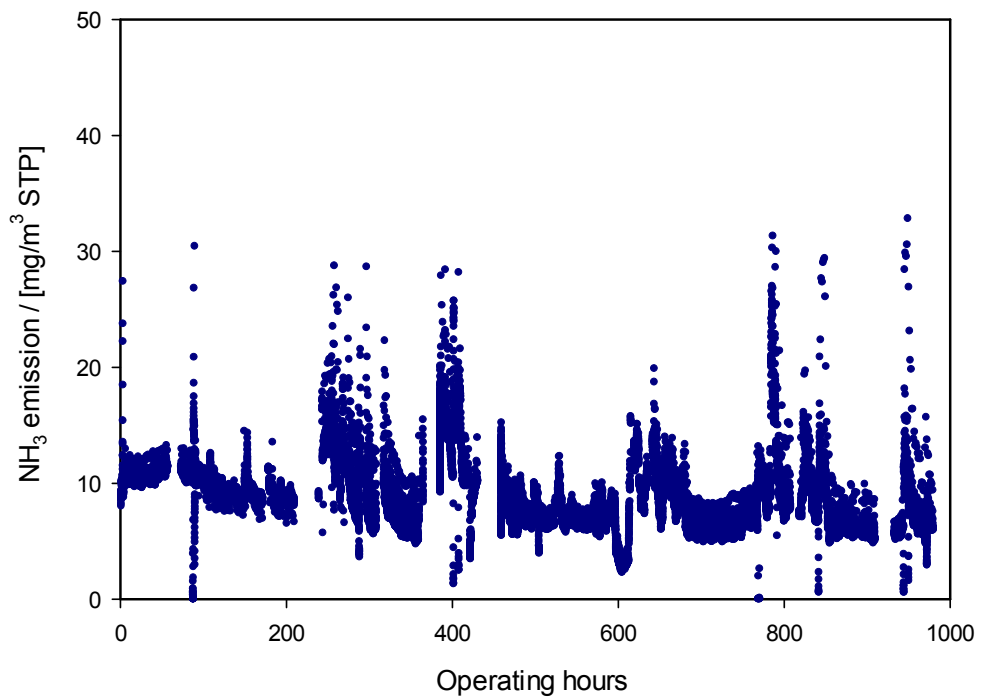


Figure 3.7. Ammonia emission (mg/m³ STP) during the pilot plant campaign (~1000 operating hours), using 30 wt% MEA.

The pH of the acid liquid in the pilot plant experiments was increased by accumulating ammonia in the acid liquid in the absence of any additional acid dosage. To maintain the same approach, the sulphuric acid concentration in the model was kept constant whereas the ammonia concentration was increased to increase the pH of the acid liquid. In the model the liquid was not recirculated, to independently change the composition of the inlet acid liquid and avoid convergence issues. Table S8 of the Appendix lists the corresponding concentrations of ammonia in the inlet acid liquid. The sulphuric acid concentration was kept constant at 0.5 mmol/L. It is important to note that the acid liquid inlet in the experiments would contain ammonium sulphate accumulated over a period of time.

3.3 Results and discussion

3.3.1 Campaign overview

The pilot plant campaign to implement various settings to test the acid wash was carried out for a duration of six weeks. The pilot plant was also operated during weekends at steady state. During the entire campaign, the settings of the CO₂ capture pilot plant were constant, as shown in Table S9 of the Appendix. Fresh solvent (30 wt.% MEA) was used for the campaign. Typical CO₂ loadings were 0.23 and 0.47 mol CO₂/mol MEA for lean and rich solutions, respectively.

Table 3.1. Summary of acid wash settings for parametric tests.

Parameter	Experiments without spiking	Experiments with spiking
Inlet liquid pH	2.87, 3.2, 4.14, 4.97, 6.81	2.87, 3.2, 4.14, 4.95, 5.92, 6.67, 8.09
Inlet liquid flow rate (L/min)	50.5, 58.3, 66.6, 75.0, 82.8, 90.3	50.2, 58.3, 66.7
Temperature of the flue gas entering the acid wash column (°C)	39.8, 43.9, 48.6, 55.6	43.9

Figure 3.7 shows that the ammonia emissions after the water wash section during the campaign as measured by the FTIR spectrometer, remained fairly constant at around 15-20 mg/m³ STP. Temporary peaks in the ammonia emissions were observed due to changes in certain operating conditions, which led to temporary shifts in the equilibrium of ammonia in the gas and liquid phases. The time period of actual operation of the pilot plant during the campaign was ca. 1000 h.

3.3.2 Parametric study for NH₃

This section describes the results of the parametric study to test the efficiency of the acid wash system for NH₃ removal. The acid strength (pH), the liquid flow rate, and the temperature of the flue gas entering the acid wash column were varied to test the efficiency of the acid wash scrubber for NH₃ removal. Typical ammonia emissions were in the range of 5-15 mg/m³ STP for the first few weeks of the campaign. Ammonia emissions can increase to values greater than 100 mg/m³ STP after several weeks of operation due to degradation of the solvent. Because the duration of this campaign was short, additional ammonia (spiking) was added to the flue gas entering the acid wash column to mimic a state of high solvent degradation state and, thus, test the efficiency of the acid wash system under extreme conditions. The ammonia spiking was done so that the total ammonia concentration entering the acid wash column was ca. 150 mg/m³ STP.

Table 3.1 presents the average values of the settings for the parametric study. The pH of the acid liquid was varied from 3 to 7 and an additional setting of pH 8 was tested with spiking of ammonia in the flue gas. The acid liquid flow rate was varied from 50 to 90 l/m (litres per minute). It must be noted that a flow rate of 50 l/m (i.e. 3 m³/h) is lower than the minimum recommended for the liquid distributor (4.09 m³/h) however, this had no impact on the ammonia capture efficiency, as seen in section 3.3.2.2. The temperature of the flue gas to the acid wash was varied from 40 to 55°C. The base setting for all tests was acid liquid at pH 3 with a flow rate of 75 l/m and a flue gas inlet temperature at 40°C.

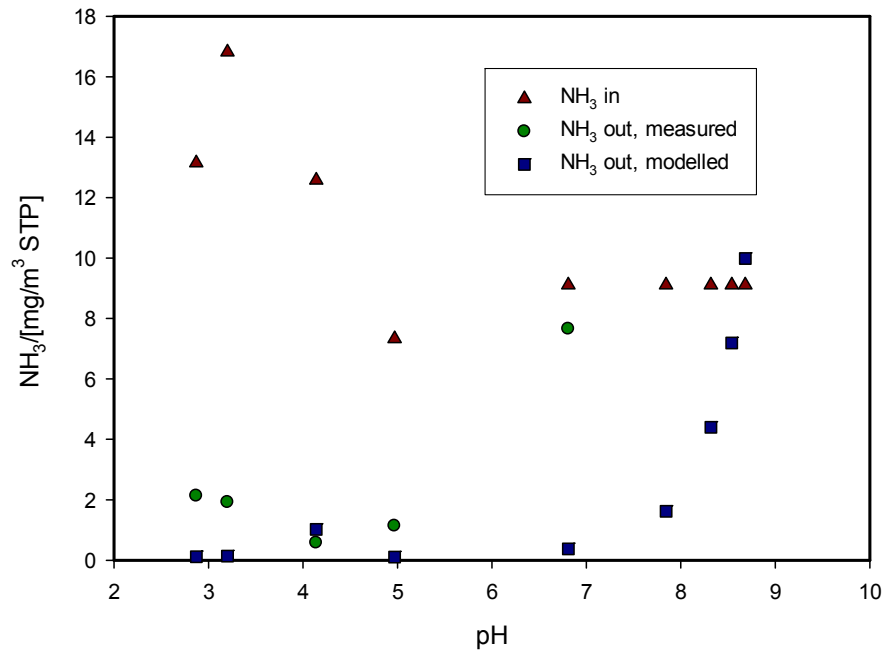
3.3.2.1 Effect of pH

Ammonia is highly soluble in water, but when the same liquid is used in a continuous countercurrent absorption system, an equilibrium between the gas phase and liquid phase ammonia is reached. After this point, no further absorption of ammonia occurs. Thus, it is necessary to keep the ammonia in ionised form by using an acid. The pH of the acid liquid was increased by the accumulation of ammonia over a period of time without any further dosing of acid. When the required pH was reached, acid was dosed to maintain the necessary pH. A pH of 3 was considered as the base setting.

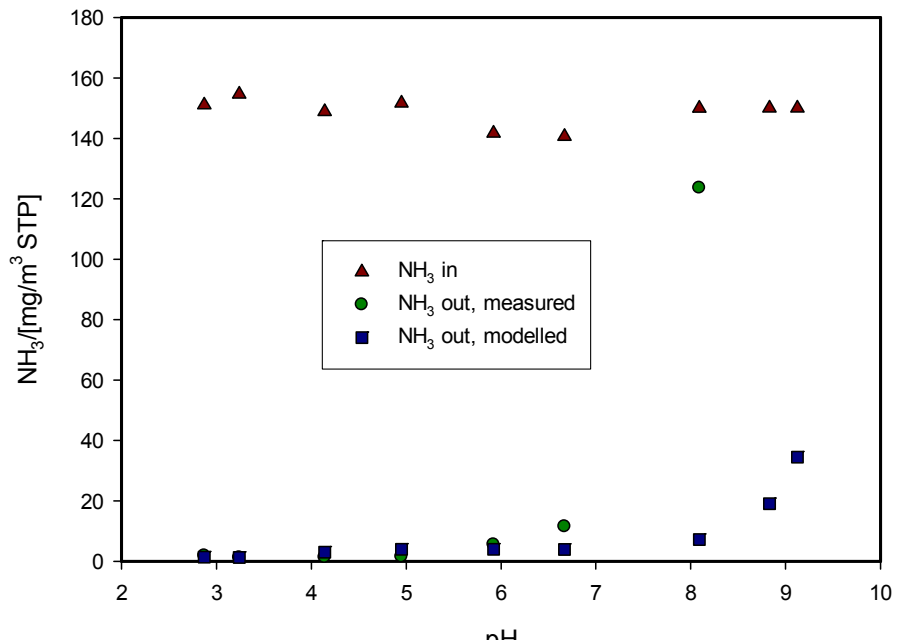
Figure 3.8 shows the ammonia concentrations in to and out of the acid wash for the parametric tests for a change in pH. For experiments conducted without spiking of ammonia in the flue gas, the inlet ammonia concentration was in the range of 7–17 mg/m³ STP. The outlet concentration was below 2 mg/m³ STP for liquid up to pH 5, whereas there was hardly any ammonia removal at a liquid pH of 6.8. The results from the model for the outlet ammonia concentration up to pH 5 are consistent with the experimental results. However, the model predicts that, even at a liquid pH of 6.8, the acid wash liquid is capable of reducing the ammonia outlet concentration to below 2 mg/m³ STP. The modelled outlet ammonia concentration increases gradually up to pH 8.7, after which there is no further capture of ammonia by the acid wash. Thus, the breakthrough of ammonia capture, defined as less than 20 % capture efficiency, for experiments without spiking was between pH 5 and 6.8, which is significantly lower than the predicted pH of 8.7.

For the experiments conducted with spiking, the inlet ammonia concentration varied from 140 to 155 mg/m³ STP. The outlet ammonia concentration for experiments with ammonia spiking remained below 5 mg/m³ STP up to a pH of 5.9. Increasing the pH further reduced the capture efficiency, and at pH 8.1, an insignificant amount of ammonia capture occurred. According to the model, the outlet ammonia concentration should be in the range of 1-3 mg/m³ STP up to a pH of 6.8. Thus, the model predicts the breakthrough of ammonia capture at pH 9.7 whereas experiments indicate that the breakthrough of ammonia capture by the acid wash occurs already at pH 8.1.

It can be seen that, for experiments both with and without spiking, the breakthrough point is at a lower pH than predicted by the model, as shown in Figure 3.9. The pK_a value of ammonia is 9.37 (at 20°C) and the reaction of ammonia with an acid is instantaneous ¹²³. Thus, the capture of ammonia can be considered to be gas-side mass transfer limited. However, the liquid-side mass transfer resistance can increase at higher pH values so that a higher driving force is required to achieve the same capture efficiency ¹²⁴. One possible explanation for the different breakthrough points for the model and the experiments is that the capture efficiency of the absorption column decreases owing to the increase in liquid side mass transfer resistance. This is verified by the fact that the breakthrough pH for spiking experiments (8.1) is at a higher pH than that for nonspiking experiments (6.8).

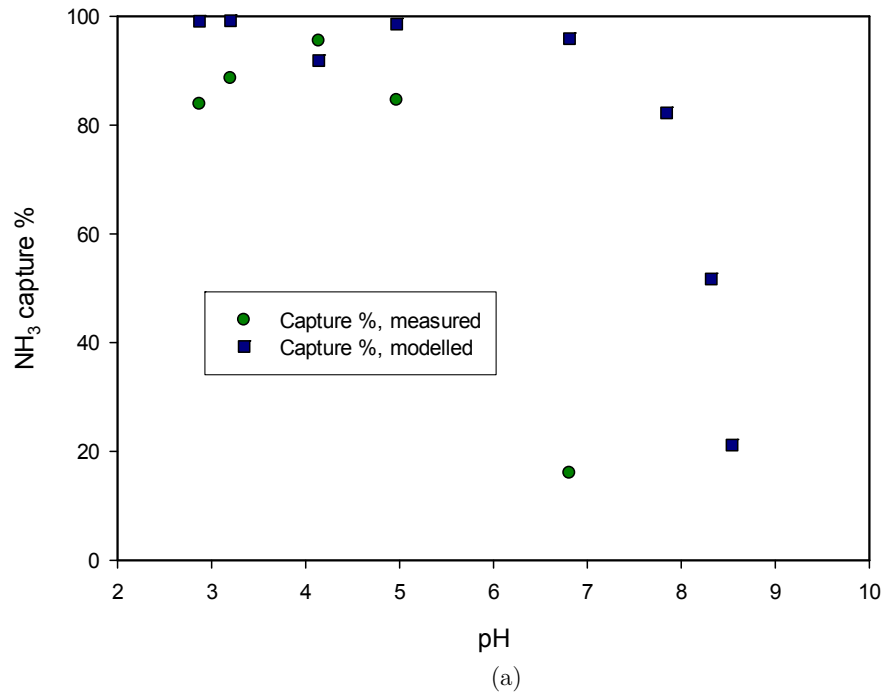


(a)

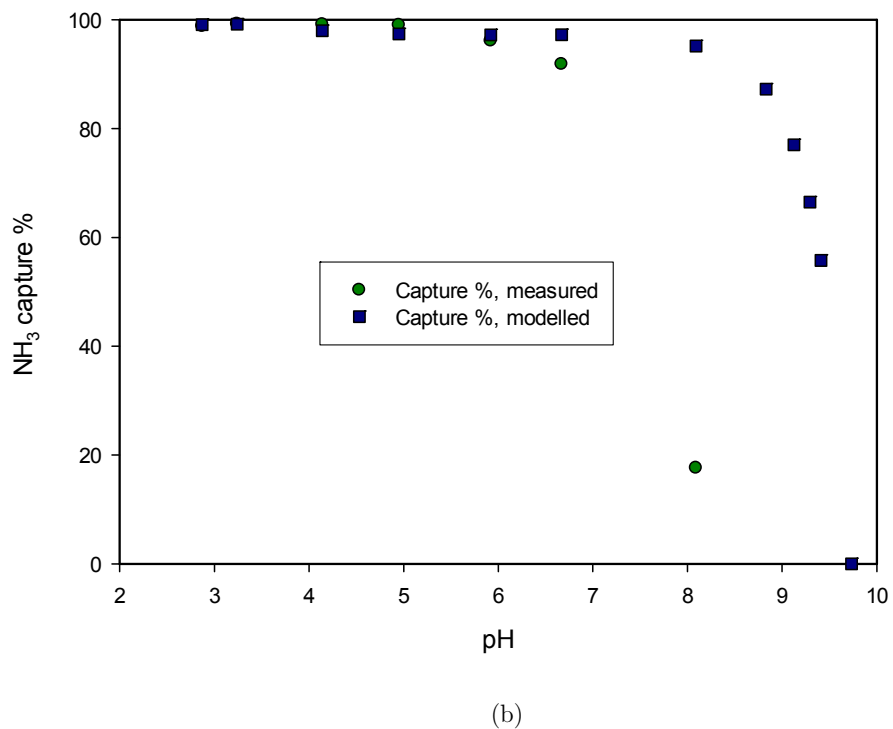


(b)

Figure 3.8. Ammonia gas phase concentration across the acid wash as compared to the modelling results at different pH values: experiments (a) without spiking, and (b) with spiking.



(a)



(b)

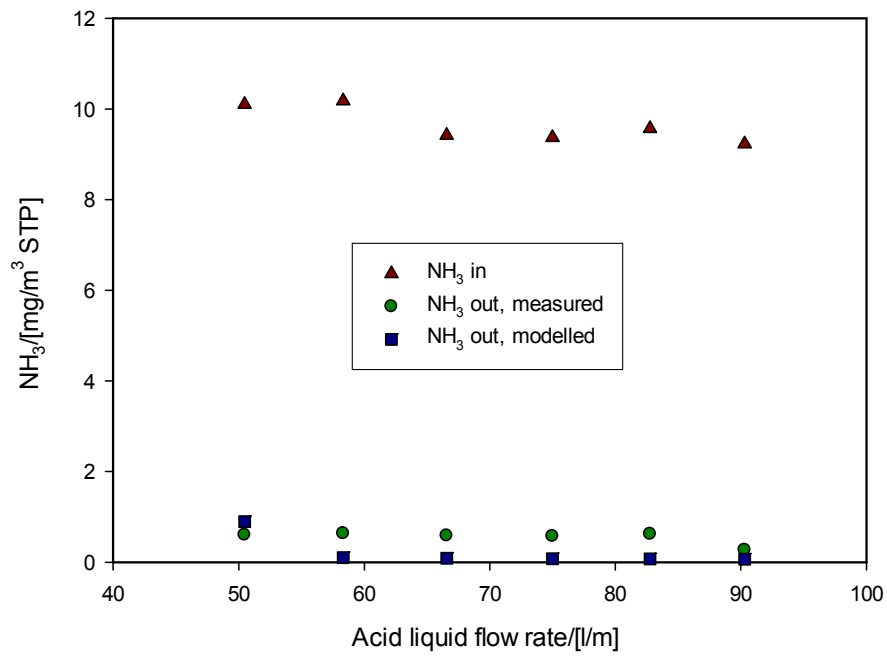
Figure 3.9. Ammonia capture percentage across the acid wash as compared to the modelling results at different pH values: experiments (a) without spiking and (b) with spiking.

Thus, to achieve the same capture efficiency at a higher pH and the same driving force, (i.e. ammonia gas phase concentration), a longer column is required. Further tests, such as increasing the height of the column and changing the flue gas flow rate should be done to understand the cause of the decrease in the efficiency of the absorption column and its internals at high pH values in such processes.

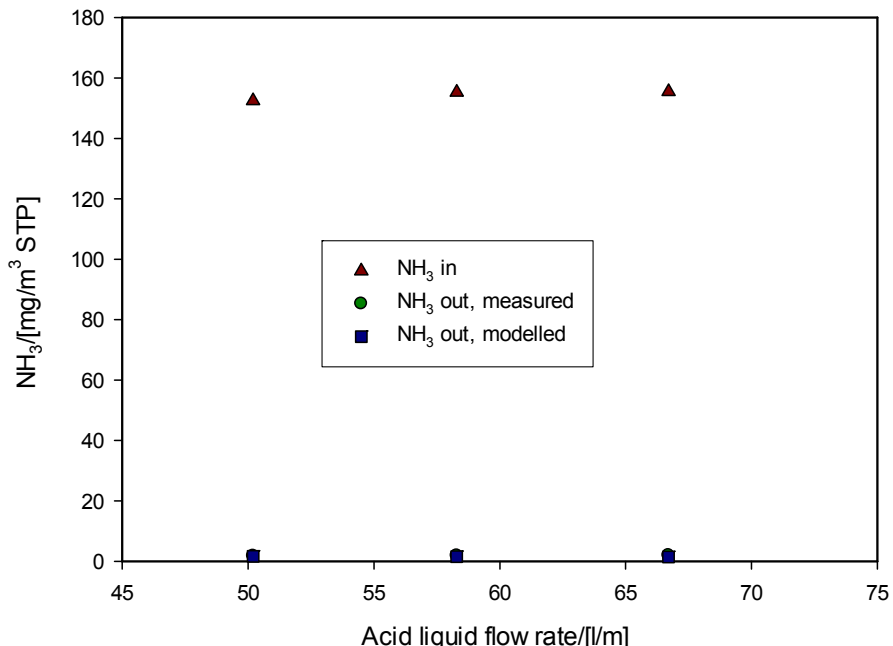
3.3.2.2 Effect of flow rate

In addition to pH, the absorption capacity also depends on the total volume of the liquid available. Moreover, changing the liquid flow rate also changes the gas to liquid ratio in the column which affects the absorption performance. Thus, the acid liquid flow rate was varied to test whether an increase in flow rate led to an increase in ammonia removal. The base setting of the flow rate of acid liquid was 75 l/m. The pH of the acid liquid was maintained at the base setting of pH 3.

Figure 3.10 shows the ammonia concentrations in to and out of the acid wash column for the tests with changing acid liquid flow rate. For experiments conducted without spiking of ammonia in the flue gas, the inlet ammonia concentration was in the range of 9-11 mg/m³ STP whereas for the experiments conducted with spiking, the inlet ammonia concentration varied from 152 to 155 mg/m³ STP. The acid wash reduced the ammonia concentration below 1 mg/m³ STP for all liquid flow rates, whereas for experiments with spiking, the outlet ammonia concentration remained below 2 mg/m³ STP. For both spiking and nonspiking experiments, the absolute outlet NH₃ concentrations at the outlet for the different flow rates were within the measurement error and can be considered to be the same. This implies that, even at the lowest flow rate of 50 l/m which is below the recommended flow rate for the liquid distributor, the acid wash is effective in the capture of ammonia. Thus, increasing the acid liquid flow rate does not lead to any further increase in the capture efficiency for the range of flow rates tested here. The model predicts this behaviour with good accuracy for all tests.



(a)



(b)

Figure 3.10. Ammonia gas phase concentration across the acid wash as compared to the modelling results at different flow rates: experiments (a) without spiking and (b) with spiking.

3.3.2.3 Effect of the temperature of the flue gas entering the acid wash column

The temperature of the gas is an important parameter for gas-liquid absorption. The thermodynamic equilibrium of a component and the rate of mass transfer are determined by the temperature of the system. The temperature of the flue gas entering the acid wash column was changed by changing the parameters of the water wash section in the absorption tower. The base setting for the flue gas leaving the water wash section was 40°C, to maintain the water balance in the CO₂ capture system. The pH of the acid liquid was maintained at the base setting of pH 3. For the parametric tests, the temperature of the flue gas entering the acid wash liquid was varied from 40 to 55°C. Figure 3.11 shows the ammonia concentrations in to and out of the acid wash when the temperature of the gas inlet to the acid wash column was changed. It must be noted that the temperature of the acid liquid was also increased in-line with that of the flue gas inlet to avoid condensation of the flue gas in the column.

For experiments conducted without spiking of ammonia in the flue gas, the inlet ammonia concentration was in the range of 11-14 mg/m³ STP, whereas one experiment was conducted with spiking at an ammonia concentration of 149 mg/m³ STP in the flue gas. The ammonia emissions levels after the acid wash were below 2 mg/m³ STP at all temperatures. The absolute values of ammonia emissions at the acid wash outlet are within the error of the measurement device. Therefore, no conclusions were drawn on the trends for the effect of flue gas temperature on the efficiency of the acid wash. Thus, the temperature appears to have no observable effect on the NH₃ capture efficiency. For this parametric test as well, the model predicts the outlet ammonia concentration with good accuracy.

Table 3.2 shows the amounts of ammonium ion measured in the solvent and water wash. The extents of ammonia dissolved in the solvent and the water wash appeared to be relatively constant in time. This is expected because ammonia generated by degradation is immediately stripped owing to its high volatility. Moreover, the gas phase ammonia concentration measured by FTIR spectroscopy after the water wash also appeared to be constant (~10-20 mg/m³ STP), as seen in Figure 3.7.

3.3.3 Parametric study for MEA

The gas phase concentration was measured by FTIR spectroscopy. Thus, during the parametric tests for ammonia removal by acid wash, information about the MEA emissions across the acid wash was also obtained. The inlet MEA concentration was in

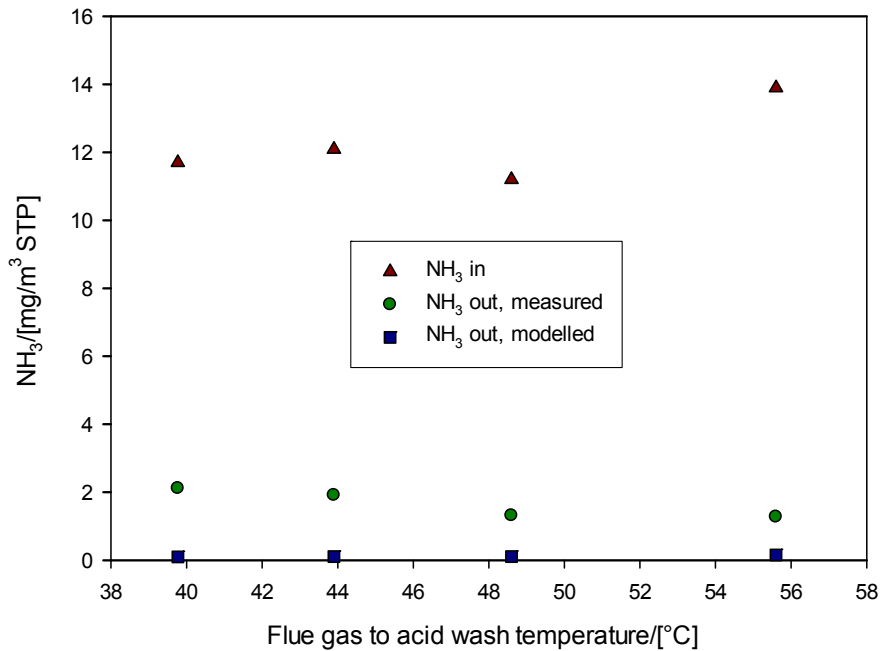


Figure 3.11. Effect of the temperature of the flue gas entering the acid wash column on NH₃ emissions across the acid wash without spiking. The experiment with spiking was performed at 44°C with an inlet concentration of 149 mg/m³ STP. The measured outlet concentration was 1.8 mg/m³ STP whereas the model predicted it to be 1.3 mg/m³ STP.

Table 3.2. Ammonia concentration in the solvent and water wash.

Matrix	Operating time (h)	NH ₃ (µg/ml)
Solvent	88.7	64.5
	432	54.8
	936	54.8
Water wash	88.7	25.5
	432	20.9
	936	13.2

the range of 1.2 to 26.8 mg/m³ STP, but was generally below 10 mg/m³ STP. MEA was found to be strongly captured in all of the parametric tests with variations within the uncertainty of the FTIR analysis. The results (given in Figures S1-S3 of the Appendix) indicate that the acid wash is capable of lowering the MEA emissions to 1-3 mg/m³ STP, mostly below 1 mg/m³ STP.

Table 3.3. Dimensions of the scaled-up acid wash column for a full scale CO₂ capture plant.

Column diameter (m)	14.4
Packing height (m)	1.26
Column length (m)	4.7
Packing type	Sulzer Mellapak 250Y

Table 3.4. Preliminary cost estimate for an acid wash column per absorption train in a full scale CO₂ capture plant. The costs have been adjusted as per the CEPC Index for 2008=560.9 and CEPC Index for 2012=584.6.

Item	Purchased cost (k€ @2012)
Vessel cost (Material:SS 304)	950
Packing: Sulzer Mellapak 250Y	300
Total	1250

3.4 Scale up and cost estimation of an acid wash for a full scale CO₂ capture plant

The acid wash system tested at TNO's CO₂ capture plant at Maasvlakte, The Netherlands, was scaled up to a CO₂ capture plant attached to an Advanced Supercritical (ASC) Pulverized Fuel (PF) bituminous coal-fired power plant as described in the European Benchmarking Task Force (EBTF) guideline document in the EU project, CESAR¹²⁵. First, the scale up of the acid wash on the basis of the pilot plant results presented in this study are discussed. Subsequently, the purchased equipment cost of the scaled-up acid wash is estimated based on the methodology described in the EBTF guidelines.

3.4.1 Sizing of full scale acid wash

The CO₂ capture plant utilizes all the flue gas from an 800 MW_e ASC PF power plant. The CO₂ capture plant uses MEA (30 wt.%) as the solvent. Because of the large amount of gas to be treated, three absorber trains were considered. The acid wash scrubber was installed downstream of the water wash for each absorber train. The column dimensions and packing type were as mentioned in Table 3.3.

The diameter of the acid wash was kept the same as the diameter of the CO₂ capture absorber at 14.4 m because the additional acid wash section can be installed on the same absorption tower. The height of the scaled-up acid wash column was kept the same as the one used in the pilot plant. The column height was determined based on the desired separation efficiency. Because the column height used in the pilot plant tests proved to be sufficient for the required ammonia removal, it was expected that the separation efficiency would also be maintained for the larger scale. The packing used in

the pilot plant tests was Sulzer Mellapak 250Y, and the same packing was considered for the scaled-up acid wash column.

3.4.2 Cost estimation

A preliminary cost calculation is presented based on the sum of the vessel and packing costs. Based on an in-house economic estimation tool that includes information from vendors and suppliers regarding material of construction and limitations in equipment size and capacity, the resulting acid wash column cost is shown in Table 3.4. The material of construction was chosen to be stainless steel 304.

The purchased equipment cost for the acid wash for a single absorption column with the packing material was estimated to be ca. €1.25 million. Thus, for three absorption trains the purchased equipment cost for all of the acid washes would be €3.75 million. This should be added to the list of equipment for the capture plant to give the final cost, including those for installation, commissioning, piping and instrumentation, and so on. In general, absorption columns are expensive pieces of equipment. For comparison, the purchased equipment costs for the three absorption trains and the entire capture plant is ca. €18.4 million and €75 million euros, respectively. It is important to note that the costs were adjusted from 2008, as given in the EBTF document, to 2012. The acid and the waste produced from the acid wash scrubber add to the operating cost of the capture plant. However, the cost of an acid such as sulphuric acid is very low, and with an appropriate operation strategy, the waste generated can be kept to a minimum. Thus, the operating cost can be neglected in comparison to the purchased equipment cost.

3.5 Conclusions

Acid wash scrubbing is a well-known countermeasure for ammonia emissions from industrial gas streams. The tests performed in this work have shown that an acid wash system is a simple and robust countermeasure for reducing ammonia emissions from a Post Combustion CO₂ capture plant. The acid wash scrubber did not influence the operation of the CO₂ capture plant. Parametric tests were performed to test the efficiency of the acid wash by means of changing the acid liquid pH, the acid liquid flow rate and the temperature of the flue gas temperature entering the acid wash. The parametric tests were also performed with spiked ammonia concentrations of ca. 150 mg/m³ STP to test the operation of the acid wash in the case of a highly degraded solvent. The base setting for the acid liquid of pH 3 and a flow rate of 75 l/m was effective in removing ammonia emissions to below 5 mg/m³ STP, even under extreme ammonia gas phase concentrations of 150 mg/m³ STP. The parametric studies indicated that an acid wash can be operated at higher pH values such as 5-6. However, the ammonia capture efficiency reduces at higher pH, due to the increase in the liquid side mass transfer resistance. An acid wash is highly effective in removing MEA emissions from the gas phase and the MEA emissions after the acid wash were mostly

below 3 mg/m³ STP. Because the measured MEA concentrations after the acid wash were so low, no clear relation between operating conditions and MEA removal efficiency was seen. Therefore, the acid wash was confirmed to be effective in reducing ammonia emissions below the expected environmental limit of 5 mg/m³ STP. It is recommended that additional parametric tests be performed at higher pH, such as 5-6, to evaluate the effects of the different operating parameters such as acid liquid flow rate, flue gas flow rate, and flue gas temperature.

It is expected that the purchased equipment cost of an acid wash scrubber for a full scale CO₂ capture plant would be ca. €3.75 million which would increases the total purchased equipment cost by 5 %. Moreover, the operating costs would be negligible, and therefore, the acid wash can be considered to be an economically viable technology for reducing ammonia emissions from a CO₂ capture plant. The final application of an acid wash system in a full scale CO₂ capture plant must be determined based on several factors including expected emissions, environmental permits, alternative technologies, available space, and project costs.

Chapter 4

Investigation of aerosol-based emissions of MEA due to sulphuric acid aerosol and soot in a post combustion CO₂ capture process.

This chapter is based on the following publication:

Khakharia, P., Brachert, L., Mertens, J., Huizinga, A., Schallert, B., Schaber, K., Vlugt, T.J.H., Goetheer, E., Investigation of aerosol based emission of MEA due to sulphuric acid aerosol and soot in a Post Combustion CO₂ capture process, *Int. J. Greenh. Gas Control*, 19, 138–144, 2013.

4.1 Introduction

Monoethanolamine (MEA, 30 wt.% aqueous solution) based CO₂ absorption can be considered as state of the art technology for a PCCC plant ^{79,126,127}. The main disadvantage of such a process is the substantial energy demand and the subsequent reduction in the power plant efficiency by about 11 percentage points ¹²⁸. Besides this large energy penalty, there has been a growing concern about emissions, especially of solvent ⁶⁹. The loss of solvent leads to higher operating costs as well as affects the environment in and around the area of the PCCC plant ¹²⁹.

Volatility of amines has been studied extensively and is well understood under laboratory conditions ^{66,88,130–133}. As an example, volatility of 30 wt. % aqueous MEA at 40°C and a lean loading of 0.25 mol CO₂/mol amine is 54 ppm (~147 mg/m³ STP) (STP; 0°C and 101.325 kPa) ⁶⁶. This is still high as compared to the design criteria of ca. 12 mg/m³ STP in the treated flue gas of a PCCC plant ¹³⁴. Thus, in practice a water wash is used at pilot plant scale to minimise these emissions. Water wash, is a packed bed with a pump around of water to condense and solubilise volatile MEA in order to minimise its emissions. In a typical PCCC pilot plant, MEA emissions in the order of 1.4 mg/m³ STP in the CO₂ free flue gas stream are expected ⁷¹. Moreover, very high MEA emissions have been observed from field tests ^{72,135}. These high amine emissions have been attributed to aerosol formation in the absorber section of pilot plants that could not be removed by conventional emission counter-measures such as a water wash and demisters.

It has been reported that SO₃ present in the flue gas can cause aerosol formation in an absorption based capture process ⁷⁴. SO₃ is known to be present in the flue gases upon combustion of sulphur containing fuel (e.g. in coal fired power plants). Along with SO₃ formation in the boiler, it is formed mainly in the Selective Catalytic Reduction (SCR) unit of the flue gas treatment train by oxidation of SO₂ present in the flue gas ¹³⁶. This SO₃ will be present in the flue gas as sulphuric acid (H₂SO₄) due to the water vapour present in the gas phase. Wet Flue Gas Desulphurization (FGD) is a common technology to remove SO_x from gas phase prior to its emission. However, the gas phase H₂SO₄ condenses in a FGD as it crosses its dew point and thus, leads to formation of sulphuric acid aerosols. Moreover, flue gas contains other particulate matter (PM) such as soot, fly ash, etc. as a result of coal combustion. These H₂SO₄ aerosols along with other particulate matter present in the flue gas can act as nuclei for further aerosol formation and growth in the absorber column of a PCCC plant.

The aim of this research work was to study the influence of particles/nuclei in the form of soot and H₂SO₄ aerosols on solvent (here: MEA) emissions from a typical absorption-desorption based CO₂ capture process. A clear relation of particulate matter on amine emissions has been observed. Moreover, for the first time a quantitative understanding of the effect of particles in flue gas on amine emissions for a typical PCCC plant has been realized.

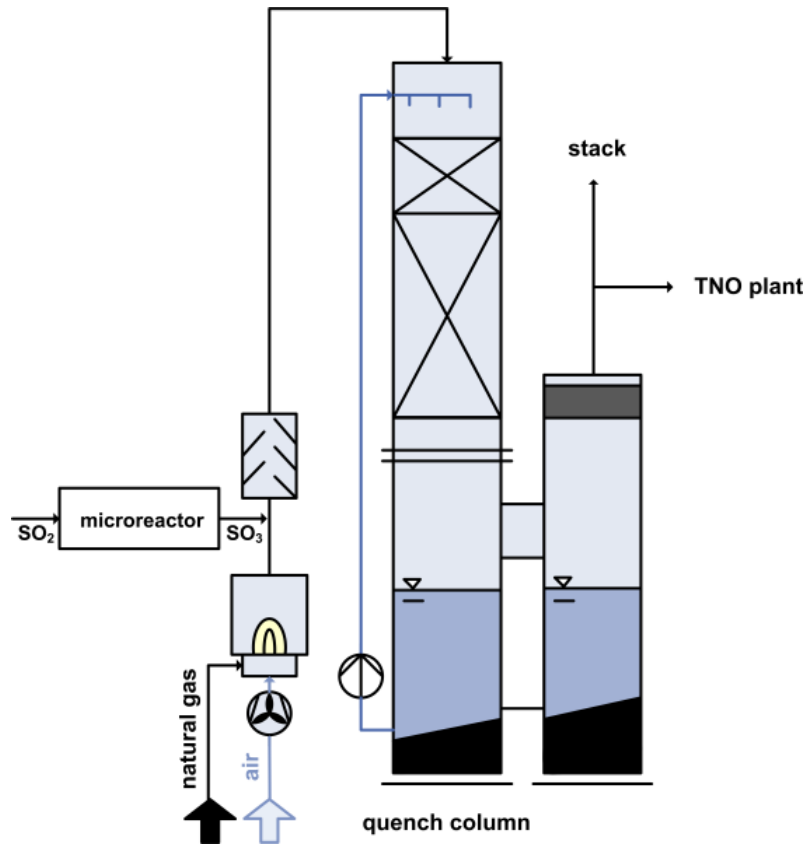


Figure 4.1 Schematic representation of the pilot plant for sulphuric acid aerosol generation at Karlsruhe Institute of Technology. SO_2 is converted into SO_3 in a microreactor and added to the hot flue gas ($\sim 220^\circ\text{C}$) generated from natural gas combustion which leads to H_2SO_4 aerosol formation in the quench column as a result of co-current cooling by water to the adiabatic saturation temperature of $\sim 46^\circ\text{C}$. A slip stream of this aerosol containing flue gas is used for the CO_2 capture mini-plant.

4.2 Test equipment

4.2.1 Aerosol generator setup

For the generation of flue gas containing nuclei, the pilot plant at the Institute for Technical Thermodynamics and Refrigeration, Karlsruhe Institute of Technology (Figure 4.1) has been used. This pilot plant has been extensively described in literature¹³⁷. The pilot plant has been used to simulate a FGD and understand H_2SO_4 aerosol formation. Moreover, the pilot plant has been used to understand heterogeneous nucleation mechanism using other components such as HCl ¹³⁸. Natural gas is burned in order to provide a flue gas volume flow of $\sim 180 \text{ m}^3 \text{ STP/h}$. The particle concentration due to incomplete burning can be varied between 10^4 and 10^6 per cm^3 by changing the burning mode (earlier/later addition of air). SO_3 is generated by the catalytic oxidation of SO_2 in a microstructured reactor¹³⁹. This SO_3 is added to the flue gas, where it is completely converted into H_2SO_4 vapour by combining with water vapour from combustion¹⁴⁰. The generated flue gas is rapidly cooled down with water from 220°C to the adiabatic saturation temperature ($\sim 46^\circ\text{C}$) in a co-current modus in a quench tower.

The column has a 300 mm diameter and a packing height of 1.5 m filled with Hiflow-rings (type 20-4 and 25-7). The liquid load of the column is $42 \text{ m}^3/(\text{m}^2\text{h})$. The rapid cooling of the flue gas and the phase equilibrium of the binary system, sulphuric acid – water, leads to high supersaturations and as a consequence to homogeneous nucleation. This leads to aerosols with number concentrations in the order of 10^8 per cm^3 and sizes well below 100 nm^{141,142}. At the outlet of the quench, a split stream has been used as a flue gas source to the CO₂ capture mini-plant. A T-connection enables the simultaneous measurement of the aerosol number concentration by means of a condensation particle counter (UFCPC, Palas).

4.2.2 CO₂ Capture plant

TNO's mobile carbon capture mini-plant is a fully automated conventional absorption-desorption system with a capacity of 4 m³ STP/h of flue gas. The absorber section is a packed bed (Sulzer Mellapak 2X) totally 3.5 m high with 4 packed beds each of 0.5 m and a diameter of 4.5 cm. In this configuration, the absorber section was equipped neither with a water wash section nor a demister. The stripper section has the same dimension as the absorber. The total liquid inventory of the system is ca. 20 litres. Additional CO₂ was added to the stream entering CO₂ capture mini-plant to obtain CO₂ concentrations in the range of 0.7 to 13 vol.%.

Typically, the CO₂ concentration in the flue gas was adjusted to ca. 12 vol.% to mimic power plant flue gas conditions. TNO's mobile CO₂ capture mini-plant along with the aerosol generator at the test location is shown in Figure 4.2. Further information regarding the main principles of a conventional absorption-desorption based CO₂ capture process can be found in literature^{126,143}.

4.2.3 FTIR (Fourier Transform InfraRed)

A FTIR analyser (GASMET CX 4000) was used to analyse the gas phase. This has been described in section 3.2.2. The concentration of MEA measured by FTIR is the sum of vapour phase MEA and MEA present in the aerosols⁶⁹.

4.2.4 CPC (Condensation Particle Counter) and dilution system

The particle number concentration was measured by a Condensation Particle Counter (CPC; PALAS UFCPC with sensor 200). In the CPC, the particles are enlarged by means of condensation of a working fluid (here: 1-Butanol) which are subsequently large enough to be detected optically. The saturation temperature used was 42°C with a condensation temperature to 12°C (default factory settings). The aerosol has to be diluted before being measured because the number concentration is too high for the CPC. The dilution with a factor of 10^4 has been realized with the PALAS dilution cascade DC 10000. The accuracy of this device is $\pm 5\%$. Further information about its working principle and other features can be found in literature¹⁴⁴.

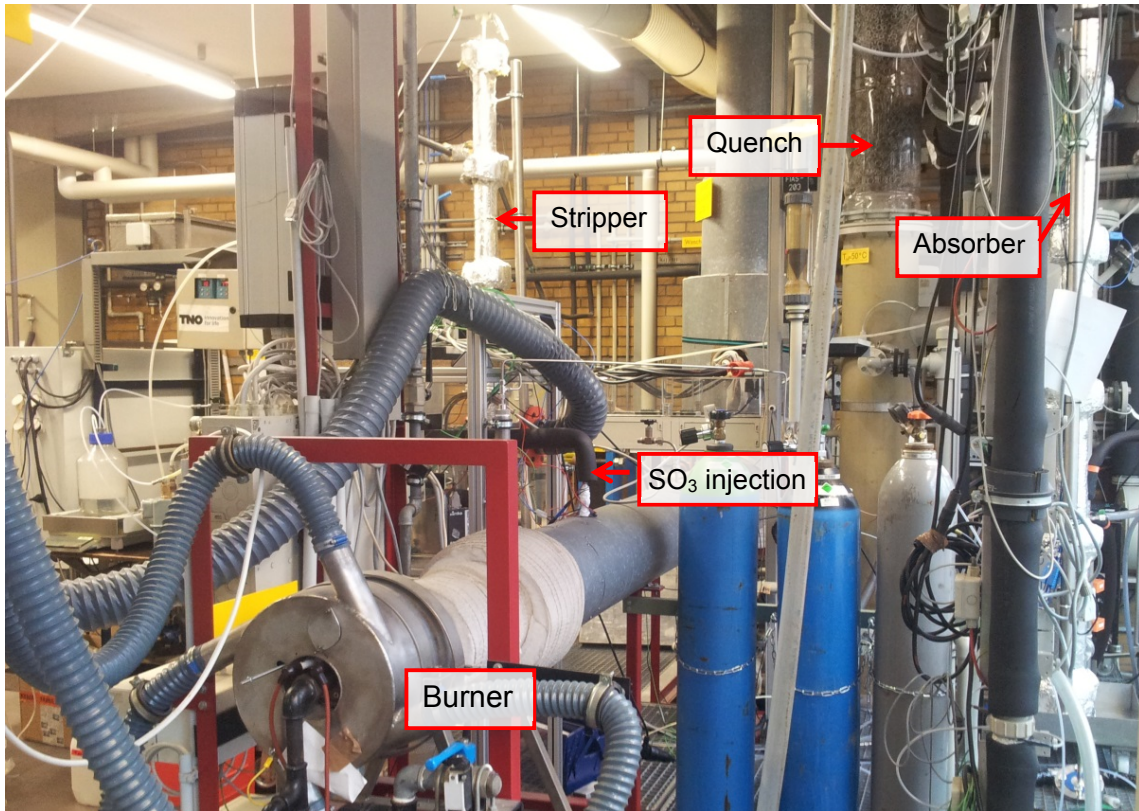


Figure 4.2. Test set up including TNO's mobile CO₂ capture mini-plant and aerosol generator located at Karlsruhe Institute of Technology. In this figure; the burner which produces the flue gas by natural gas combustion, SO₃ injection point from the microreactor to the flue gas; quench column which causes H₂SO₄ aerosol formation and the CO₂ capture mini-plant's absorber and stripper can be seen.

Table 4.1. Typical operating conditions of the CO₂ capture mini-plant. These conditions are representative of a typical PCCC plant.

Lean pH	9.8 (± 0.2)
Rich pH	8.9 (± 0.2)
MEA lean solvent concentration	4.9 mol/L (± 0.2 mol/L)
Stripper temperature (bottom)	120°C (± 0.5 °C)
Stripper pressure (top)	1.8 bar (± 0.05 bar)

Table 4.2. Flue gas composition to the absorber of CO₂ capture mini-plant.

CO ₂	12.8 vol. % (± 0.2 vol. %)
O ₂	14.6 vol. % (± 0.5 vol. %)
CO	43.5 mg/m ³ STP (± 1 mg/m ³ STP)

4.3 Results and discussion

4.3.1 Typical CO₂ capture plant operating conditions

The CO₂ capture mini-plant was operated on a stable and continuous basis (absorption and desorption cycles) in order to maintain constant conditions in the absorption column. Typical operating conditions of the capture plant are shown in

Table 4.1. The stripper was operated such that the lean pH was maintained at 9.8 (± 0.2). Typical lean and rich loadings were 0.18 and 0.49 mol CO₂/mol amine, respectively.

The CO₂ content of the flue gas from the natural gas burner was ca. 0.7 vol.%. Additional CO₂ was added using a CO₂ gas bottle to simulate flue gas composition from a power plant. The flue gas composition without solvent circulation as measured by FTIR (without any correction) at the absorber outlet is as shown in Table 4.2. This corresponds to the normal burning mode of the aerosol generator setup.

The typical temperature profile in the absorber is as shown in Figure 4.3. The temperature maximum in a typical CO₂ absorption process occurs at the upper half of the column since the maximum amount of CO₂ is absorbed in that region. Further upwards in the column, the temperature reduces owing to the cooling by the relatively cold lean solvent. The exact temperature profile depends on several factors such as liquid to gas ratio, CO₂ content in the flue gas, lean loading, etc.^{126,143}.

The temperature of the flue gas to the CO₂ capture plant was maintained at 50°C ($\pm 2^\circ\text{C}$) using a heated line to maintain the same temperature as the flue gas from the aerosol generator setup. The lean solvent temperature was maintained at 39°C ($\pm 2^\circ\text{C}$). The corresponding gas temperature at the absorber outlet is ca. 38°C ($\pm 2^\circ\text{C}$). A baseline study was performed to quantify the emissions in absence of soot and H₂SO₄ aerosol droplets. The conditions for this test were as shown as in Table 4.3. A mixture of ambient air with CO₂ (up to 12.1 vol.%) was used. The corresponding MEA emission was ca. 45 mg/m³ STP, which can be considered as a baseline for comparison in this study. The entire test setup was operated as stable as possible. Nevertheless, certain variations are unavoidable on a day-to-day basis and thus, the corresponding emission and particle number concentrations mentioned here must not be considered as absolute, but within an accuracy of ca. 10 %.

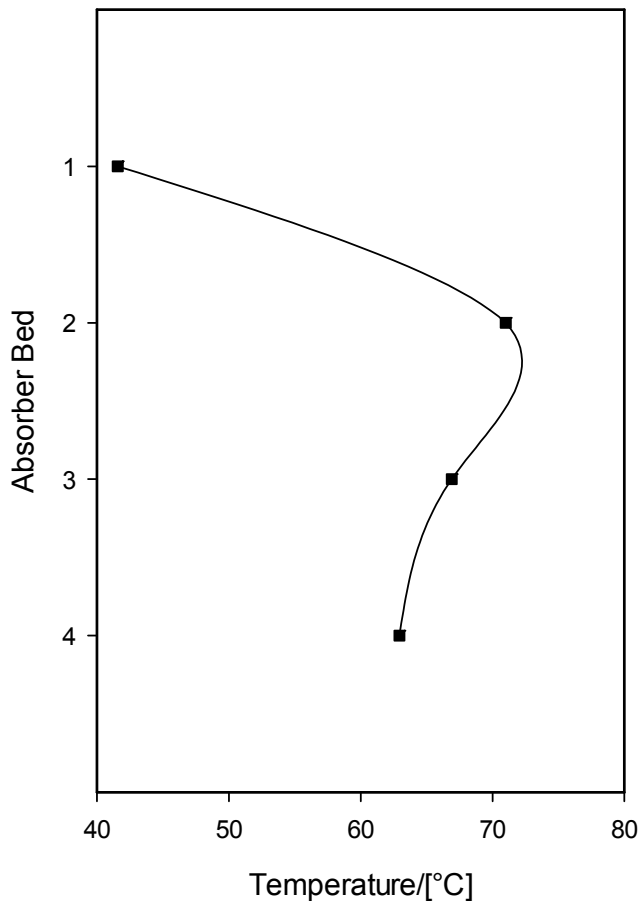


Figure 4.3. Typical temperature profile in the CO₂ capture absorption column. Absorber Bed 1 is the TOP while Absorber Bed 4 is the BOTTOM. (■) indicate actual temperature measurement points. The line is a guide to the eye.

Table 4.3. Operating conditions for the CO₂ capture mini-plant for the baseline study. Corresponding baseline MEA emission is ca. 45 mg/m³ STP.

Lean pH	9.9
Absorber outlet temperature	34°C
CO ₂ in flue gas	12.1 vol.%
CO ₂ in treated gas	2.5 vol.%
Lean loading	0.21 mol CO ₂ /mol amine
MEA emission	~45 mg/m ³ STP

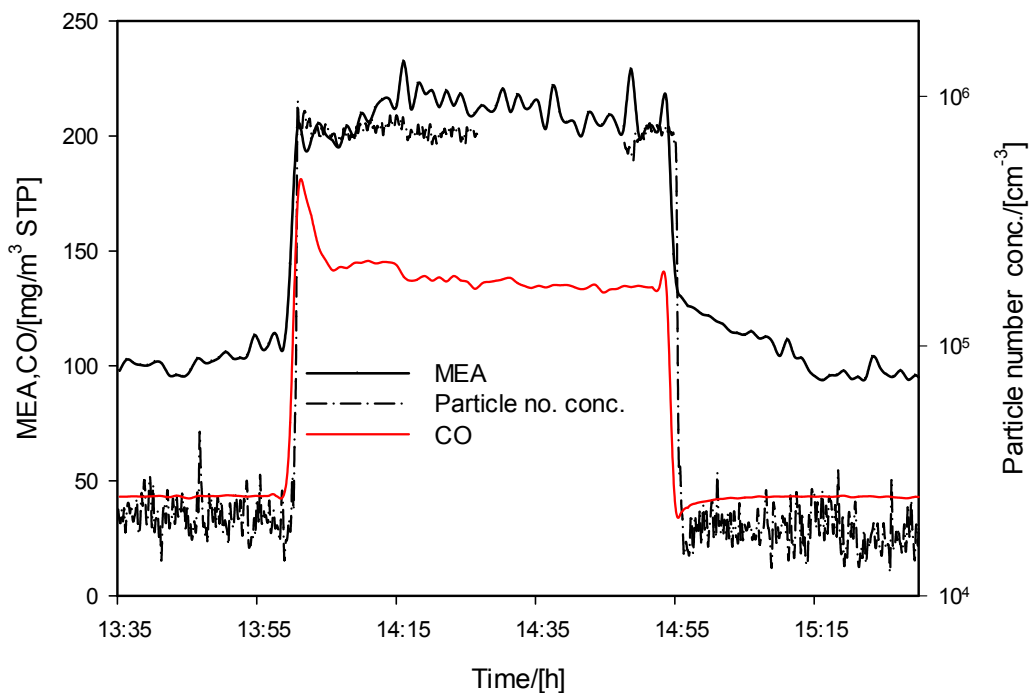


Figure 4.4. Effect of particle number concentration of soot on MEA emissions. CPC which measures the particle number concentration was not connected for short intervals and thus, there are no measurement data points for this time interval. The horizontal axis represents the time of the day in hours during which the experiment was performed.

4.3.2 Effect of Soot

The soot is produced from the combustion of domestic natural gas by using excess air (CH_4 : Air $\approx 1: 155$ (volume/volume)). The mixing point of air and fuel can be changed which alters the combustion efficiency and thus, higher amount of soot can be generated. As shown in

Figure 4.4, MEA emission increases strongly and instantaneously as soon as the burning mode is changed. The change in burning mode can also be observed by the increase in CO concentration.

MEA emissions are increased to ca. $100 \text{ mg/m}^3 \text{ STP}$ due to the low soot concentration in the aerosol generator flue gas, which is more than twice the baseline emissions of $45 \text{ mg/m}^3 \text{ STP}$. During high soot combustion mode, the particle number concentration increased two orders of magnitude from 10^4 to 10^6 per cm^3 while, the corresponding MEA emission increased from ca. 100 to $200 \text{ mg/m}^3 \text{ STP}$ as observed in Figure 4.4. This behaviour is reversible and instantaneous. When decreasing the particle numbers by changing to low soot combustion mode, the MEA emissions decrease back to $100 \text{ mg/m}^3 \text{ STP}$.

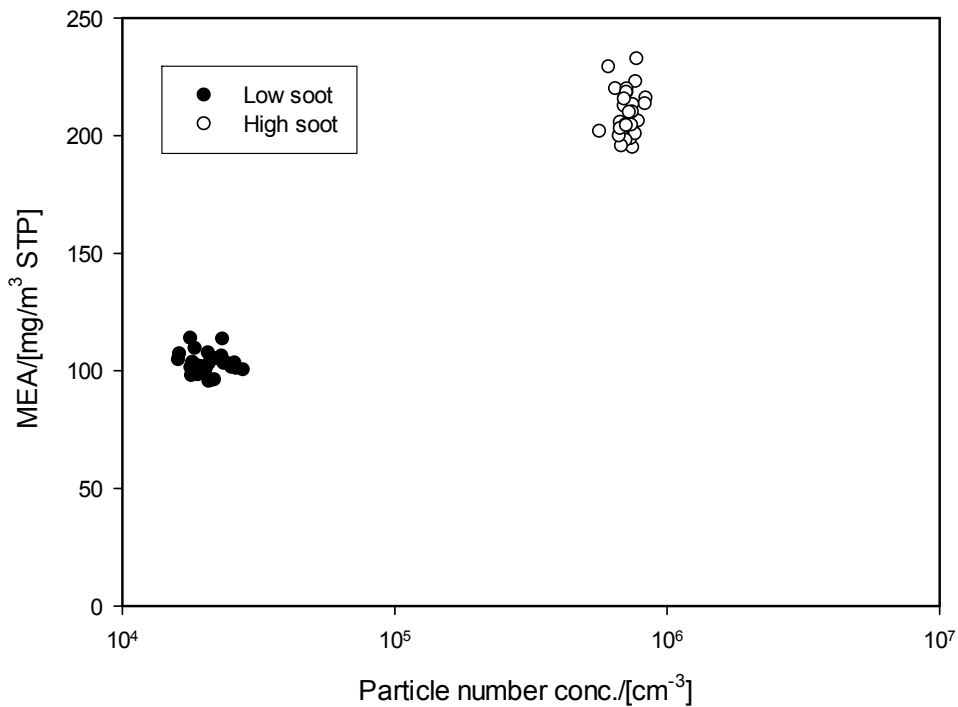


Figure 4.5. Effect of change in particle number concentration of soot particles in flue gas on MEA emissions.

Table 4.4. Average particle number concentration measured at different H_2SO_4 aerosol concentrations in flue gas as measured by the CPC. These measurements represent the average of the measured particle number concentration on-line during the experiments.

Levels	Average particle number conc. (cm^{-3})
Low	$1.02 \cdot 10^8$
Middle	$1.18 \cdot 10^8$
High	$1.42 \cdot 10^8$

As can be observed in Figure 4.5, the MEA emission almost doubles when the particle number concentration increases about two orders of magnitude. This observation clearly shows the influence of the change in particle number concentration, in this case soot, on MEA emissions. It is important to note, that the general combustion mode for the burner of this aerosol generator is the low soot mode.

4.3.3 Effect of H_2SO_4 aerosols

Adding SO_3 to the flue gas and subsequent homogeneous nucleation in the 1st stage quench produces sulphuric acid aerosols. Varying the added amounts of SO_3 to the flue gas changes the concentration of H_2SO_4 aerosol. The particle number concentration of the H_2SO_4 aerosol is in the order of $10^7\text{-}10^8$ per cm^3 . Wix et. al., were able to model the

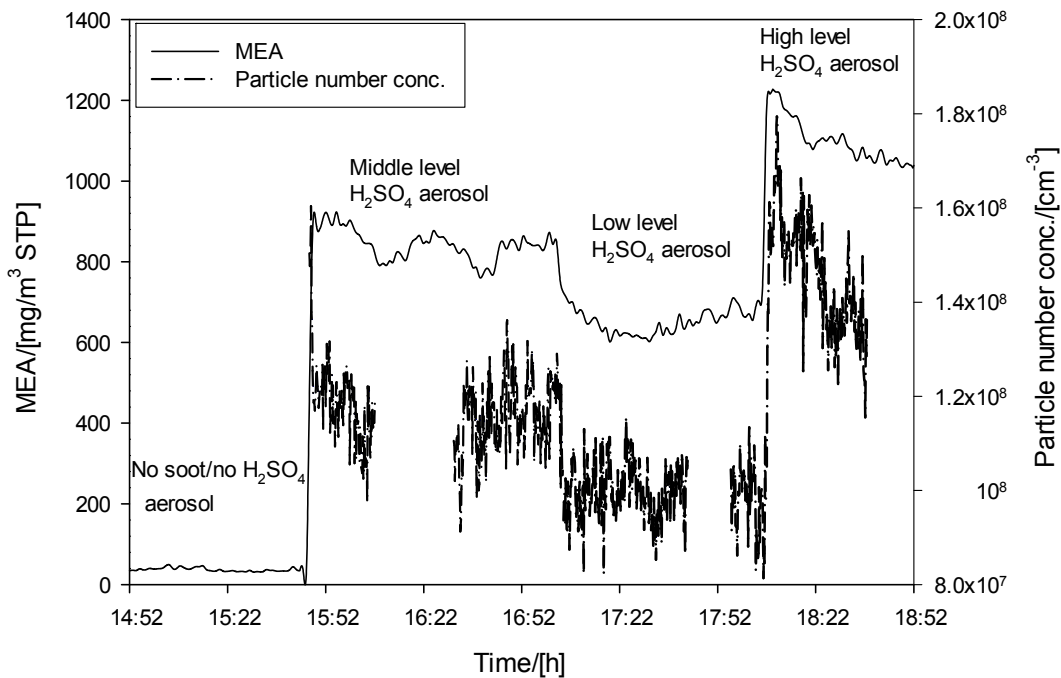


Figure 4.6. Effect of change in H_2SO_4 aerosol concentration in flue gas ($\text{CO}_2 \sim 12.8$ vol.%) on absorber MEA emissions at low soot conditions. CPC which measures the particle number concentration was not connected for short intervals and thus, there are no measurement data points for this time interval. The horizontal axis represents the time of the day in hours during which the experiment was performed.

relationship of size with the H_2SO_4 aerosol droplet concentration using an in-house simulation tool¹⁴². They found that the particle number concentration is within the same order of magnitude for all different H_2SO_4 concentrations but, the aerosol sizes are larger at higher concentrations. It has been confirmed by latest experimental results that the number concentration remains in the same order of magnitude throughout the entire tested concentration range¹⁴¹. As mentioned in section 4.2.1, the particle sizes are below 100 nm for the range of sulphuric acid concentrations tested in this work.

In a typical experiment, three different H_2SO_4 aerosol concentrations were used by changing the SO_2 concentration in the microreactor. The exact H_2SO_4 concentration entering the absorber column depends on several factors such as length of gas inlet line, gas velocity etc. and thus, cannot be accurately measured. Therefore, the different concentrations are described as ‘levels’. The particle number concentrations for the different amount of H_2SO_4 aerosol levels are shown in Table 4.4. The mass concentration of H_2SO_4 expected from the aerosol generator is in the range of 1-5 mg/m^3 STP. SO_3 concentration at the outlet of Wet FGD (just before the stack) has been reported to be ca. 0.3 ppmv ($\sim 1 \text{ mg}/\text{m}^3$ STP of SO_3) from coal-fired utility boilers¹⁴⁵. However, the typical stack SO_3 concentration in power plants can vary significantly based on several factors for which additional information can be obtained in literature¹³⁶.

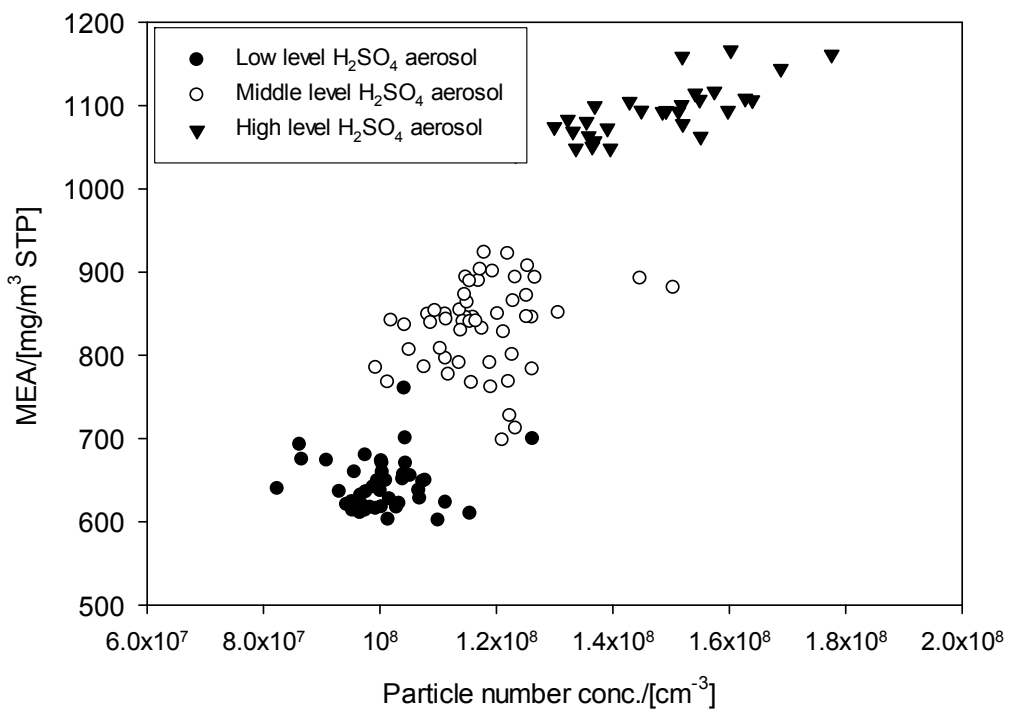


Figure 4.7. Effect of different H₂SO₄ aerosol number concentrations in flue gas on MEA emissions. (●) represents the low level H₂SO₄ aerosol concentration with average particle number concentration of $1.02 \cdot 10^8$ per cm³, (○) represents the middle level H₂SO₄ aerosol concentration with average particle number concentration of $1.18 \cdot 10^8$ per cm³ and (▼) represents the high level H₂SO₄ aerosol concentration with average particle number concentration of $1.42 \cdot 10^8$ per cm³.

Figure 4.6 shows the MEA emissions when the H₂SO₄ concentration in the gas phase was changed over time. As compared to the baseline emissions i.e. flue gas without H₂SO₄ aerosol droplets, the MEA emission increases substantially from 45 mg/m³ STP to 600-1100 mg/m³ STP depending on the amount of H₂SO₄. Moreover, the effect of aerosols and subsequent change in particle number concentration is instantaneous on MEA emissions.

As shown in Figure 4.7, there is a clear correlation of MEA emissions with the change in H₂SO₄ aerosol number concentration. The MEA emission doubles from about 600 to 1100 mg/m³ STP while the particle number concentration increases by 1.6 times. It must be noted that the MEA emissions from this capture unit would not be exactly the same as compared to a large scale capture facility as the absolute emissions strongly depends on the flue gas quality of the power plant, configuration and operating conditions of the CO₂ capture plant such as direct contact cooler, water wash section, lean pH and absorber temperature profile.

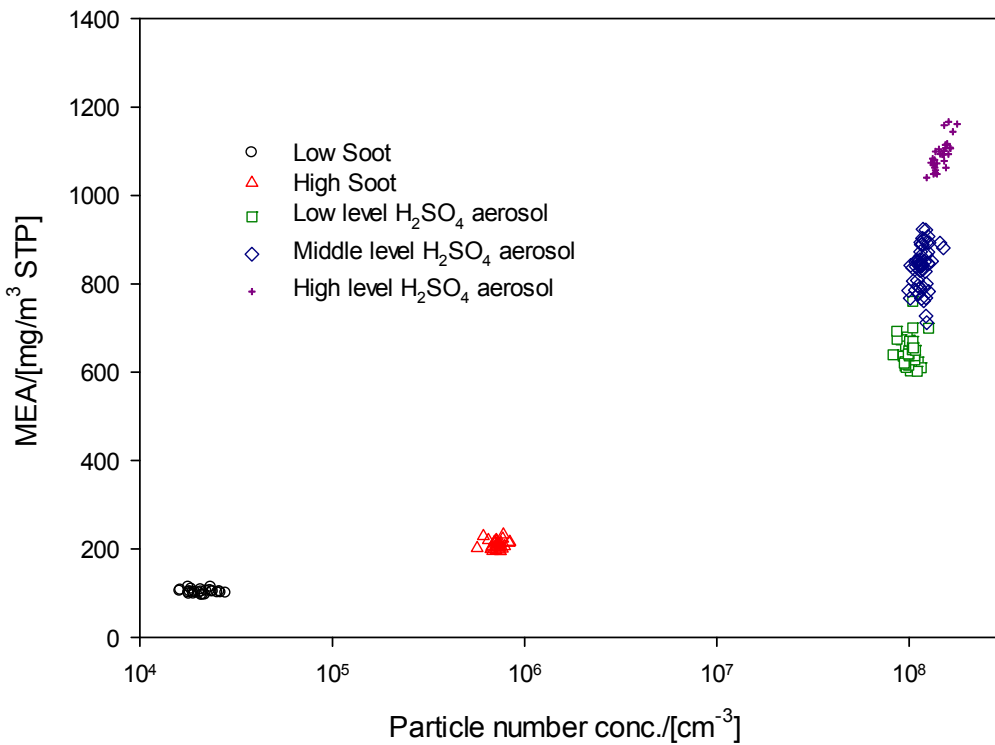


Figure 4.8. MEA emissions as function of particle number concentration of soot and H_2SO_4 aerosols in flue gas.

4.3.4 Effect of particle number concentration on MEA emission

The effect of particle number concentration on MEA emissions is summarised in Figure 4.8. The soot particle number concentration ranges from 10^4 - 10^6 per cm^3 while, H_2SO_4 aerosol particle number concentration is in the range of 10^8 per cm^3 . The MEA emission doubles from about 100 to 200 mg/m^3 STP when the particle concentration increases 34 times from low soot to high soot. The MEA emission increases only five times from about 200 to 1100 mg/m^3 STP when, the particle number concentration increases by a factor of 200 from high soot to high sulphuric acid aerosol level. Thus, it seems that the effect of particle number concentration of soot on MEA emissions is relatively more than sulphuric acid aerosols. However, a fair comparison between the types of particles (soot and H_2SO_4 aerosol) can only be made at similar particle number concentrations.

4.3.5 Effect of capture plant parameters on MEA emissions

The extent of emissions strongly depends on the capture plant parameters and in particular, on the operating conditions in the absorber column. Factors such as temperature profile, CO_2 gas phase concentration and lean pH also provides an insight into the mechanism of aerosol formation in the absorber.

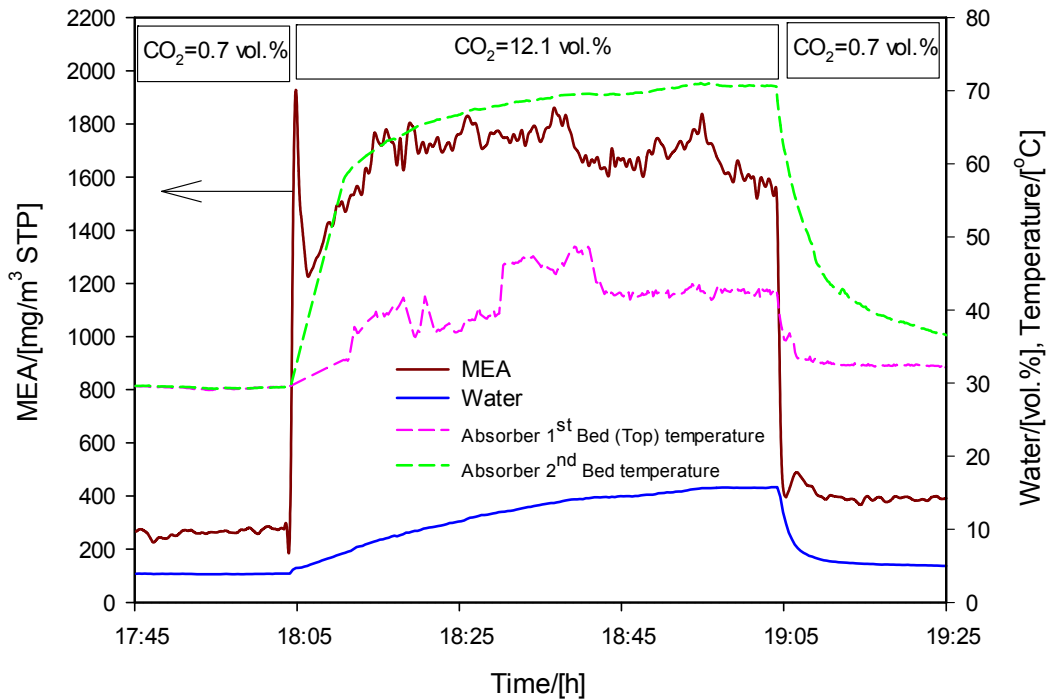


Figure 4.9. Effect of the flue gas CO₂ content and absorber temperature profile on MEA emission at a constant H₂SO₄ aerosol level (middle level). The horizontal axis represents the time of the day in hours during which the experiment was performed.

In a further experiment, the CO₂ content of the flue gas was varied, while the H₂SO₄ aerosol concentration in the flue gas was maintained constant at the middle level. As can be observed in Figure 4.9, at the start of the experiment MEA emissions of ca. 220 mg/m³ STP were measured wherein the flue gas contained H₂SO₄ aerosol without additional CO₂ (only 0.7 vol.% CO₂ from aerosol generator). The absorber column was also at ambient temperature (~30°C) as there was only a minor reaction of CO₂ and MEA. Then, the CO₂ flow was increased to a total CO₂ content of 12.1 vol.% CO₂ in the flue gas. The MEA emissions increase instantaneously (~seconds) to measured values in the range of 1600-1800 mg/m³ STP while, the temperature profile in the absorber increases much slower. The change in absorber temperature profile is not rapid as the column is made up of metal (SS 316L) and is insulated. The temperature bulge; defined as the difference between the hottest section (2nd Bed) and the 1st bed takes a few minutes before it stabilizes. The gas outlet temperature seems to be increasing throughout the experiment although slowly, as seen by the measured water content in the absorber outlet gas.

After 1 h, the CO₂ concentration is lowered to 0.7 vol.%. The MEA emission instantaneously lowers, close to the baseline value of ~220 mg/m³ STP as observed at the start of the experiment. The 2nd bed temperature takes much longer to reach a stable temperature and thus, the temperature bulge lowers only after several minutes.

The absorber top bed temperature and the water content in the gas phase take few minutes before it reaches the baseline value as measured at the start of the experiment.

The MEA emission measured with middle H₂SO₄ aerosol level is higher in this experiment (1600-1800 mg/m³ STP) as compared to results as mentioned in Figure 4.6 (800-900 mg/m³ STP). This could be explained by the different loadings for this experiment, 0.13 mol CO₂/mol amine as compared to 0.21 mol CO₂/mol amine for the results of the experiment as shown in Figure 4.6. This is reflected in the higher lean pH (10 as compared to 9.8) and the higher CO₂ capture rate, 77%, as compared to 70% for this experiment. The lower loading implies, more free MEA is available to be evaporated from the liquid to the gas phase and subsequently, be present in the aerosol phase. This leads to high emission level of MEA.

One of the proposed mechanism of aerosol formation in the absorber, is condensation aerosol formation by heterogeneous nucleation ^{138,146}. Owing to the temperature bulge or cooling down at the top of the absorber column, the MEA present in the gas phase condenses on the H₂SO₄ aerosol nuclei rather than the bulk liquid phase, which causes the high MEA emissions. This experiment indicates that even in presence of a temperature bulge and very low CO₂ (~0.7 vol.%), MEA emissions can be low (~220 mg/m³ STP) while, in the presence of CO₂ and no temperature bulge, the MEA emissions can be high (~1 g/m³ STP). The observations from this experiment indicate that the presence of CO₂ could be a much more dominating factor in the mechanism of aerosol formation than temperature bulge. The effect of CO₂ on the aerosol formation can be due to the supersaturation profile in the column and/or the reaction of CO₂ with the MEA in the aerosol phase.

4.4 Conclusions

This study highlights the influence of particles such as soot and H₂SO₄ aerosol droplets in the flue gas on solvent emissions from a typical CO₂ capture process. This is important to design Post Combustion CO₂ Capture plants with low amine emissions to not only to reduce operating costs but also, to meet the necessary regulatory requirements. Particles in the form of soot (10⁶ per cm³) can cause MEA emission in the order of 200 mg/m³ STP. H₂SO₄ aerosols with a particle number concentration in the order of 10⁸ per cm³ can lead to MEA emissions in the range of 600-1100 mg/m³ STP under tested conditions. The emission levels observed in this study are 1-2 orders of magnitude higher than the design criteria of 12 mg/m³ STP considered for design of Post Combustion CO₂ Capture plant. The observed MEA emissions are much higher than vapour pressure based MEA gas phase concentration. This proves that foreign nuclei, especially H₂SO₄ aerosols can lead to significant aerosol-based solvent emissions. Moreover, there is a clear relation between the particle number concentration of particles/foreign nuclei and MEA emissions. It is also clear that both temperature bulge and CO₂ in the gas phase are necessary for aerosol-based emissions. There are indications that CO₂ could play a very important role in the aerosol formation process

itself. Further experiments are being currently conducted to understand the mechanism of aerosol formation. This will help in appropriate design of counter-measures for avoiding high solvent emissions.

Chapter 5

Understanding aerosol-based emissions in a post combustion CO₂ capture process: parameter testing and mechanisms.

This chapter is based on the following publication:

Khakharia, P., Brachert, L., Mertens, J., Anderlohr, C., Huizinga, A., Fernandez, E.S., Schallert, B., Schaber, K., Vlugt, T.J.H., Goetheer, E., Understanding aerosol based emissions in a Post Combustion CO₂ Capture process: Parameter testing and mechanisms, *Int. J. Greenh. Gas Control*, 34, 63–74, 2015.

5.1 Introduction

Solvent emission is one of the challenges in the realisation of a full-scale absorption-desorption based Post Combustion CO₂ capture plant ^{69,71,74}. Typically, aqueous solutions of amines are used as solvent. The most widely known and studied solvent is 30 wt.% monoethanolamine (MEA) solution ^{17,18,79}. Other amines e.g. 2-amino-2-methylpropoanol (AMP), piperazine (Pz), N-methyldiethanolamine (MDEA), have been developed to improve various aspects of the capture process, e.g. the solvent capacity for CO₂, stability, specific reboiler duty, over MEA ^{108,147–152}. Some of these amines are known to be volatile and therefore, can be emitted to the atmosphere via the treated flue gas stream ^{66,69}. Amino acids such as taurine, alanine, glycine, sarcosine, proline, etc. and their salts with bases such as KOH are also being evaluated as capture solvents ^{19,153–156}. As they are in a salt form, they have an advantage of no vapour emissions.

The emission of solvent and its components can occur by means of (i) vapour emissions due to the volatility, (ii) carryover as a result of mechanical entrainment, and (iii) aerosols. The first two means of emissions are well understood. Recently, aerosol-based emissions have been reported from typical Post Combustion CO₂ Capture pilot plants in literature ^{72,74,107} and, in Chapter 4. These studies indicate that aerosol-based emissions can be significant, in the order of grams/m³ STP (STP; 0°C and 101.325 kPa), as compared to few mg/m³ STP of vapour emissions. Moreover, they cannot be reduced by conventional counter-measures such as a water wash or a demister. Therefore, these emissions can lead to environmental hazard and huge solvent losses, increasing the operating cost ¹²⁹. The cause of these aerosol-based amine emissions were investigated in a controlled environment using 30 wt.% MEA as the capture solvent, see Chapter 4. The extent of solvent emissions was correlated to the aerosol particle number concentration entering the CO₂ capture absorber. The particles, in the range of 10⁷–10⁸ per cm³, were of H₂SO₄ and H₂O, generated by homogeneous nucleation of gas phase SO₃ in a combustion flue gas. Moreover, these tests indicated that the operating parameters of the CO₂ capture plant could play an important role in determining the extent of aerosol-based emissions.

In this study, various operating parameters of a CO₂ capture process are evaluated for their impact on aerosol-based emissions. The lean solvent temperature, the pH of the lean solvent, and the CO₂ concentration in the flue gas were varied. Moreover, different solvents were used to investigate if the aerosol-based emissions are specific for MEA. A blend of AMP (2.6 M) and Piperazine (0.9 M) (hereafter denoted by AMP-Pz), and a blend of AMP (2.2 M) and potassium taurate (1.5 M) (hereafter denoted by AMP-KTau) were used as capture solvent. AMP has a high capacity for capturing CO₂ however, it has very slow reaction kinetics ¹⁵⁷. Therefore, a fast reacting molecule with CO₂ such as piperazine or taurate is added as an activator ^{150,158,159}. A mixture of AMP and Pz has been shown to reduce the steam reboiler duty as compared to MEA in a typical CO₂ capture process ^{160,161}. Amino acid salts, such as taurate, are expected not to

result in aerosol-based emissions as they are non-volatile. Moreover, the reaction kinetics of amino acid salts is similar to that of amines¹⁵⁶.

5.2 Saturation and aerosol growth

Aerosols formation and growth in gas-liquid contact devices such as absorption columns has been extensively studied for the quenching of acid gases^{137,138,141,142,146,162}. The mechanism of aerosol formation and growth can be understood by considering the degree of saturation. The degree of saturation (S) is defined by the ratio of the total partial pressure of all the condensing components to its equilibrium partial pressure at the same composition and temperature^{137,163}. The gas is considered to be supersaturated when the degree of saturation (S) is greater than 1. Aerosol nucleation can be initiated by two mechanisms: (i) homogeneous nucleation: at high saturation ratios ($S>2$, depending on temperature and composition), nucleation of molecules of condensable components leads to aerosols, and (ii) heterogeneous nucleation: fine particles in the gas phase can form aerosols even at low saturation ratios ($S\sim 1$). Subsequently, the growth of aerosol particle occurs by (i) coagulation and (ii) condensation¹⁴⁶.

An example of aerosol formation by heterogeneous nucleation in a counter-current absorption of HCl in water was studied by Wix et al., 2007 using an in-house model¹³⁸. The temperature of the gas phase decreased and liquid temperature increased as compared to their inlet temperatures due to the heat of absorption. In the absence of heterogeneous nuclei in the gas, the gas was supersaturated ($1.3 < S < 1.5$) and increasing the number of heterogeneous nuclei led to a reduction in the supersaturation due to condensation on foreign nuclei. Upon increasing the particle number concentration in the inlet gas stream, the total concentration of HCl in the aerosol phase was found to increase and was attributed to the higher surface area.

A similar mechanism can be expected to occur in a counter-current absorption of CO₂ in a solvent. The flue gas is heated up (60-70°C, as seen in this study) along the column due to the reaction of the solvent component with CO₂. At the top of the column, the flue gas comes in contact with cold lean solvent, typically at 40°C. This leads to a so called, temperature bulge, where the temperature reaches a maximum, typically at a distance of 2/3rd of the total packing height from the bottom and further cools down at the top of the column. This can lead to a significant temperature difference between the gas and liquid phases resulting in a supersaturated environment. The degree of saturation along a CO₂ capture absorber column was calculated using a rate based approach in Aspen Plus¹⁶⁴. The maximum saturation was found to be at the top of the column and in the range of 1.05-1.2 depending on the operating parameters. In the presence of nuclei and supersaturation in the flue gas, the volatile components can condense on these nuclei leading to a growth of aerosol droplets. Mertens et al., 2014 measured a slightly lower particle number concentration at the outlet of the absorber than at the inlet and attributed this to possible coagulation in the absorber

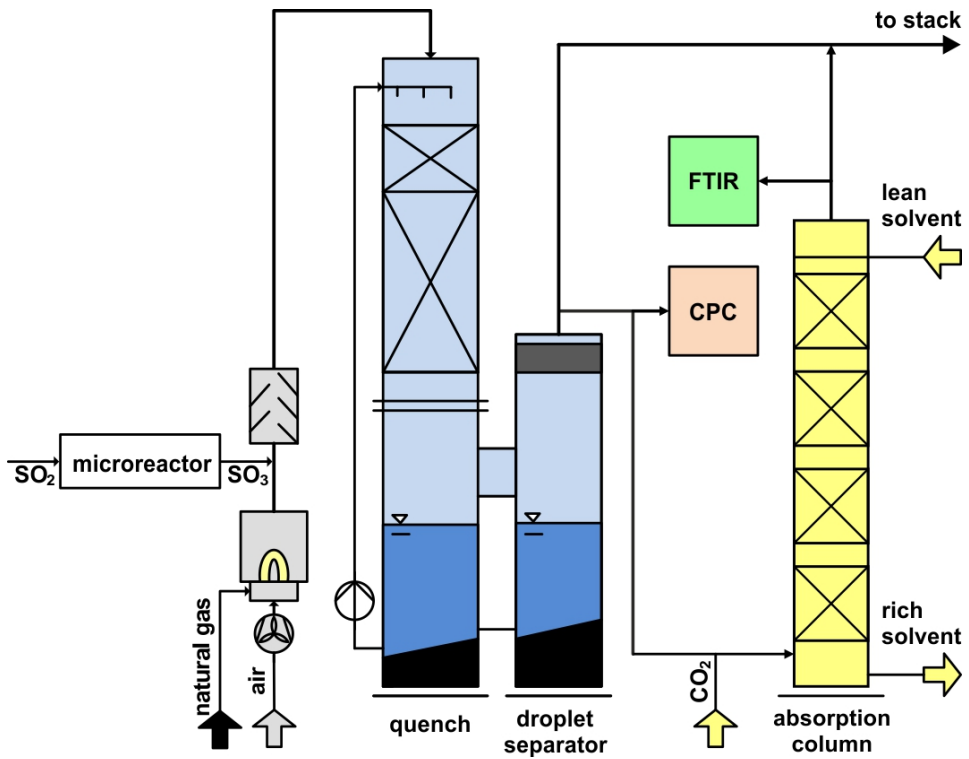


Figure 5.1. Schematic representation of the pilot plant for sulphuric acid aerosol generation and the absorber section of the CO_2 capture mini-plant at Karlsruhe Institute of Technology. A slip stream of this aerosol containing flue gas is used for the CO_2 capture mini-plant, while the emissions are measured by the FTIR analyser in the treated flue gas stream at the top of the absorber ¹⁶⁵ (see Chapter 4).

column ¹⁰⁷. However, the growth of particles by means of condensation is expected to be the dominant mechanism.

5.3 Test equipment and methods

5.3.1 Pilot plant for aerosol generation

The flue gas containing sulphuric acid aerosols was generated using the pilot plant at the Institut für Technische Thermodynamik und Kältetechnik, Karlsruhe Institute of Technology. The pilot plant has been described in detail in literature ^{106,137,141}. At the outlet of the quench column, a split stream has been used as a flue gas source to the CO_2 capture mini-plant as shown in Figure 5.1. The different sulphuric acid concentration leads to particle number concentrations in the range of $10^7\text{-}10^8$ per cm^3 . The particles grow in size when the sulphuric acid concentration is increased remaining below 100 nm, while the particle number concentration are in the same order of magnitude ^{107,141,142}. The flue gas generated from the pilot plant has been characterized by two measuring instruments, a condensation particle counter (UFCPC, PALAS GmbH) and an electrical low pressure impactor (ELPI⁺, Dekati Ltd.) ^{107,165}.

5.3.2 CO₂ capture mini-plant

TNO's mobile continuous absorption-desorption based carbon capture mini-plant was used as described in 0. The absorber consists of 4 packed beds, each of 0.5 m, with temperature sensors in between each bed. The diameter of the absorber column is 4.5 cm. The top bed is referred to as the 1st bed, while the bottom bed is referred to as the 4th bed. It is important to note that in the configuration used, the absorber section was equipped neither with a water wash section nor a demister. Additional CO₂ was added to the flue gas stream from the pilot plant and prior to the absorber, with resulting CO₂ concentrations in the range of 0.7 to 13 vol.% with a typical CO₂ concentration of 12 vol.% in the flue gas to mimic power plant flue gas conditions. The temperature of the flue gas to the absorber column was maintained at about 50-55°C using a heated line.

5.3.3 FTIR (Fourier transform infraRed)

An FTIR analyser (GASMET CX 4000) was used to analyse the gas phase leaving the absorber section. This has been described in section 3.2.2.

5.3.4 CPC (Condensation Particle Counter) and dilution system

The number concentration of particles, in this case sulphuric acid aerosols, was measured by a Condensation Particle Counter (CPC; PALAS UFCPC with sensor 200). The particle laden gas stream is diluted with a PALAS dilution cascade DC 10000 in order to restrict the particle number concentration to the measuring range of the CPC. Further information about its working principle and its comparison with other measuring principles can be found in literature ^{144,165}.

5.4 Results and discussion

This section presents the effect of the changes in various parameters on the amine emissions. Subsequently, the mechanisms explaining the observations are discussed. Finally, an overall hypothesis for aerosol formation and growth in a CO₂ capture absorption column is presented.

Table 5.1. Operating conditions of the CO₂ capture mini-plant during the test of change in lean solvent temperature.

MEA (4M)	
Gas flow rate (m ³ STP/h)	2
Liquid flow rate (kg/h)	10
Stripper temperature (bottom) (°C)	120
Stripper pressure (bar)	1.82
CO ₂ inlet flue gas (vol.%)	13.3
Lean loading (mol CO ₂ /kg)	0.60
Rich loading (mol CO ₂ /kg)	1.60

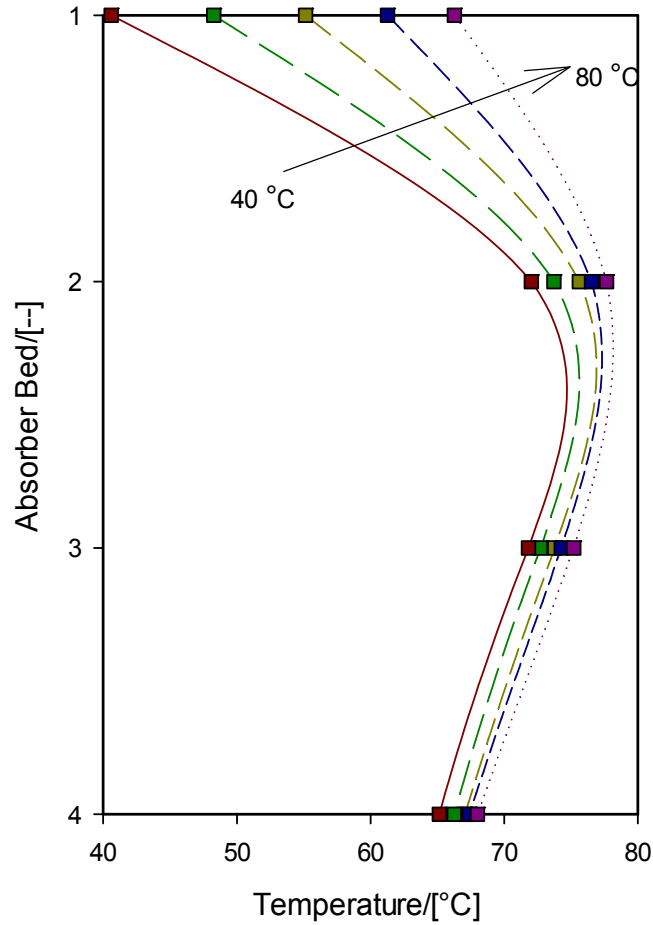


Figure 5.2. Temperature profile along the absorber column when the lean solvent temperature was increased from 40°C to 80°C, in steps of 10°C. Feed gas temperature was maintained at 45°C.

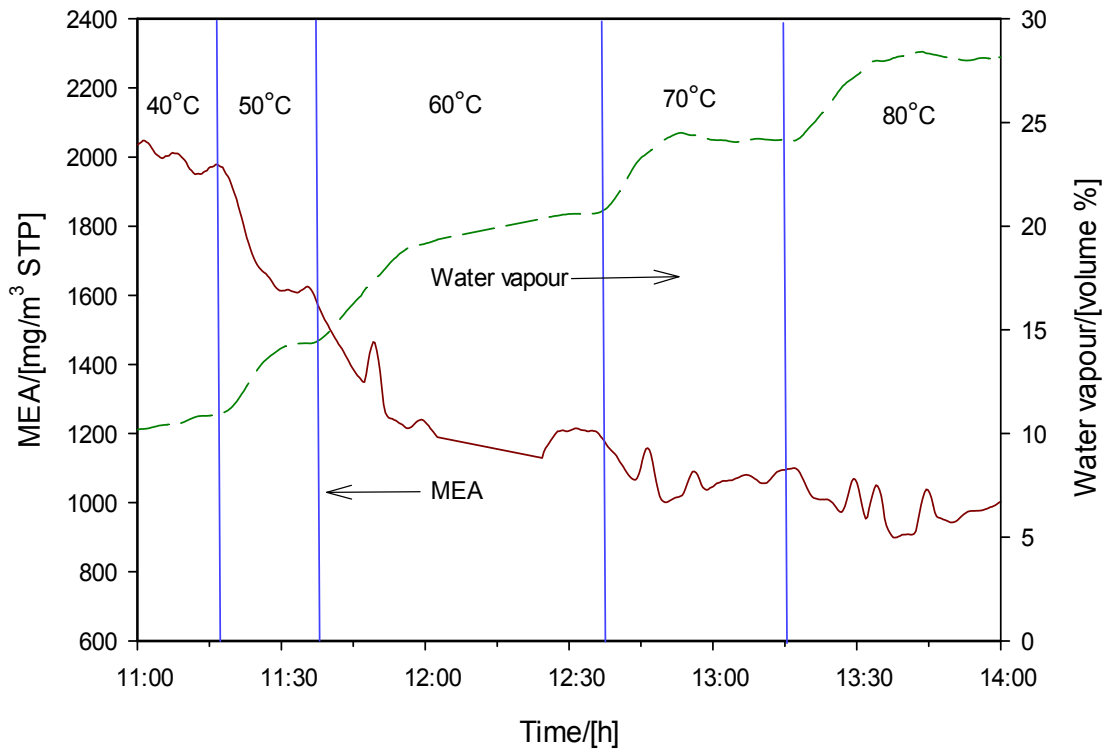


Figure 5.3. Effect of increasing the lean solvent temperature, indicated by the water content, on the MEA emissions. Vertical lines indicate change in the lean solvent temperature.

5.4.1 The lean solvent temperature

The temperature profile and therefore, the supersaturation along the column can be altered by changing the temperature of the lean solvent. For this, the operating conditions of the CO₂ capture mini-plant with MEA as the solvent were kept constant at the values shown in Table 5.1. The lean solvent temperature is typically maintained at 40°C. The operating parameters of the CO₂ capture mini-plant and the particle number concentration in the inlet flue gas were kept constant at ca. 1.05 · 10⁸ per cm³, while the lean solvent temperature was increased in steps of 10°C, from 40°C to 80°C. The corresponding rich loading was 1.61 mol CO₂/kg and the CO₂ capture percentage was in the range of 97-100 %.

The corresponding temperature profile in the absorber column was as shown in Figure 5.2. Upon increasing the lean solvent temperature, the temperature along the column increases, especially the 2nd bed and 1st bed temperatures. The temperature bulge, i.e. the difference between the hottest bed (2nd bed) and the cooler, top bed (1st bed) reduces at higher solvent inlet temperatures. The water content of the treated flue gas increases from ca. 10 vol.% to ca. 28 vol.% as the temperature of the gas stream is increased, as shown in Figure 5.3. The treated flue gas stream is saturated with water vapour and thus, the amount of water vapour is directly related to the flue gas temperature. The emissions of MEA at a lean solvent temperature of 40.5°C are ca.

1900 mg/m³ STP indicating these are aerosol-based emissions. The emissions of MEA decreases from ca. 1900 mg/m³ STP to 1600 mg/m³ STP as the lean solvent temperature is increased from 40°C to 50°C. The lean temperature is further increased to 60°C resulting in a further decrease of MEA emission to ca. 1200 mg/m³ STP. Further increase in the lean solvent temperature only decreases the MEA emissions slightly, to ca. 1000 mg/m³ STP. The volatility of 5M MEA at 60°C and at a loading of 0.11 mol CO₂/mol MEA is ca. 700 mg/m³ STP ⁶⁶. Therefore, the emissions of MEA at high lean solvent temperatures of 70°C and 80°C, indicates that the emissions are caused mainly by volatile MEA. Therefore, the aerosol-based emission of MEA decreases with increasing temperature of the lean solvent, while the vapour emission increases.

5.4.2 AMP-Pz as the CO₂ capture solvent

Due to the relevance of AMP-Pz as a next generation CO₂ capture solvent, an aqueous mixture of 2.6M AMP and 0.9M Pz was used as the capture solvent to evaluate if aerosol-based emissions are observed for other commonly used CO₂ capture solvents as well. The operating conditions of the CO₂ capture mini-plant using AMP-Pz as the capture solvent were as shown in Table 5.2 and the corresponding temperature profiles in the column were as shown in Figure 5.4. The temperature along the column is lower than MEA as the solvent, however, there is an increase in the temperature of the gas from the inlet to the fourth bed. Therefore, there is a temperature bulge but is located at the bottom of the column.

The lower absolute temperatures are due to the following reasons: (a) the liquid to gas ratio is higher in this experiment as compared to the experiment with MEA and therefore, there is more cooling by the lean solvent, (b) the absorption enthalpy of primary amines like MEA is known to be higher than secondary amines such as Pz or hindered amine like AMP ¹⁶⁶.

Figure 5.5 shows the emissions of AMP and Pz at varying levels of sulphuric acid aerosols. One can observe that the emissions of AMP and Pz directly follow the trend of particle number concentration. Thus, when the particle number concentration increases from 9.7·10⁷ at the low H₂SO₄ aerosol level to 1.4·10⁸ at the high H₂SO₄ aerosol level, the AMP emission increases from 2146 mg/m³ STP to 2940 mg/m³ STP, while the Pz emissions increase from 312 mg/m³ STP to 416 mg/m³ STP. The corresponding vapour emission levels, i.e. in the absence of H₂SO₄ aerosols, of AMP and Pz were 393 mg/m³ STP and 15 mg/m³ STP. Thus, aerosol-based emissions are observed for both AMP and Pz. A similar instantaneous behaviour in the change of emissions with changing number concentrations is also observed.

Based on this observation, the risk of aerosol-based emission can be expected from other solvents containing volatile components when treating flue gas containing particles.

Table 5.2. Operating conditions of the CO₂ capture mini-plant using AMP-Pz as the capture solvent.

Gas flow rate (m ³ STP/h)	3.2
Liquid flow rate (kg/h)	20.4
Stripper temperature (bottom) (°C)	118
Stripper pressure (bar)	1.82
CO ₂ inlet flue gas (vol.%)	12.1
Lean solvent temperature (°C)	40
Lean loading (mol CO ₂ /kg)	0.34
Rich loading (mol CO ₂ /kg)	1.19
CO ₂ capture (%)	94

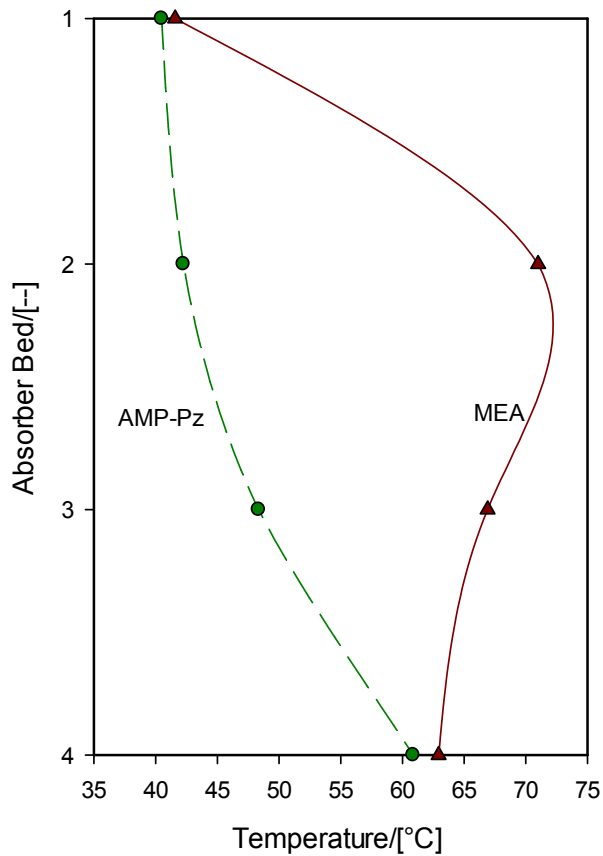


Figure 5.4. Temperature profile along the absorber column using 2.6M AMP-0.9M Pz as the CO₂ capture solvent. The temperature of the feed gas was 45°C and lean solvent temperature was maintained at 40°C. The temperature profile with MEA as the CO₂ capture solvent as presented in Figure 4.3 is also shown for comparison.

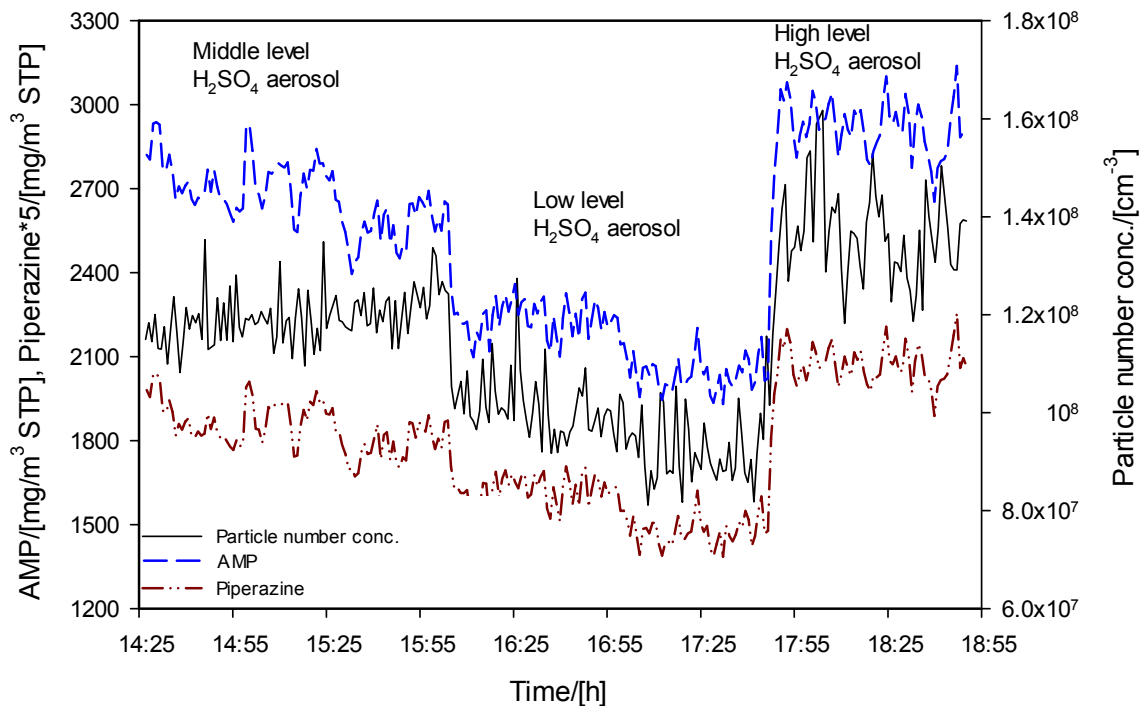


Figure 5.5. Emissions of AMP and Pz and the measured particle number concentration at different levels of H_2SO_4 aerosols in the flue gas.

Table 5.3. Operating conditions of the CO_2 capture mini-plant using AMP-Pz as the capture solvent with varying lean pH.

Gas flow rate ($\text{m}^3 \text{ STP/h}$)	2.4
Liquid flow rate (kg/h)	16.1
CO_2 inlet flue gas (vol.%)	12.3
Lean solvent temperature ($^\circ\text{C}$)	40.5
Particle number concentration inlet flue gas (cm^{-3})	$1.02 \cdot 10^8$

5.4.3 The pH of the lean solvent

The lean loading and thus, the pH are determined by the operating conditions of the stripper. Typically, the stripper is operated at a constant temperature ($\sim 120^\circ\text{C}$), while the pressure is fixed based on the vapour-liquid equilibrium value. In this study, the temperature set point of the stripper was changed from 100°C to 120°C in order to strip more CO_2 from the solvent and increase the pH of the lean solvent. The average particle number concentration was $1.02 \cdot 10^8$ per cm^3 and the remaining operating conditions of the CO_2 capture mini-plant were also kept constant, as shown in Table 5.3.

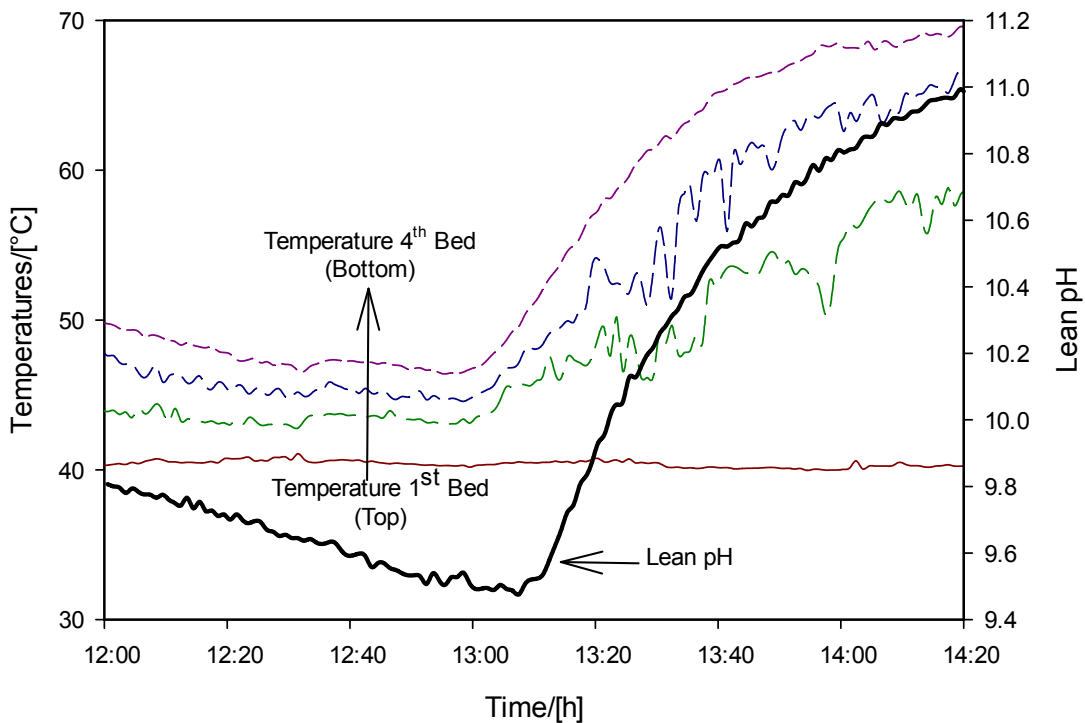


Figure 5.6. Effect of lean pH on the temperature profile along the absorber column. The temperature of the feed gas was 45°C and lean solvent temperature was maintained at 40.5°C. The temperature of the gas increases from the top to the bottom and is indicated by the arrow.

The corresponding temperature profile along the absorber column was as shown in Figure 5.6. Initially, the solvent has a relatively high CO₂ loading as indicated by a pH of 9.4. Therefore, there is hardly any CO₂ captured and thus, the temperature in the column is low, below 50°C. However, there is still a temperature gradient in the column, as the gas temperature increases from 45°C to ca. 49°C from the inlet to the 1st bed and subsequently cools down in the column to 41°C at the top. The pH of the lean solvent starts to increase as the temperature in the stripper rises, leading to a lower CO₂ loading in the lean solvent. This leads to more capture of CO₂ and, therefore, higher temperatures in the absorber. The temperature bulge, in this case the difference between 4th bed (hottest bed, bottom) and the top bed temperature which is constant at 41°C, increases as the lean pH increases. It is important to note that the temperature of the gas leaving the absorber (inlet of FTIR analyser) was constant at ca. 33°C as the temperature of the 1st bed was constant at ca. 40°C.

The resulting emissions of AMP, Pz and the pH of the lean solvent during the experiment were as shown in Figure 5.7. Initially, only emissions of AMP are observed, while the emissions of Pz are below the detection limit of the FTIR analyser. As the lean pH was increased, the emissions of both AMP and Pz increase. The maximum emissions of AMP and Pz were 2249 mg/m³ STP and 350 mg/m³ STP, respectively at a lean pH of 11. Initially, at low lean pH the emissions of AMP (~100 mg/m³ STP) are

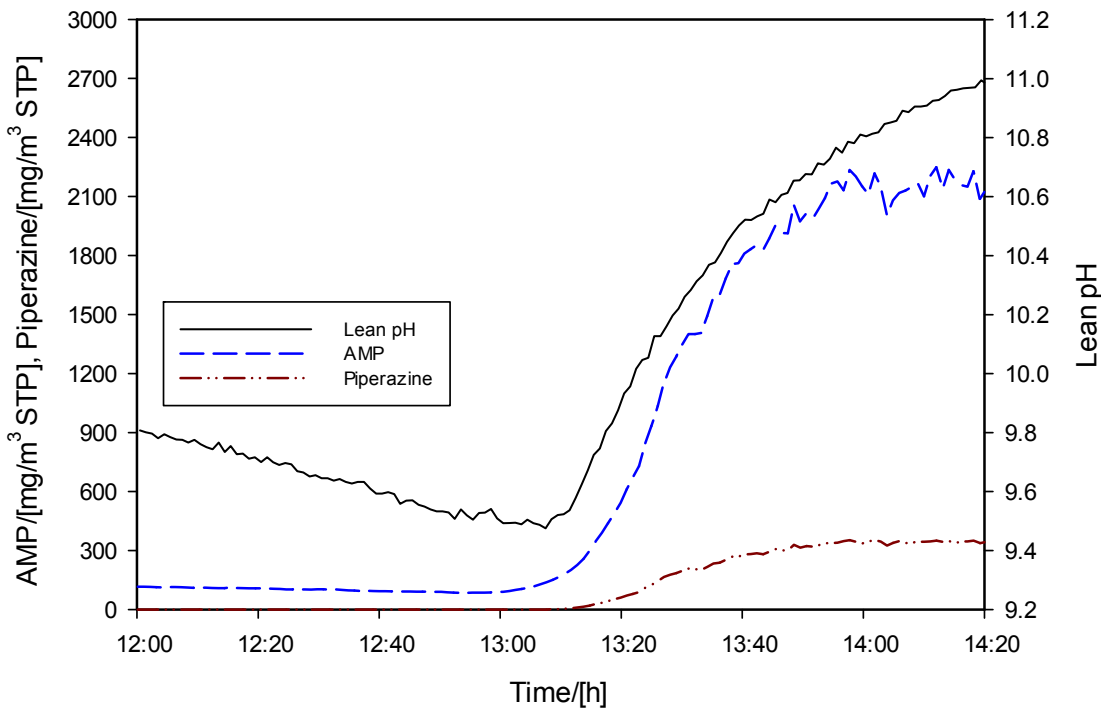


Figure 5.7. Effect of change in pH of lean solvent on emissions of AMP and Pz. The pH of the lean solvent is changed by changing the temperature in the stripper column.

expected to be mainly volatile emissions at the gas temperature of 33°C entering the FTIR analyser⁶⁶. Moreover, there is hardly any emission of Pz. At a high CO₂ loading, the activity of Pz is expected to be low as it is likely to be in a carbamate form, which is non-volatile. Higher activity implies a higher amount of free amine available for evaporation. Moreover, the concentration of Pz was low (at 0.9M) and its volatility is almost two orders of magnitude lower than that of AMP. The increase in emissions can be attributed to the following two reasons: (a) increasing the lean pH implies lower the CO₂ loading in the solvent and therefore, higher activity of the amine components. The higher activity leads to a higher volatility and thus, higher emissions; (b) as the lean pH increases the amount of CO₂ captured increases, resulting in higher temperatures as well as higher temperature bulge in the column. Both effects lead to an increase in emissions and specifically, aerosol-based emissions. This is further explained in section 5.5.3.

5.4.4 CO₂ concentration in the flue gas

Typically, the CO₂ content in a coal fired flue gas is ca. 13 vol.%, while in natural gas combined cycle fired flue gas it is ca. 4 vol.%. In this experiment, the CO₂ content of the flue gas was varied from 12.7 vol.% to 0.7 vol.%, in steps of 2 vol.%, using AMP-Pz as the capture solvent. The total flue gas flow rate was kept the same and only the CO₂ flow was changed. This led to an increase in the flue gas flow from the aerosol

Table 5.4. Operating conditions of the CO₂ capture mini-plant using AMP-Pz as the capture solvent with varying CO₂ concentration in inlet flue gas. The capture rate changes as the CO₂ concentration in the flue gas is varied.

Gas flow rate (m ³ STP/h)	2.8
Liquid flow rate (kg/h)	14.2
Stripper temperature (bottom) (°C)	118
Stripper pressure (bar)	1.82
Lean solvent temperature (°C)	40.6

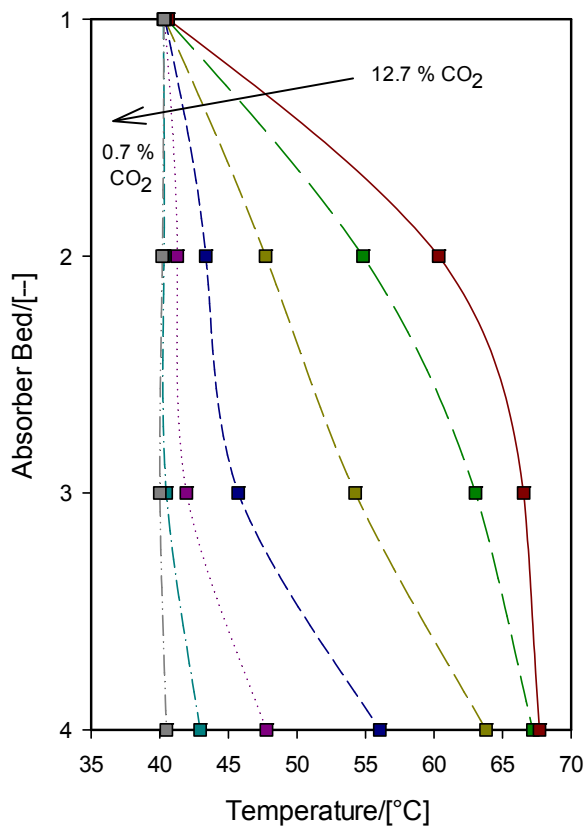


Figure 5.8. Temperature profile along the absorber column when the CO₂ content in the flue gas is varied from 12.7 to 0.7 vol.% using AMP-Pz as the CO₂ capture solvent. The arrow indicates the temperature profile obtained by decreasing the CO₂ content in the flue gas, from the left (at 12.7 vol.%) to the right (at 0.7 vol.%).

generator and thus, higher particle number concentration with decreasing CO₂ concentration. The CPC measures the particle number concentration at the flue gas extraction point (as shown in Figure 5.1) and thus, the exact particle number concentration entering the absorber at different CO₂ concentrations is not measured. However, the increase in particle number concentration is expected to be only 5-10% and thus, does not have a significant impact on the observed emissions.

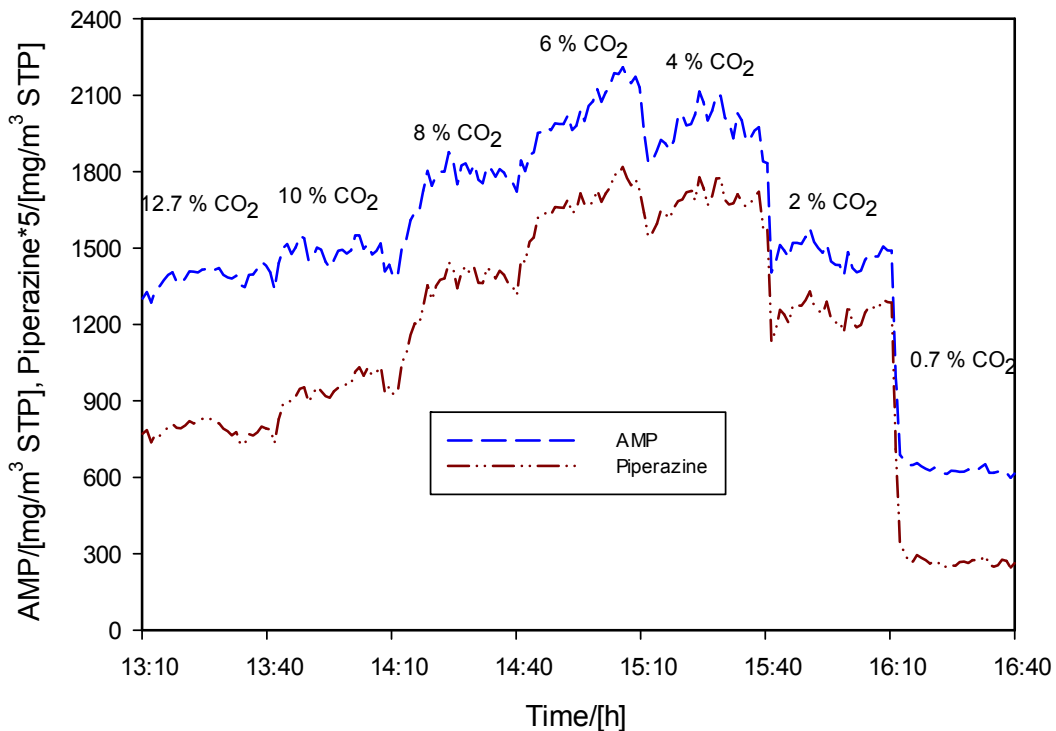


Figure 5.9. Emissions of AMP and Pz during the test where the CO₂ content in the inlet flue gas was changed from 12.7 vol.% to 0.7 vol.% in steps of 2 vol.%, approximately every half hour.

The corresponding temperature profile along the column was as shown in Figure 5.8. As the CO₂ content of the flue gas was decreased, the temperature in the column decreased too. The heat released due to the reaction was lower as the amount of CO₂ captured decreases at lower CO₂ content in flue gas. When no additional CO₂ was added to the flue gas, the CO₂ content was 0.7 vol.% from the aerosol generator and the corresponding temperature profile along the column was almost constant at 40°C.

The emissions of AMP and Pz were as shown in Figure 5.9. The emission of AMP and Pz increases as the CO₂ content was reduced from 12.7 vol.% to 6 vol.% of CO₂. A maximum value in emissions was observed at 6 vol.% CO₂ and thereafter, the emissions of both components reduce till 0.7 vol.%. The maximum emission of AMP and Pz at 6 vol.% are ca. 2200 mg/m³ STP and 226 mg/m³ STP. The temperature bulge was seen to decrease continuously as the CO₂ content in the flue gas was reduced. However, the emissions show a clear maximum. A similar experiment was performed with MEA as the CO₂ capture solvent and the same behaviour, i.e. a maximum in emissions at CO₂ 6 vol.%, was observed. It is important to note that the treated flue gas temperature remained constant and thus, the volatile emissions will not vary significantly. A clear maximum in the trend of emissions at decreasing CO₂ concentration in the flue gas indicates there are at least two competing mechanisms which are responsible for aerosol-based emissions.

Table 5.5. Operating conditions of the CO₂ capture mini-plant using AMP-KTau as the CO₂ capture solvent.

Gas flow rate (m ³ STP/h)	1.9
Liquid flow rate (kg/h)	15
Stripper temperature (bottom) (°C)	120
Stripper pressure (bar)	1.81
CO ₂ inlet flue gas (vol.%)	13.4
Lean solvent temperature (°C)	40
Lean loading (mol CO ₂ /kg)	0.45
Rich loading (mol CO ₂ /kg)	1.06
CO ₂ capture (%)	88.7

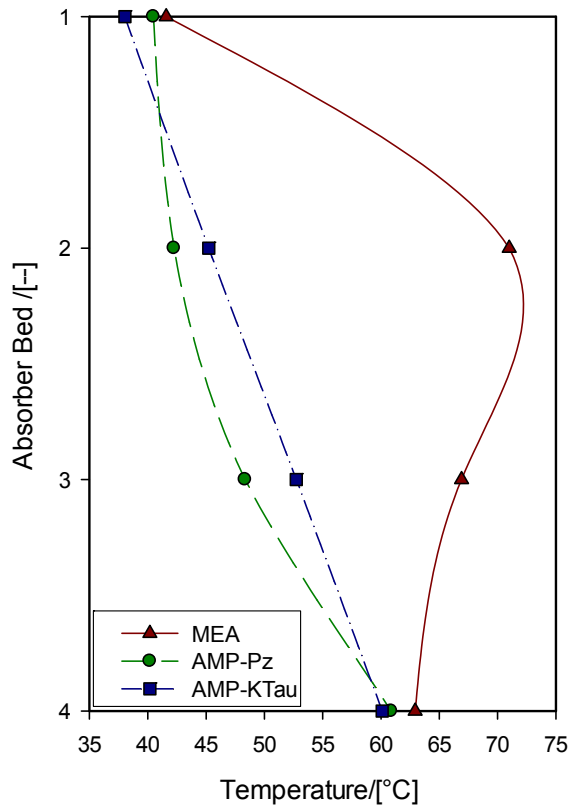


Figure 5.10. Temperature profile in the absorber column with AMP (2.2M) and Potassium taurate (1.5M) as the solvent. Its temperature profile is compared with that of AMP-Pz and MEA as the CO₂ capture solvent.

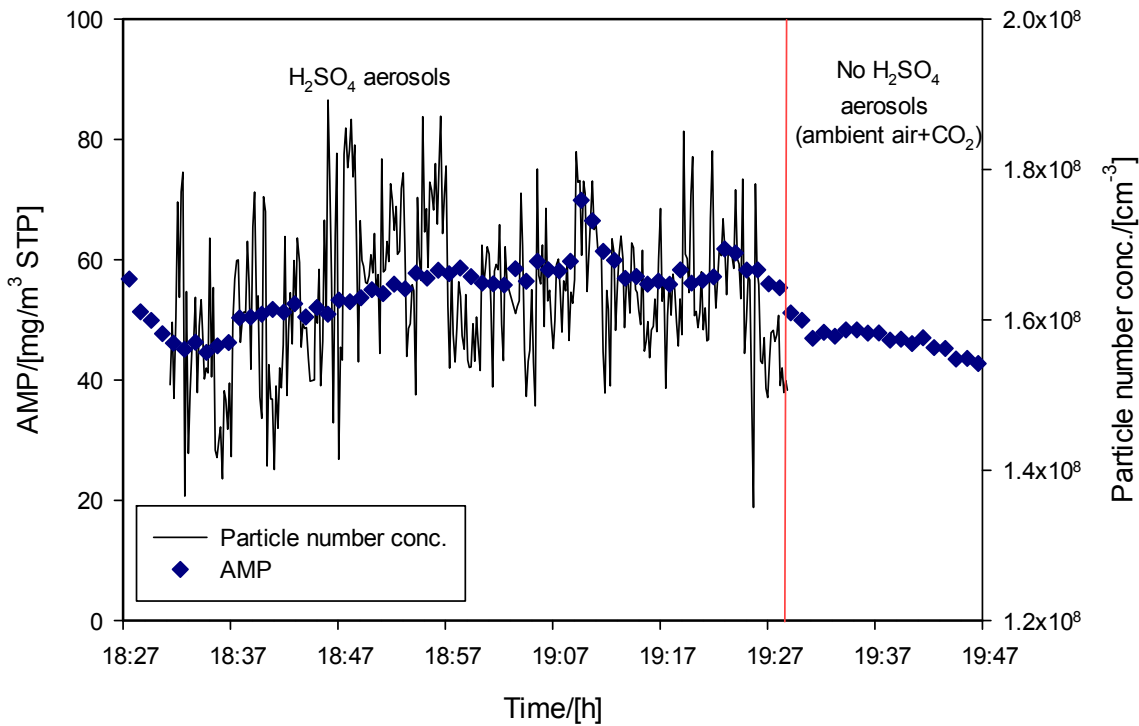


Figure 5.11. Emissions of AMP with and without H_2SO_4 aerosols in the inlet flue gas. AMP (2.2M) and Potassium taurate (1.5M) was used as the CO_2 capture solvent. The particle number concentration in the ambient air is expected to be ca. $10^4\text{-}10^5$ per cm^3 . The red lines indicates the time at which no H_2SO_4 aerosols were present in the inlet flue gas to the absorber.

5.4.5 AMP-KTau as CO_2 capture solvent

Amino acid salts are known to be non-volatile. Therefore, neither vapour nor aerosol-based emissions are expected from such a solvent. However, in a solvent mixture of a volatile and non-volatile component, aerosol-based emissions of the volatile component is to be expected. Thus, in order to verify this, a solvent mixture of AMP (2.2M) and potassium taurate (1.5M) was used. The operating parameters of the CO_2 capture plant were as shown in Table 5.5.

The corresponding temperature profile was as shown in Figure 5.10 and is compared with the experiment with MEA and AMP-Pz as the CO_2 capture solvent. The maximum temperature was observed at the bottom of the column indicating most of the CO_2 capture occurs at lowest bed. This is a solvent similar in terms of its CO_2 capacity and absorption enthalpy to AMP-Pz and moreover, the operating conditions of the CO_2 capture mini-plant were similar. Therefore, its temperature profile too is similar to AMP-Pz.

The emissions of AMP (volatile component) and the measured particle number concentration during the test were as shown in Figure 5.11. Initially, flue gas from the aerosol generator with H_2SO_4 aerosols in the range of $1.4\text{-}1.7 \cdot 10^8$ per cm^3 was used.

After one hour, the flue gas was replaced with ambient air. In the presence of H_2SO_4 aerosols the AMP emissions were in the range of 40-60 mg/m³ STP. Subsequently, in the absence of H_2SO_4 aerosols the AMP emissions reduces only slightly, to ca. 40 mg/m³ STP. Thus, the emissions of AMP were about the same in the presence and absence of H_2SO_4 aerosols. It is important to note that the set point of the CO_2 flow was not changed in order to compensate for the 0.7 vol.% CO_2 contribution from the flue gas from the aerosol generator. Thus, the CO_2 content is lower by 0.7 vol.% in the test with ambient air. This leads to only a small change in the operating conditions of the CO_2 capture mini-plant and thus, has minimal impact on the emissions.

The low emissions of AMP in the presence of H_2SO_4 aerosols indicate that AMP was not present in the aerosol droplets, but only in the vapour phase. The process conditions of this test were similar to the tests with AMP-Pz and MEA. Therefore, even in the presence of all necessary elements for aerosol emissions, i.e. temperature bulge and volatile amine, no aerosol-based emissions were observed. This is an important observation, as there is a striking difference in aerosol-based emissions between AMP-Pz and AMP-KTau due to a different solvent chemistry. This observation is further discussed in section 5.5.3.2.

5.5 Mechanisms

Aerosol-based emission in a CO_2 capture absorber is a multi-parameter phenomenon. In this section, the observations are explained by relating them to possible mechanisms. The three main parameters identified are; (i) the particle number concentration, (ii) the supersaturation, and (iii) the reactivity of the amine.

5.5.1 Particle number concentration

As reported in Chapter 4 and shown in the results presented in section 5.4.2, the emissions of MEA and AMP-Pz increase as the particle number concentration in the flue gas increases. Therefore, the extent of aerosol-based emission depends strongly on the number of particles present in the flue gas. Although small, the aerosol droplets offer a surface for heterogeneous nucleation. This indicates a preference for the amine to be in the aerosol phase rather than in the bulk liquid phase.

5.5.2 Supersaturation

As seen in section 5.4.1, increasing the lean solvent temperature decreases the emissions of MEA. As the lean solvent temperature is increased, the difference between the gas and liquid temperature decreases. At higher liquid temperatures the equilibrium partial pressure of the volatile components increases. Both these effects lead to a decrease in the supersaturation of the gas phase and therefore to less growth of aerosol droplets by condensation.

The lean pH decreases as a result of the lower CO₂ loading of the solvent. The solvent then has a higher capacity for capturing CO₂ leading to a temperature increase in the column. The resulting increase in the temperature gradient along the column leads to an increased supersaturation of the gas phase and thus, increased aerosol-based emissions.

As the CO₂ content in the flue gas stream is decreased, two competing phenomena take place. When the CO₂ content reduces, the amount of CO₂ captured by the liquid reduces, resulting in a higher activity and thus, higher volatility of the amines. At the same time, the heat released due to the reaction lowers, reducing the temperature in the column and thereby reducing the volatility of amines. The former effect is expected to be dominant for CO₂ content from 12.7 to 6 vol.%, while the latter effect is dominant at lower CO₂ content. Both these effects lead to a change in the supersaturation profile in the column and a maximum driving force for aerosol-based emission is expected at 6 vol.% CO₂ in the flue gas. Therefore, sufficient supersaturation is necessary for aerosol formation and growth. Moreover, the extent of supersaturation determines the extent of aerosol-based emissions.

5.5.3 Reactivity of the amine

5.5.3.1 Ratio of AMP to Pz

Each amine has unique intrinsic reaction kinetics with CO₂. Typically, hindered primary amines such as AMP and tertiary amines are known to have slow reaction kinetics with CO₂ as compared to primary amines like MEA or Taurine ¹⁴⁷. Using a blend of AMP and Pz enables us to understand the influence of CO₂ kinetics on the mechanism of aerosol formation. As seen in Figure 5.7, initially, the emissions of AMP are low and correspond to its vapour pressure, while the Pz emissions are below limit of detection limit at low lean pH (~9.2). It is interesting to note that there is CO₂ capture and a temperature gradient at the start of the experiment and thus, aerosol-based emissions are expected to a small extent. Significant aerosol-based emissions are observed only when increasing the lean pH. At higher pH, the activity of Pz increases leading to its emission and aerosol-based emissions of both AMP and Pz. This indicates that volatility of the promoter, Pz, is required for aerosol-based emissions of AMP.

Figure 5.12 shows the change in ratio of AMP: Pz emissions during the change in pH of the lean solvent. At higher lean pH relatively more Pz is present than AMP. This is due to the fact that at higher lean pH the activity of Pz is higher than that of AMP and thus, more Pz is able to evaporate in the gas phase and subsequently condense on the aerosols. The higher sensitivity for the activity of Pz for different CO₂ loadings was shown by Nguyen et al., 2010 ⁶⁶ for a MDEA-Pz mixture and a similar behaviour can be expected for AMP-Pz too.

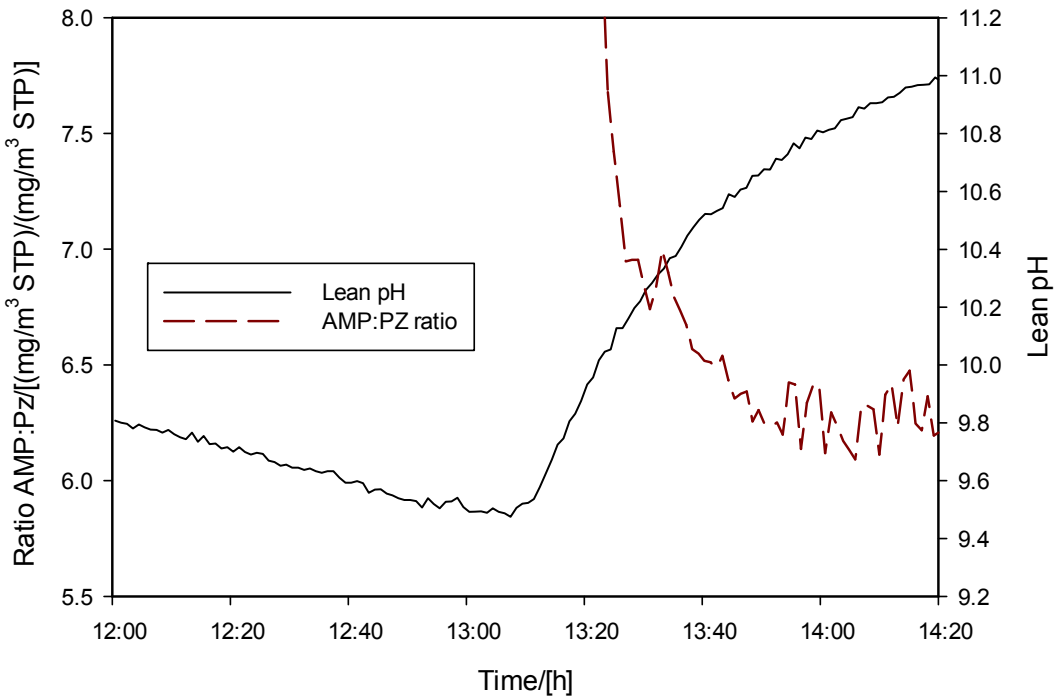


Figure 5.12. Effect of change in pH of lean solution on ratio of AMP:Pz emissions. The pH of the lean solvent is changed by changing the temperature in the stripper column.

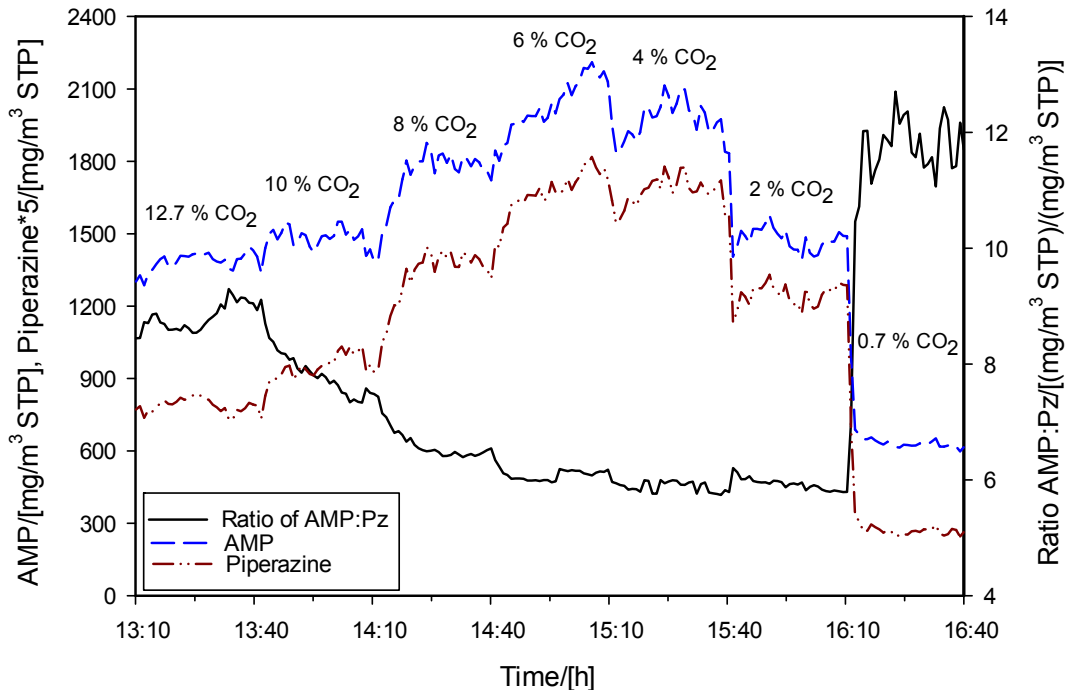


Figure 5.13. Effect of change in CO₂ content of the inlet flue gas on the ratio of AMP:Pz emissions during the test where the CO₂ content in the inlet flue gas was changed from 12.7 vol.% to 0.7 vol.% in steps of 2 vol.%, approximately every half hour.

The ratio of AMP:Pz emissions decreases as the CO₂ content in the inlet flue gas is reduced as shown in Figure 5.13. In the absence of aerosol nuclei in the flue gas, the ratio of AMP:Pz emissions was about 26, which correspond to volatile emissions. A lower ratio (5-12) indicates that relatively more Pz is present than AMP in the aerosol droplets. As the CO₂ content in the flue gas is reduced the activity of the amines also changes as a result of decreased CO₂ loading in the solvent. As mentioned before, the activity of Pz changes significantly at varying CO₂ loadings than that of AMP. This leads to relatively more Pz at lower CO₂ content in the flue gas and thus, a lower ratio of AMP:Pz.

5.5.3.2 Volatility of promoter

No aerosol-based emissions are observed when taurate is used as the promoter instead of AMP. However, in a mixture of AMP-Pz, aerosol-based emissions of both the components are observed at a similar temperature profile and operating conditions. This indicates that reaction kinetics plays a significant role for the amine aerosol growth. Slower reacting solvent component such as AMP needs to be promoted in the aerosol phase by the faster reacting component such as Pz for significant growth of the aerosols. This observation leads to formulation of an overall hypothesis for aerosol growth in a CO₂ capture system and is discussed in the following section.

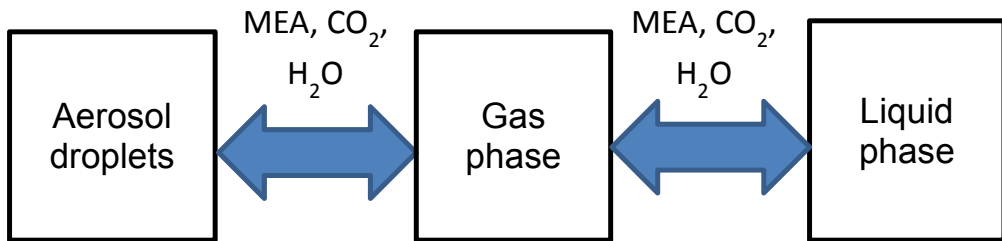


Figure 5.14. Schematic representation of the phases and components present in the absorber column with flue gas containing nuclei and using MEA as the capture solvent. The arrows indicate the interaction between the three phases by means of the volatile components, MEA, CO₂ and H₂O.

5.6 Overall hypothesis

An important difference in a CO₂ capture absorption system, as compared to other studies on heterogeneous nucleation, is the reversible reaction of CO₂ and the active component in the solvent. CO₂ can react with the solvent component to form a salt, carbamate or bicarbonate, which is then non-volatile ¹⁶. The amine and the other species formed are weak electrolytes.

Hereby, an overall hypothesis is presented to describe the phenomena occurring during aerosol formation in a CO₂ capture system. The environment at the entrance of a CO₂ capture absorption column using MEA as the solvent and flue gas containing H₂SO₄ aerosol nuclei, is schematically represented in

Figure 5.14. The gas phase and liquid phase are in contact, especially on the packing material, while the aerosol droplets and the gas phase are in contact and have the same velocity. The liquid phase contains the amine, protonated amine and its reaction product in the form of carbamate ¹⁶. The gas phase contains CO₂, N₂, O₂, the volatile components of the solvent, namely MEA, and water vapour. The aerosol droplets contain sulphuric acid and water.

The total specific surface area of all the droplets is ca. 0.4 m²/m³ at the inlet of the absorber column. This is much less as compared to the surface area of the packing material (~100 m²/m³) on which the bulk liquid phase is present. The resistance to mass transfer of CO₂ can be considered to be on the liquid side for both of the interfaces, gas-liquid phase and gas-aerosol droplets. At the bottom of the column, the gas temperature increases as a result of reaction of CO₂ with the amine. The temperature of the gas is expected to be lower than that of the liquid. As the gas temperature increases, the temperature of the aerosol droplets is also expected to increase. This can lead to some evaporation of water from the aerosol phase and therefore, possible shrinking of the droplet. The gas temperature reaches a maximum and is subsequently cooled by the relatively cold lean solvent. In this zone, the gas temperature is expected to be higher than the lean solvent temperature creating a supersaturation zone. The particles present in the gas, although smaller than at the inlet, offer a surface area for condensation of volatile components. In this zone, the

condensable components such as water vapour and amine accumulate on the droplet. Additionally, the amine present in the boundary layer of the aerosol droplet can further react with the CO₂ in the gas phase. This leads to a further reduction in the activity of the amine in the aerosol droplet and more accumulation of amine in the aerosol droplet as compared to the bulk liquid. The promoter, such as Pz, acts as a CO₂ transfer agent to the slower reacting more volatile component, such as AMP. Once the AMP reacts with the CO₂ in the form of bicarbonate it becomes non-volatile and remains in the aerosol droplet. Moreover, its activity is reduced causing further condensation of AMP on to the aerosol droplet. In the case of taurate as the promoter, it is not present in the vapour phase and therefore, cannot condense on the aerosol droplet. The AMP on its own reacts very slowly with CO₂ and does not form bicarbonate ions in the aerosol droplet. Therefore, hardly any AMP is found in the aerosol droplet when AMP-KTau is used as the solvent.

5.7 Conclusions

The level of emission by aerosols is a function of flue gas quality and operating conditions. Several parametric tests were performed which provide an insight into the mechanism of aerosol-based emissions in a CO₂ capture absorption process. Aerosol-based emissions were observed as a function of particle number concentration in the flue gas, for both the amine components when a blend of AMP-Pz was used as the capture solvent. Increasing the lean solvent temperature led to a decrease in the aerosol-based emission of MEA. This decrease was attributed to the reduction in the difference of gas and liquid temperatures at the top of the column and thus, reduction of supersaturation. At a low pH of the lean solvent, no aerosol-based emissions were observed, while as the pH of the lean solvent was increased the emissions of both AMP and Pz increased. A maximum in amine emissions was observed at 6 vol.% CO₂ as the CO₂ content in the flue gas was decreased from 12.7 to 0.7 vol.%. No aerosol-based emissions were observed when AMP-KTau was used as the CO₂ capture solvent due to the slower reactivity of AMP.

As expected, heterogeneous nucleation and growth by condensation is the main mechanism leading to aerosol-based emissions in a CO₂ capture absorption column. Moreover, the amine-CO₂ reactivity is essential for aerosol growth from volatile amine species. This is exemplified by the striking difference between AMP-KTau and AMP-Pz, where significant aerosol-based emissions of AMP were seen for the latter. It can be concluded that relatively fast reaction kinetics or the presence of volatile promoters such as Pz are required for aerosol-based emission.

The phenomenon of aerosol-based emissions from a CO₂ capture absorption presents a new facet to the current understanding of aerosol formation and growth in reactive absorption systems. The key difference as compared to already studied systems, is the varying reactivity of the volatile components with the gas phase and the presence of weak electrolytes. In order to further understand this mechanism, a dual approach of

semi-empirical modelling and performing experiments specifically to validate the model is proposed. A rigorous model similar to the modelling tool made by Wix et al., 2010, 2007^{138,142}, would be extremely difficult to formulate and validate. Thus, a semi-empirical model can be made, which includes the effect of both supersaturation and CO₂ reactivity. Further understanding of the mechanism and influence of the operating parameters on the aerosol-based emission from a theoretical point of view will help in formulating solvents which inherently do not give rise to aerosol-based emissions, design of suitable countermeasures, and guide the plant operators in the case of high aerosol-based emissions.

Chapter 6

Field study of a Brownian Demister Unit to reduce aerosol-based emission from a post combustion CO₂ capture plant.

This chapter is based on the following publication:

Khakharia, P., Kvamsdal, H.M., da Silva, E.F., Vlugt, T.J.H., Goetheer, Field study of a Brownian Demister Unit to reduce aerosol based emission from a Post Combustion CO₂ capture plant, *Int. J. Greenh. Gas Control*, 28, 57–64, 2014.

6.1 Introduction

The loss of solvent and its degradation products lead to higher operating cost as well as negative effects on the environment in and around the area of the PCCC plant¹²⁹. Typically, countermeasures such as a water wash and standard demisters are employed for emission reduction as they are capable of reducing emissions to acceptable levels (~ppm)⁷³. A water wash section consists of a packed bed with a continuous recycle of water (5–10°C lower than the gas temperature) to condense and absorb volatile components and thus, reduce their emission. Standard demisters consist of a wire mesh, which can remove droplets larger than 10 µm with 99.99% efficiency¹¹⁸. For a typical PCCC plant, it is expected that emissions of MEA are up to 12 mg/m³ STP (STP; 0°C and 101.325 kPa) and emissions of NH₃ are ca. 5 mg/m³ STP¹¹². Along with ammonia, nitrosamines and nitramines are also degradation products of amines^{50–52}. Many of these compounds are carcinogenic in nature and thus, their emissions must be limited. There is no information available for measured gas phase nitrosamine and nitramine concentrations from CO₂ capture pilot plants. The permitted total air concentration of N-nitrosamines and N-nitramines is 0.3 ng/m³ STP for the CO₂ capture facility at Mongstad, Norway, according to the permit issued by the Norwegian Climate and Pollution Agency¹¹¹.

Emissions can not only occur in the form of gaseous components, but also in the form of aerosol droplets (0). Previously mentioned countermeasures such as a water wash and a demister are not effective in removing aerosol-based emissions, as the aerosol droplets are typically much less than 10 µm (0.04 – 4 µm). These aerosol droplets follow the trajectory of the gas molecules and are not captured by the water wash or standard demisters. A Brownian Demister Unit (BDU) consists of a filter element and is able to remove very fine droplets by means of impingement and diffusion. Therefore, it is a suitable counter-measure for removal of aerosol-based emissions. To the best of our knowledge, such a counter-measure has not been tested earlier in either a laboratory or at a pilot plant scale for PCCC applications. The aim of this research work is to evaluate the efficiency of the BDU to reduce emissions from a typical PCCC process. Emissions of MEA and other degradation products (nitrosamines and nitramines), across the water wash as well as the BDU were studied using an impinger measurement technique. The BDU shows a high removal efficiency for aerosol-based MEA emissions. NH₃ and nitrosamines are not removed by the BDU as they are present in the gas phase. The possibility of scale up of BDU and its impact on the additional electricity consumption and thus, costs are also discussed. A maximum increase of 1 €/tonne CO₂ captured can be expected for a BDU in a full scale CO₂ capture plant.

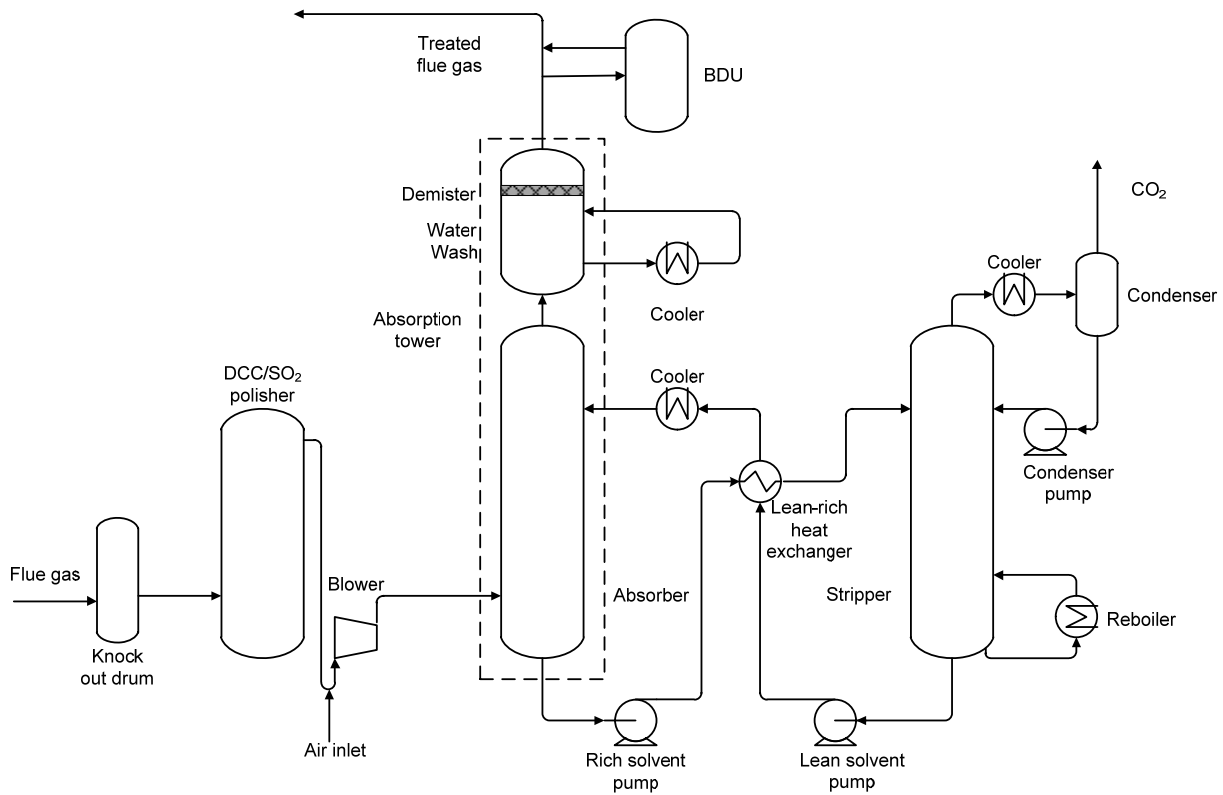


Figure 6.1. Flowsheet of TNO's CO₂ capture pilot plant at Maasvlakte, The Netherlands. The water wash section is integrated in the absorption tower but shown here as a separate unit here. It is a typical absorber-desorption based CO₂ capture plant. The BDU was installed after the wash section and prior to the emission point. The treated flue gas stream and product CO₂ stream are combined to be sent to the stack.

6.2 Test equipment and methods

6.2.1 TNO's CO₂ capture pilot plant

The tests were performed at TNO's (post-combustion CO₂ capture pilot plant located at Maasvlakte, The Netherlands. This has been described in detail in section 2.2.1 and 3.2.1. The BDU was installed after the water wash section as shown in Figure 6.1.

6.2.2 Operating conditions of the CO₂ capture plant

The flue gas was mixed with air (1:2.7, volume/volume) in order to resemble the composition of flue gas as obtained from a natural gas fired power plant. The resulting gas composition is shown in Table 6.1.

All tests were conducted over a period of two weeks. Typical operating conditions of the pilot plant are shown in Table 6.2. 30 wt.% MEA was used as the absorption solvent. The experiments associated with the BDU were part of a larger experimental campaign at the pilot plant and thus, the solvent was already in use for about 1000 h.

Table 6.1. Flue gas composition after mixing with air to the absorber of the CO₂ capture pilot plant. The temperature of the flue gas from the power plant is typically around 50°C, while the temperature of the flue gas entering the CO₂ capture absorber is ca. 25°C as it was mixed with ambient air (~15-20°C).

Component	Composition (vol.%)
CO ₂	3.4
O ₂	17.2
N ₂	76
H ₂ O	3.4*

* Depending on humidity of ambient air

Table 6.2. Range of operating conditions for the CO₂ capture pilot plant.

	Range
Flue gas flow rate	800-900 m ³ STP/h
Liquid flow rate	3-6 ton/h
Solvent inventory	2400-2600 L
Stripper temperature	113-115°C
Stripper pressure	0.9-1.1 barg
Absorber top temperature	25-35°C
Wash section temperature drop	12-14°C
Wash section specific liquid load	3.6 m ³ /m ² h

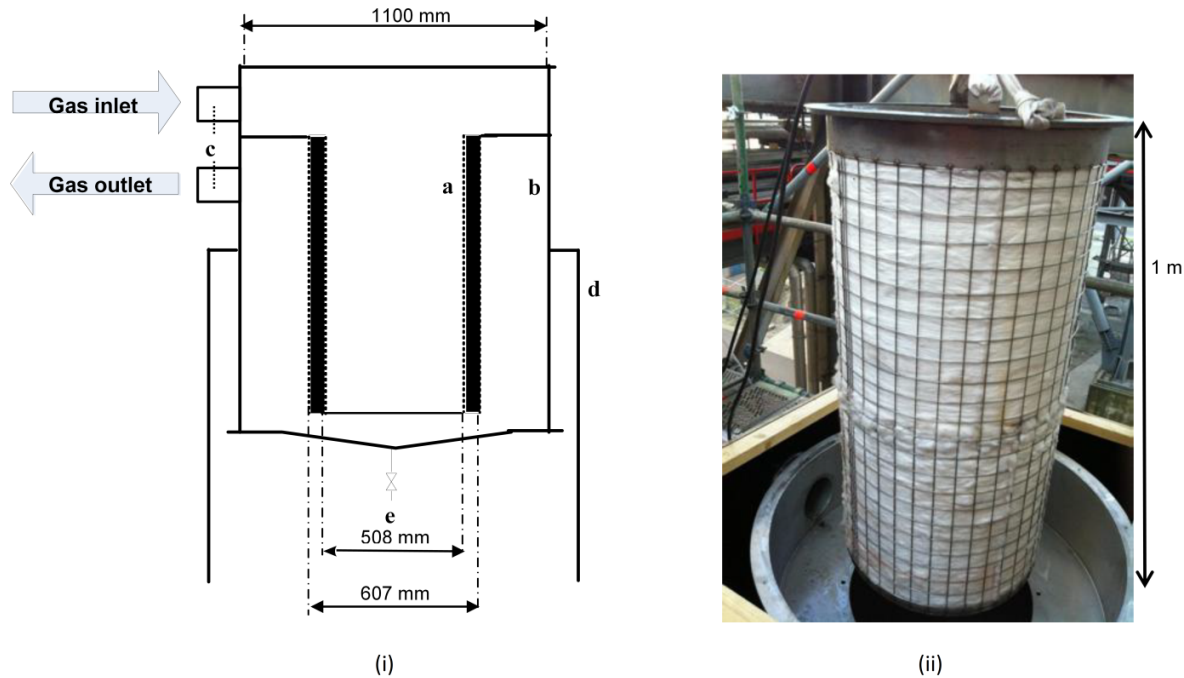


Figure 6.2. (i) Schematic representation of the BDU with the dimensions as installed at CO₂ capture pilot plant. (a) BDU filter element (polypropylene PP 13.5), (b) BDU housing, (c) sampling and measurement points, (d) stands of BDU and (e) drain collector. (ii) Polypropylene filter element (height 1 m) of the BDU at the CO₂ capture pilot plant. The housing consists of the stainless steel vessel and wooden housing in order to maintain a constant temperature.

6.2.3 Brownian Demister Unit (BDU) and its working

The BDU (Begg Cousland, U.K.) is intended primarily for the removal of very fine mist droplets of less than 2 μm . The mechanism of operation of the BDU is combination of impingement for removing particles larger than 1–2 μm and diffusion for finer particles where Brownian motion becomes predominant. The unit consists of a candle filter element made up of polypropylene (type: PP 13.5) along with a housing to maintain isothermal conditions. The filter element is installed vertically and gas passes horizontally through the filter from inside to outside. The filter element is composed of millions of fibres. Although the efficiency of each individual fibre is low, the cumulative efficiency is very high. Low approach velocities are necessary in order to attain the diffusion velocities associated with Brownian movement. Figure 6.2a shows a schematic representation of the BDU and Figure 6.2b shows the picture of the filter element during its installation. The total height of the BDU including the housing and support was 2 m. The filter element was 1 m long with an internal diameter of ca. 50 cm and a thickness of ca. 5 cm. The trapped particles coalesce and drain through the filter bed. The liquid collected in the filter can be drained and collected for further analysis. A heater was placed in order to maintain the same temperature as the gas entering the BDU and avoid any condensation.

6.2.4 Gas sampling

6.2.4.1 Impinger measurement technique

A schematic representation of the measurement technique used for gas phase sampling is as shown in Figure 6.3. The gas is sampled using a vacuum pump through an insulated probe tube in the flue gas duct. Subsequently, the gas passes through a series of three impingers placed in an ice bath. The gas velocity at the impinger nozzle is ca. 82–93 m/s for a 95% collection efficiency of 1.4–1.5 μm droplets in the first impinger. The first and second impingers are filled with sulphuric or sulfamic acid, while the third is kept empty to trap any remaining condensable components. The sampling time period was in the range of 2.5–4 h and a total 3–6 m^3 of gas was sampled. It is important to note that the final MEA concentration refers to the average emission during this sampling period. Moreover, this sampling technique captures both vapour based emissions as well as entrained droplets and aerosol droplets.

6.2.4.2 Fourier transform infrared (FTIR)

An FTIR analyser (GASMET CX 4000) was used to analyze gas phase components. This has been described in section 2.2.3.

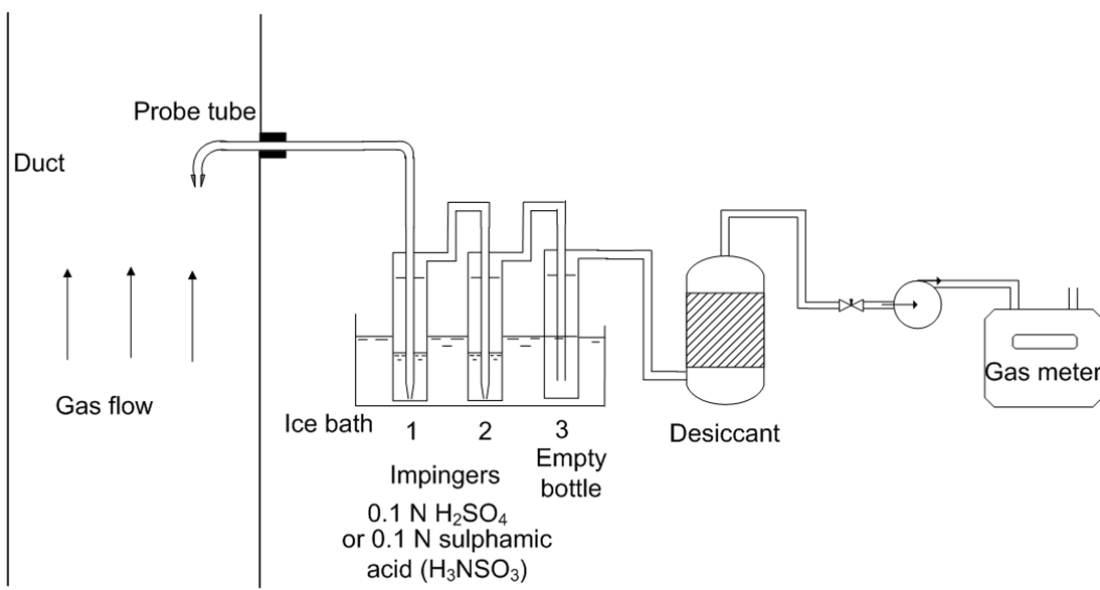


Figure 6.3. Schematic representation of the gas sampling technique used for analysing MEA and Nitrosamines in the gas phase. The gas is sucked by means of a vacuum pump through a probe tube from the duct of the gas flow. Two impingers containing liquid (sulfamic acid or sulphuric acid) captures the gaseous components and a third impinger is kept empty to trap any carryover liquid.

6.2.5 Liquid analysis

The following components: MEA, nitrosamines (N-nitrosodimethylamine, NDMA; N-morpholine, NMOR; N-nitrosodiethanolamine, NDELA) and MEA-nitramine were analyzed in samples of wash water, solvent, BDU condensate, and impinger liquids (sulfamic acid and sulphuric acid). The components were measured using tandem liquid chromatography triple quadruple mass spectrometry (LC–MS–MS–QQQ) technique on an Agilent1290/6460 instrument (Agilent Technologies, USA). The samples were prepared by dilution, direct injection, or sample preparation by liquid-liquid or solid phase extraction. The limits of quantitation were: 0.6 µg/L for MEA and 0.1 µg/L for NDMA, NMOR, NDELA and MEA-nitramine in solution. More information can be found in literature¹⁶⁷.

6.3 Results and discussion

6.3.1 MEA emissions

Public information about emission of amines from CO₂ capture plants is limited due to the confidential nature of the used solvent and its components. However, there are a few reports of MEA emissions from pilot plants as it is a widely tested and used solvent. MEA emissions in the range of 0.02–0.7 mg/m³ STP have been measured at the pilot plant of Dong Energy at Esbjerg (Denmark) using an impinger measurement technique¹⁶⁸. MEA emissions of 4 mg/m³ STP (maximum) have been reported from a mobile CO₂ capture pilot plant of Aker Clean Carbon at Longannet (Scotland)¹⁶⁹. The

Table 6.3. MEA emission measurements across the water wash and the BDU using impingers along with its removal efficiency. Test periods represent averages over sampling time period of 2.5–4 h.

	Before water wash (mg/m ³ STP)	After water wash and demister (mg/m ³ STP)	Before BDU (mg/m ³ STP)	After BDU (mg/m ³ STP)	Water wash removal efficiency (%)	BDU removal efficiency (%)
Test period 1	407.4	241	156.9	1.2	40.8	99.2
Test period 2	466	251.6	173.2	2.1	46	98.8

pilot plant of NCCC at Alabama (USA) have reported MEA emission values of 354 mg/m³ STP of droplet (aerosol and carryover) emission, while the vapour based emissions are ca. 12 mg/m³ STP¹⁷⁰.

In Table 6.3, the results of measured MEA emission across the water wash as well as the BDU are presented. The water wash section reduces the inlet MEA emissions from 460 to 250 mg/m³ STP (~46%). The removal in the water wash section is a combination of solvent condensation, water washing, and droplet removal by the demister. The expected vapour MEA emission at the absorber outlet (before the water wash section) is ca. 200 mg/m³ STP at the corresponding temperature of ca. 30–40°C. The MEA emission at the outlet of the water wash is expected to be lower than at least 5 mg/m³ STP based on an in-house model from SINTEF⁷³. The model predicts the emission values considering the thermodynamic equilibrium of the components at the actual operating conditions. The MEA emissions measured across the water wash and the BDU inlet are much higher than the values obtained from the model.

Additionally, solvent entrainment tests were performed using lithium and rubidium carbonate (Li_2CO_3 , Rb_2CO_3) as tracers. These tests indicated no major contribution to emissions after the water wash due to solvent entrainment or carryover. This implies that along with vapour based emission there is a significant contribution due to emission by aerosols. There seems to be a further reduction in MEA emissions after the water wash and before BDU by about 30–35%. This is likely due to the different sampling conditions in the duct for the probe tube of the impingers (see Figure 6.3). The velocity in the duct ($\phi = 0.65$ m) for the sampling across the water wash section is ca. 0.7 m/s, while the velocity in the duct ($\phi = 0.13$ m) for sampling across the BDU was ca. 17 m/s. This could lead to non-isokinetic sampling in the impingers. Nevertheless, the measured MEA emission levels are of the same order of magnitude and thus, a relative comparison is justified.

Table 6.4. MEA emission measurements across the BDU and the corresponding removal efficiency of the BDU.

	MEA before BDU (mg/m ³ STP)	MEA after BDU (mg/m ³ STP)	BDU removal efficiency (%)
Test period 3	86.6	1.2	98.6
Test period 4	128.8	1	99.2
Test period 5	152.1	1.3	99.2
Test period 6	139.3	1.9	98.6
Test period 7	178.9	4	97.8

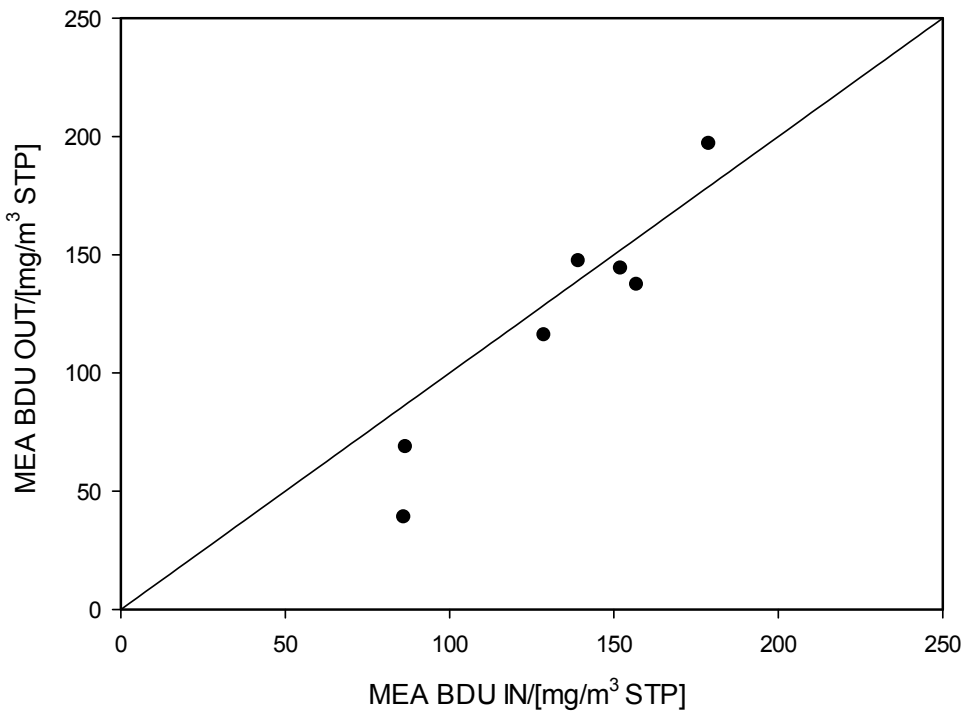


Figure 6.4. MEA levels entering and leaving the BDU represented as mg/m³ STP (dry gas) for the different tests. BDU OUT (vertical axis) is the sum of the MEA emission in the gas phase at the BDU outlet and its concentration in the collected liquid. BDU IN (horizontal axis) is the MEA emission in the gas phase at the BDU inlet.

Table 6.4 presents the results of MEA gas phase measurements before and after the BDU using an impinger measurement technique. MEA emissions at the BDU inlet are in the range of 85–180 mg/m³ STP. For all the tests, the BDU shows a removal efficiency of larger than 97%. This results in MEA emission after the BDU of below 5 mg/m³ STP and mostly below 2 mg/m³ STP. The BDU removes most of the aerosol-based emission and MEA is present only in the vapour phase at the BDU outlet. The MEA emissions at the BDU outlet remain relatively constant as vapour emission depends only on the temperature which also remains constant at the BDU

outlet. Therefore, the water wash is capable of reducing vapour based emissions, while the BDU is capable of removing only aerosol-based emissions.

The MEA emission levels at the BDU inlet vary significantly as shown in Table 6.3 and Table 6.4. Aerosol-based emissions have been attributed to several factors and flue gas composition being the most important amongst all the factors (Chapter 4 and Chapter 5). The flue gas quality can vary on a day to day basis leading to varying extent of aerosol-based emissions. Moreover, the gas sampling before and after the BDU was performed at different time period on the same day using the same apparatus. As mentioned earlier, these results represent an average over a sampling period of 2.5–4 h and thus, certain variations in the measured emissions are expected. Nevertheless, the values are in the same order of magnitude.

6.3.1.1 MEA mass balance across BDU using impinger measurements

The droplets removed by the BDU were collected for further analyses. The MEA concentration was measured in the collected liquid at the end of each test period. Based on the measured MEA emission levels across the BDU and its concentration measured in the collected liquid, the mass balance of MEA across the BDU can be validated.

The MEA levels entering and leaving the BDU for the different tests are as shown in Figure 6.4. The mass balance of MEA across the BDU is closed up to 80%. This can be considered as acceptable considering the approximations and error associated with the sampling and measurement techniques. The MEA emission levels at the BDU out-let are very low (1–4 mg/m³ STP) and thus, the measured value could have a significant error associated with it. Moreover, all the droplets entrained in the BDU may not have necessarily been rinsed off the BDU surface as no additional back flow of inert gas or water was used for rinsing the filter element.

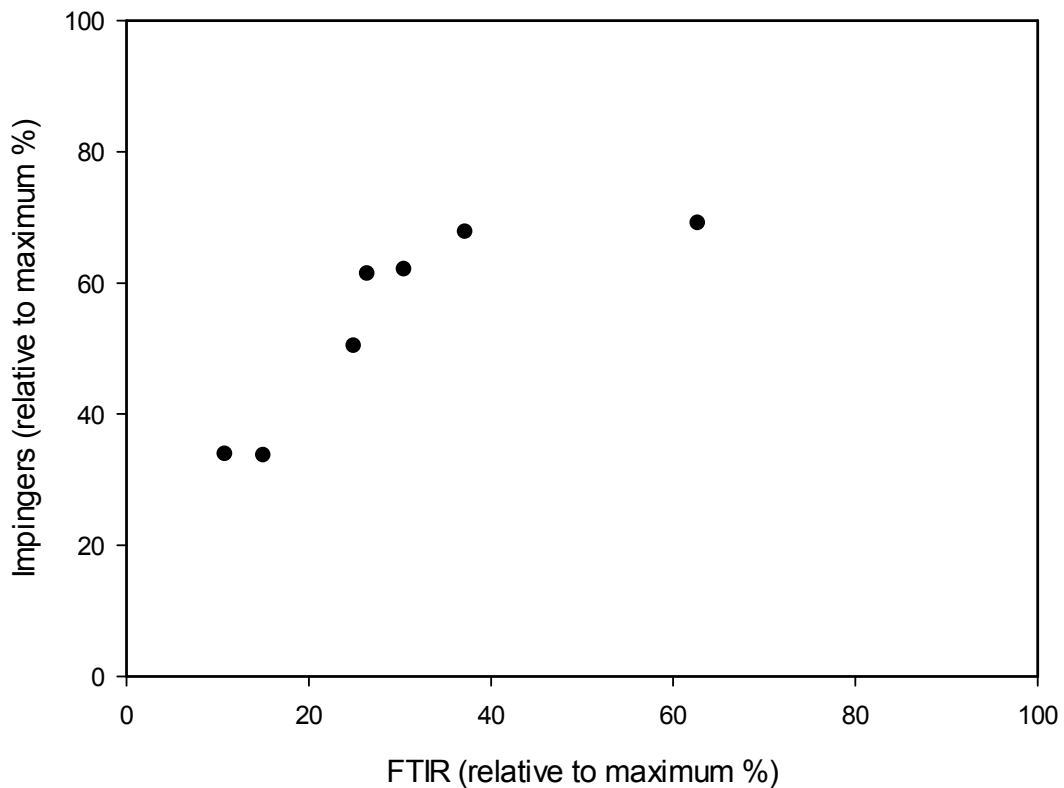


Figure 6.5. MEA emission at the BDU inlet as measured by impingers and FTIR normalized to their respective maximum value of $256 \text{ mg/m}^3 \text{ STP}$ and $33 \text{ mg/m}^3 \text{ STP}$, respectively.

6.3.1.2 Comparison of impinger measurements with FTIR for MEA

Along with gas sampling using impingers, an FTIR was also installed to measure the components in the flue gas across the BDU. The sampling location for FTIR was the same as that for the impinger measurements. It has been observed in literature that the absolute emission levels measured by each of this measurement technique vary significantly especially in the presence of aerosols and therefore, comparison based on absolute emission numbers is not recommended⁶⁹. Nevertheless, the trend in both the measurement technique is comparable as shown in Figure 6.5.

The emission level at the inlet of the BDU as a percentage of the maximum value of the respective measurement technique is plotted for each of the tests. The maximum MEA emission values for the FTIR and impinger measurement technique are $33 \text{ mg/m}^3 \text{ STP}$ and $256 \text{ mg/m}^3 \text{ STP}$, respectively. The emission levels at the outlet of the BDU are very low and they are close to the minimum limit of detection by these methods and thus, no clear trend is observed. To compare the absolute emission levels as measured by each of the technique at different sampling conditions, further improvement and validation are necessary.

Table 6.5. Measured concentration of nitrosamines (NDELA, NDMA and NMOR) in the absorption liquid, water wash liquid and gas inlet of BDU at the CO₂ capture pilot plant.

		Absorption liquid (ng/ml)	Water wash liquid (ng/ml)	BDU Inlet concentration (ng/m ³ STP)
Test period 1	NDELA	2056.2	1	13.5
	NDMA	<100	<10	7.3
	NMOR	<250	<25	4.8
Test period 2	NDELA	2048	0.4	47
	NDMA	<100	<10	8.3
	NMOR	<250	<25	22

Table 6.6. Measured MEA-nitramine concentration in the absorption liquid, water wash liquid and BDU drain.

	Absorption liquid (ng/ml)	Water wash liquid (ng/ml)	BDU drain (ng/m ³ STP)
Test period 1	1399.1	<5	37.7
Test period 2	1418.1	<5	39.2
Test period 3	1780.3	<5	25.9
Test period 4	1848.6	<5	-

6.3.2 Nitrosamines and nitramine

Nitrosamines and nitramines are secondary degradation products of MEA. These compounds are formed as result of the reaction of absorbed NO_x from the flue gas with the amines (primary and secondary) in the solvent ^{49-52,171}. The measured nitrosamines were N-Nitrosodiethanolamine (NDLEA), N-Nitrosodimethylamine (NDMA) and N-Nitrosomorpholine (NMOR). These components were measured in the absorption and water wash liquid. The gas sampling using impinger measurement technique was performed across the BDU. The analytical results are presented in Table 6.5.

In the absorption and water wash liquid, only NDELA was found to be above the limit of quantification. NDELA is present in the order of 2000 ng/ml in the absorption liquid, while in the water wash liquid its concentration is ca. 1 ng/ml. The measured nitrosamine levels across the BDU is in the order of 10s of ng/m³ STP which can be considered to be extremely low and close to the detection limit of the measurement technique. There was no significant reduction in the nitrosamine levels across the BDU. This implies that the nitrosamines were not present in the aerosol droplets but only in the vapour phase. The dispersion factor determines the actual ground level concentration of a gaseous component. If a dispersion factor of 100 is considered, the actual ground level concentration of nitrosamines would be less than 0.1 ng/m³ STP ¹⁰². Thus, the air concentration of nitrosamines would be below the permitted value of 0.3 ng/m³ STP ¹¹¹.

Table 6.7. Ammonia (NH_3) gas phase measurements across the BDU measured by FTIR. The FTIR switches its sampling location over the BDU inlet and outlet every 30 min. Therefore, the emission measurements are average values over 30 min and the inlet and outlet measurements are 30 min apart.

	NH_3 before BDU (mg/m ³ STP)	NH_3 after BDU (mg/m ³ STP)
Test period 1	28 (21-38)	28 (20-38)
Test period 2	25 (20-29)	23 (17-28)
Test period 4	45 (10-80)	50 (27-91)
Test period 6	21 (17-24)	20 (17-23)
Test period 8	69 (34-95.5)	71 (37-95)
Test period 9	13 (12-16)	13 (11-15)

In

Table 6.6, the measured MEA-nitramine concentration in the absorption liquid, water wash liquid and the drain collected in the BDU are presented. MEA-nitramine concentration in the absorption liquid ranges from 1400 to 1900 ng/ml. It is below the limit of quantification of 5 ng/ml in the water wash liquid. To the best of our knowledge, the results presented here are the only available information about MEA-nitramine from MEA based CO_2 capture process in open literature. The measured MEA-nitramine concentration in the drain of the BDU is in the range of 26–40 mg/m³ STP, which is in the same order of magnitude as NDELA. No data is available for the MEA-nitramine in the gas phase across the BDU.

6.3.3 NH_3 emissions

The presence of oxygen in the flue gas leads to oxidative degradation of amines. NH_3 is one of the major oxidative degradation product ^{38,108}. NH_3 concentrations were measured across the BDU by FTIR. The measured NH_3 concentration across the BDU is in the range of 10–70 mg/m³ STP as shown in Table 6.7.

These values are typical for CO_2 capture pilot plant using an aged solvent, as used in the tests here ^{129,170}. No significant reduction in NH_3 levels was measured across the BDU. This is expected since NH_3 is highly volatile and thus, present only in the gas phase and not in the aerosol phase. For some of the tests the NH_3 concentration at the outlet of the BDU is higher than at the inlet, but within the same order of magnitude (± 20%). This could be due to the following reason. The NH_3 emission levels are measured by FTIR which switches its sampling location every 30 min across the BDU and thus, it was not possible to have measurement points of the BDU inlet and outlet for the same time period. Moreover, the NH_3 emission values are averages during a test period of 2.5–4 h.

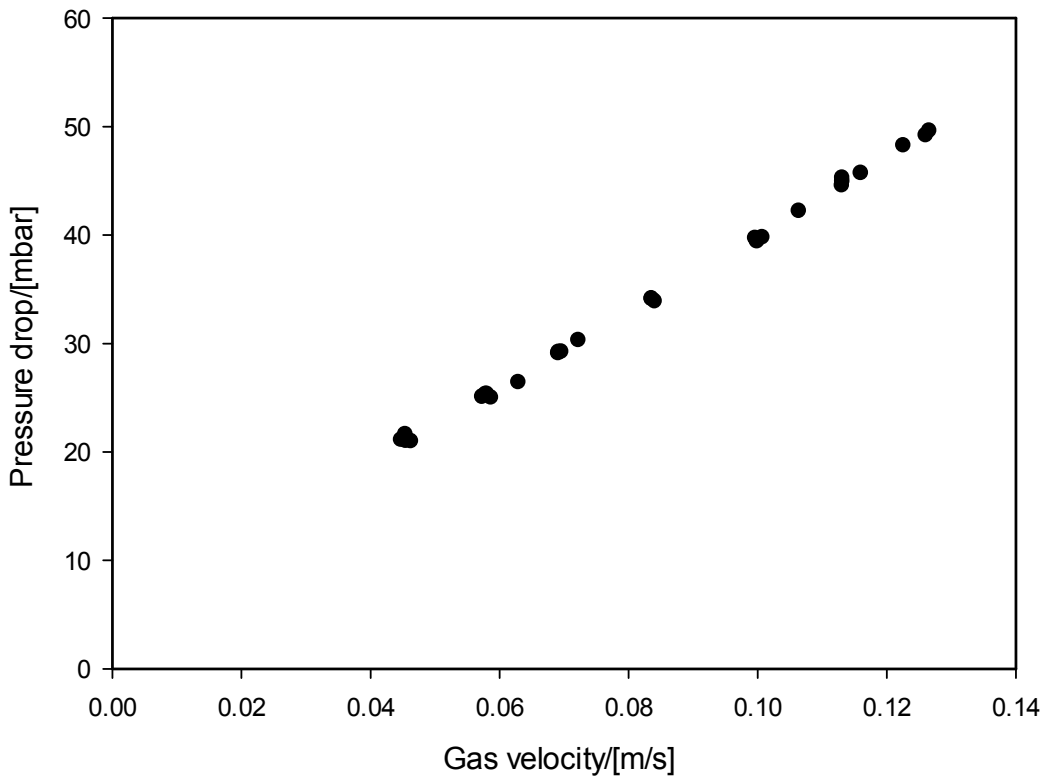


Figure 6.6. Pressure drop across the BDU as a function of the gas velocity through the filter element.

Table 6.8. Effect of pressure drop increase by BDU on electricity consumption and costs for a full scale CO₂ capture plant excluding CO₂ compression. The electricity consumption by the Lean Vapour Compressor is included. Price of electricity is assumed to be 0.057 €/kWh.

	Pressure drop (mbar)	Total Electricity consumption [GJe/ton CO ₂ captured]	Electricity Costs [€/ton CO ₂ captured]	% Increase in electricity consumption/cost
Without BDU Base case	50	0.117	1.85	-
With BDU Case a)	100	0.148	2.34	26
With BDU Case b)	150	0.178	2.82	52

6.3.4 Application of a BDU for a full scale CO₂ capture plant

The high droplet removal efficiency of the BDU is attributed to the low velocities in the fibre elements. A disadvantage of this is the resulting increase in pressure drop. A test was performed to investigate the effect of the different flue gas flow rate and thus, velocities on the pressure drop across the BDU as shown in Figure 6.6.

As expected, the pressure drop linearly increases with the flue gas flow rate. At the operating flue gas flow rate of 900 m³ STP/h (velocity through filter ~0.13 m/s), the pressure drop across the BDU was ca. 50 mbar. This implies if the flue gas flow rate is increased to 1800 m³ STP/h, the corresponding pressure drop across a single BDU would be at least 95 mbar based on extrapolation of the existing experimental data. However, it is expected that for higher flue gas flow rate several filter elements will be used in parallel resulting in a lower pressure drop per cubic metre of gas flow. The additional increase in pressure drop across the BDU has to be provided by the flue gas blower before the absorber column. This would have a significant impact on the electricity consumption and therefore, the operating costs, especially for a full scale capture plant. For a 800 MW coal fired plant, the flue gas flow rate is expected to be around 1,152,000 m³ STP/h based on a flue gas density of 1.2 kg/m³ STP ¹³⁴. The CO₂ capture plant includes a Lean Vapour Compression configuration to minimize the reboiler duty ¹⁷². The exact velocity and thus, the pressure drop across the BDU depend on the design of the BDU filter element, droplet load, etc. Two cases can be considered: (a) pressure drop of 50 mbar across BDU and (b) pressure drop of 100 mbar across the BDU. The pressure drop of 50 mbar across the BDU can be considered as the best case since based on experiments performed here, a pressure drop of 50 mbar was already obtained at 900 m³ STP/h (0.13 m/s) in a single filter element. The 100 mbar pressure drop case can be assumed to be the worst case scenario.

Table 6.8 presents the resulting increase in the electricity consumption and the corresponding increase in operational electricity costs. Typically in a CO₂ capture plant, electricity is used by pumps, blower and in the present process configuration, also by a Lean Vapour Compressor. CO₂ compression electricity requirements are not included. The blower has to overcome a minimum pressure drop of 35 mbar across the absorber. An increase of 50 mbar (case a) in pressure drop for the blower results in ca. 26% increase while, for additional 100 mbar (case b) of pressure drop results in 52% increase in the total electricity consumption in the CO₂ capture plant. The corresponding increase in operational costs is ca. 1 €/tonne CO₂ for every 100 mbar increase in pressure drop. If the total cost is considered to be 50 €/tonne CO₂ captured then the BDU would lead to a maximum of 2% increase in the total cost of CO₂ captured. The total amount of CO₂ captured in a year for a full scale CO₂ capture plant is ca. 4 million tonne of CO₂/year. Therefore, the corresponding increase in yearly operational costs can be in the order of millions of euros per year.

6.4 Conclusions

The objective of this study was to evaluate the efficiency of a BDU for removal of amines (MEA, NH₃), nitrosamines and nitramine. High level of MEA emissions are attributed to aerosol-based emissions during the test period. The water wash was effective in removal of vapour based emissions, while the BDU is effective in removing aerosol-based MEA emissions. The use of the BDU reduced MEA emissions from ca. 85–180 mg/m³ STP to ca. 1–4 mg/m³ STP, resulting in an efficiency of larger than 97%. Emissions of ammonia were in the range of 10–70 mg/m³ STP. The BDU was not effective in reducing ammonia emissions, as it is highly volatile and present only in the vapour phase. The measured nitrosamines (NDELA, NMOR and NDMA) in the treated flue gas stream from the absorber are very low and in the order of 10 ng/m³ STP (around the limit of detection). The BDU was not effective for removing nitrosamines suggesting they are present in the vapour phase. The BDU creates a significant additional pressure drop (~50 mbar) for the blower based on the configuration and type of BDU used in this study. The additional pressure drop leads to an increase in the electricity consumption by the blower. For a full scale CO₂ capture plant, the increase in electricity consumption can be in the range 26–52% and can lead to increase in operating cost by 1 €/tonne CO₂ for every 100 mbar increase in pressure drop. The corresponding increase in the total cost of CO₂ capture is ca. 2%. The application of BDU for a full scale CO₂ capture plant will depend on the seriousness of the issue of aerosol-based emission, alternative countermeasures and efficient design to have a minimum impact on blower pressure drop and thus, operational costs.

Chapter 7

Predicting aerosol-based emissions in a post combustion CO₂ capture process using an Aspen Plus model.

This chapter is based on the following publication:

Khakharia, P., Mertens, J., Vlugt, T.J.H., Goetheer, E., Predicting Aerosol Based Emissions in a Post Combustion CO₂ Capture Process Using an Aspen Plus Model, *Energy Procedia*, 63, 911–925, 2014.

7.1 Introduction

Apart from energy losses, amine losses due to emissions, thermal degradation and oxidative degradation are a major concern as these not only increase the operating cost, but also lead to adverse environmental effects^{69,129}. There are two types of solvent losses due to emissions: (1) emissions due to the component's volatility (vapour emission), and (2) emissions due to aerosols (aerosol emission)¹⁴⁶. Here the word 'aerosols' refers to 'aerosol droplets'. Solvent loss by means of mechanical entrainment can be easily controlled and therefore, not considered to occur in PCCC.

The amount of vapour emissions is (amongst others), a function of the volatility of the amine, loading of the solvent and the temperature of the gas phase^{173,174}. A number of studies (both experimental and theoretical) have been carried out to understand volatility based solvent emissions from PCCC plants^{66,69,174,175}. To reduce vapour emissions, the use of a water wash at the top of the absorber column has shown to be effective¹⁷³. MEA emissions of ca. 1.4 mg/m³ STP (STP; 0°C and 101.325 kPa) in the treated flue gas stream after water wash can be achieved⁷¹. However, the water wash section at the top of the absorber column is ineffective in controlling aerosol-based emissions^{137,173}.

The mechanism of aerosol formation and growth is related to the degree of supersaturation. The degree of supersaturation of flue gas (S) can be calculated using the following equation;

$$S = \frac{P_C(T, y_1, y_2 \dots y_n)}{P_{CS}(T, y_1, y_2 \dots y_n)} \quad (1)$$

where P_C is the total partial pressure of all condensing vapour component at the actual temperature T and mole fraction, y_i of the supersaturated gas, and P_{CS} is the total partial pressure of all the condensing components corresponding to the phase equilibrium¹³⁷.

If the supersaturation exceeds a critical value, nucleation takes places and nuclei are formed by molecules of condensing components (homogeneous nucleation) and/or on the impurities in the flue gas (heterogeneous nucleation). Heterogeneous nucleation is induced at low supersaturation ratio ($S \sim 1$) whereas, homogeneous nucleation occurs at higher supersaturation ratio ($S > 2$)^{137,146}. Heterogeneous nuclei present in the flue gas entering the absorber could be for instance sulphuric acid aerosols. Flue gas leaving the flue gas desulphurisation unit of typical coal fired power plant has been reported to have H₂SO₄ concentration in the range of 1 to 12 parts per million (ppm) equivalent of SO₃⁸⁵. The presence of impurities like H₂SO₄ in the flue gas can initiate heterogeneous nucleation even at very low supersaturation¹³⁷. The relation of the H₂SO₄ aerosols and the corresponding particle number concentration to the emissions of the solvent has been proved in Chapter 4.

Understanding and modelling of vapour emissions are relatively straight forward^{66,173,174}. Aerosol-based emission is a more complex phenomena to model and to predict.

However, modelling is an indispensable tool to understand the complex mechanism and predict the extent of aerosol-based emissions. The developed model should be accurate and at the same time be robust. As a first step, this study presents a simplified modelling approach to predict aerosol emission as a function of the operating conditions. The methodology is implemented in Aspen Plus which is a commercially available flow sheeting tool. This model is intended to serve the purpose of understanding and predicting trends. The modelling tool is an approximation and the exact local conditions within the plant can differ. Hence, it should be noted that values reported can only be compared qualitatively with experimental results.

7.2 Modelling approach and assumptions

7.2.1 Methodology

To model a CO₂ absorption column, mass and heat transfer processes occurring in each of the phase need to be solved simultaneously. However, standard flowsheeting tools such as Aspen Plus do not have the option of introducing an additional phase in an absorption column. Therefore, in this study a simplified modelling approach was used to understand aerosol-based emissions in a reactive absorption process using standard flowsheeting tools such as Aspen Plus. This is shown in Figure 1a. The absorption liquid flows counter-current to the gas phase, while the aerosol phase is co-current to the gas phase. The absorber column is divided into smaller sections and instead of the simultaneous mass and heat transfer process of all the three phases, the process is divided into two steps. The first step is the counter-current contact between liquid and gas phase. The second step is the co-current contact of aerosols with the resulting gas phase from the first step. It is assumed that there is no direct contact between the absorption liquid phase and the aerosols.

7.2.2 Implementation in Aspen Plus

The process simulation software, Aspen Plus V8.0 was used as the modelling tool. A single absorption column is divided into smaller absorber sections. Each section consist of two calculation blocks. In the first calculation block, the mass and heat transfer of the counter current gas-liquid absorption is solved using a rate based absorber model. In the second calculation block, a plug flow reactor (PFR)¹⁷⁶ model is used to simulate the co-current contact between aerosols and gas phase. Figure 1b represents the generic section '*i*' of the model. Treated flue gas from section '*i*' is mixed with the aerosols of section '*i+1*' before entering PFR model. The outlet stream of PFR model at section '*i*' is flashed to separate gas phase and aerosols before entering the next section '*i-1*'. Rich solvent from section '*i-1*' enters section '*i*' as lean solvent. Similarly, treated flue gas from section '*i+1*' is the inlet flue gas to section '*i*'.

The dimensions (length and diameter) of the PFR are similar to that of the absorber column. The PFR and flash drum operates at the same temperature and pressure as the

gas phase. To demonstrate the discretization method and to quantify the aerosol-based emission, a base case was defined as follows,

- An absorber column with a packing height of 20 m and 21 m diameter is divided into 10 sections with height of 2 m each
- A 90 % CO₂ removal from the flue gas
- A 30 MEA wt. % absorption liquid
- Lean loading of 0.23 mol CO₂/mol MEA

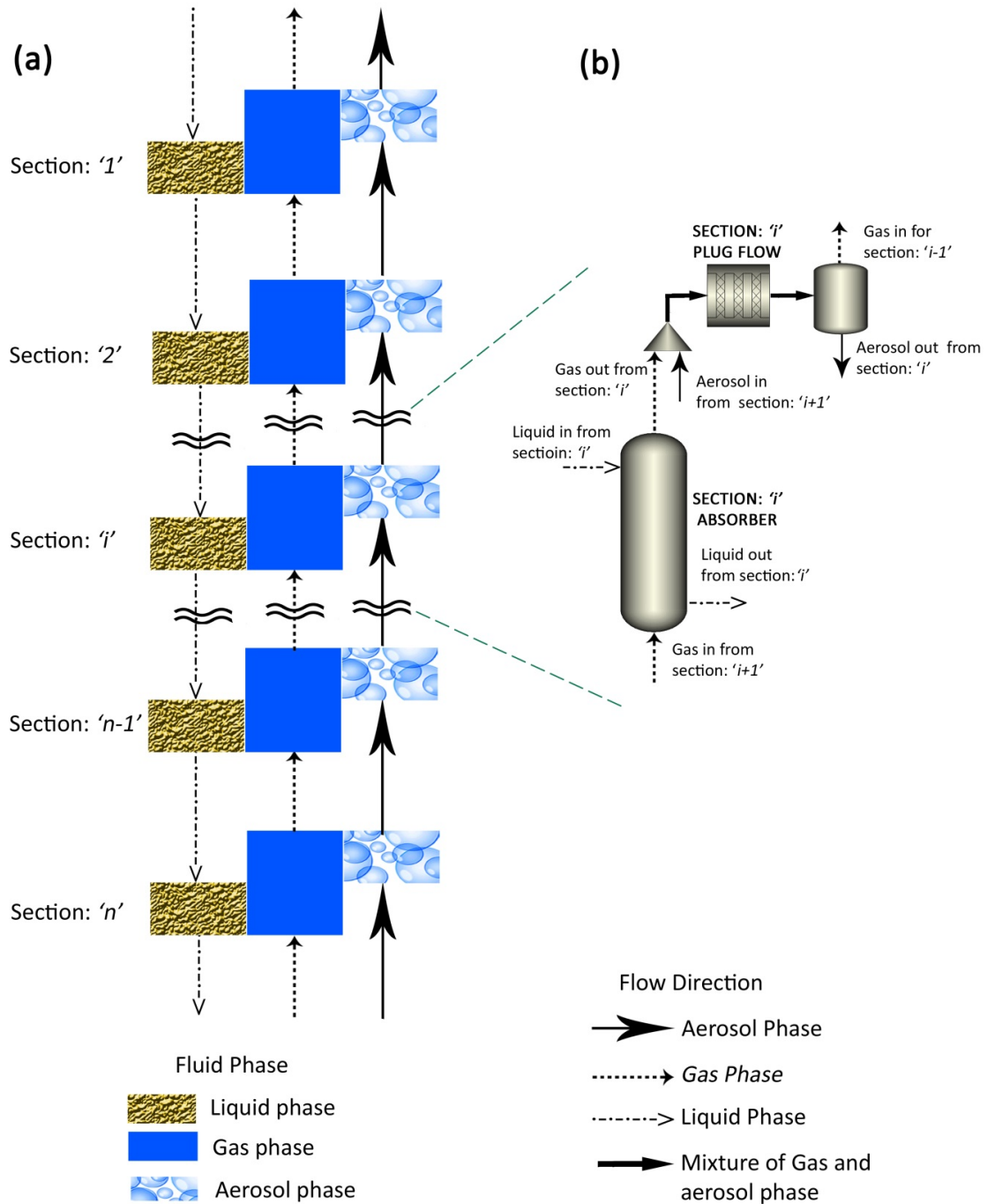


Figure 7.1. (a) Schematic representation of the modelling approach. Flue gas and aerosols enters the absorber section 'n' and lean solvent enter the absorber at section '1'; (b) Schematic representation of generic section 'i' as modelled in Aspen Plus. Aerosol phase and flue gas co-current mass and heat transfer process occurs in the Plug Flow Reactor. The solvent and flue gas counter current mass and heat transfer process occurs in the absorber column.

Table 7.1 Base Case - Inlet stream specification for the flue gas and the lean solvent.

Parameter	Flue gas	Solvent
Temperature (°C)	48	40
Flow rate (kg/sec)	616	2341
Pressure (bar)	1.016	1.016
Loading (mol CO ₂ /mol MEA)	-	0.23
Composition		
Molecule	mole fraction (Flue gas)	mass fraction (Solvent)
H ₂ O	0.1127	0.655
MEA	-	0.295
CO ₂	0.133	0.05
N ₂	0.7162	-
O ₂	0.0381	-

Table 7.2: Aspen Plus model equipment specification.

Parameter	Value
Absorber (each section)	
Packing type (-)	Norton IMTP (50 mm)
Packing material (-)	Metal
Absorber total height (m)	20
Absorber diameter (m)	21
Absorber sectional height (m)	2
Sectional Packing height (m)	2
Packing diameter (m)	21
Stages (-)	2
Plug Flow Reactor	
Length (m)	2
Diameter (m)	21

Table 7.3: Solution chemistry and kinetic reactions for MEA-CO₂-H₂O system.

Reaction name	Stoichiometry
Equilibrium	
Water Dissociation	2 H ₂ O \leftrightarrow H ₃ O ⁺ + OH ⁻
CO ₂ hydrolysis	CO ₂ + 2 H ₂ O \leftrightarrow H ₃ O ⁺ + HCO ₃ ⁻
Bicarbonate dissociation	HCO ₃ ⁻ + H ₂ O \leftrightarrow H ₃ O ⁺ + CO ₃ ²⁻
Carbamate Hydrolysis	MEACOO ⁻ + H ₂ O \leftrightarrow MEA + HCO ₃ ⁻
Amine Protonation	MEA ⁺ + H ₂ O \leftrightarrow MEA + H ₃ O ⁺
Kinetic	
Carbamate formation	MEA + CO ₂ + H ₂ O \rightarrow MEACOO ⁻ + H ₃ O ⁺
Bicarbonate formation	CO ₂ + OH ⁻ \rightarrow HCO ₃ ⁻

The flue gas flow rate and composition for 600 MWe coal fired power plant are considered for this study⁸⁰. Table 7.1 shows the flow rate and composition of flue gas and lean solvent. and Table 7.2, the specifications of absorber model used in Aspen Plus. The corresponding liquid to gas ratio (L/G) is 3.5 kg of liquid/kg of gas.

A rate based absorber model (Rad Frac is the rate based model frame work in Aspen Plus) is used. The Electrolyte - NRTL (ELECNRTL) model in Aspen Plus is used to describe the thermodynamic property of the given H₂O-MEA-CO₂ system. The chemical reactions kinetics (MEA REA in Aspen Plus V8.0) considered for absorber and PFR model⁸⁰ are as shown in Table 7.3.

The input parameters to the Aspen Plus model for the aerosols are inlet volume and composition and are calculated as follows:

- Step: 1. Assume a diameter for the aerosol droplet, say 0.1 μm .
- Step: 2. Calculate the volume of a single aerosol by considering it as perfect sphere
- Step: 3. Calculated volume in step 2 is multiplied with the aerosol number concentration to obtain the total volume of aerosol per m³ gas phase.
- Step: 4. Multiply the value in step 3 with total volume of flue gas to obtain the inlet volume flow of aerosols in m³/s.
- Step: 5. The sulphuric acid amount in the aerosols is calculated by multiply the expected sulphuric acid concentration (say 3 mg/m³ STP) with the total gas volume

7.2.3 Assumptions

Several assumption have been used in order to simplify the modelling approach. They are as follows;

- 1. The aerosols number concentration is typically in the range of 10¹³ to 10¹⁴ per m³ of gas (Chapter 4, ¹⁶⁵). Here, the particle number concentration is assumed to be constant and equal to 10¹⁴ per m³ of gas, and the H₂SO₄ concentration is assumed to be 3 mg/m³ STP. Moreover, no coagulation or deposition of aerosols is considered.
- 2. The aerosol phase is modelled as bulk liquid phase
- 3. No nucleation in the absorber column (i.e. only growth of the aerosol is studied).
- 4. Chemical reactions take place only in liquid phase.
- 5. No direct contact between liquid phase and aerosols (i.e. mass and heat transfer process takes place only between the aerosols and gas phase).
- 6. The overall mass transfer of CO₂ and MEA is predominately liquid phase controlled. Therefore, the assumption can be made that surface area of the aerosols can be neglected.

7. The Kelvin effect is neglected. The vapour pressure for a curved surface will be larger than that of the flat surface. This increase in vapour pressure is described by Kelvin effect ¹⁷⁷ :

$$\ln \frac{p}{p_0} = \frac{2\gamma V_m}{rRT} \quad (2)$$

Here, p is the actual vapour pressure, p_0 is the vapour pressure over a flat surface, γ is the surface tension, V_m is the molar volume of the liquid, r is the radius of the droplet, R is the universal gas constant, and T is the temperature. Small liquid droplets like aerosols will exhibit a higher effective vapour pressure, since the surface area is larger in comparison to the volume. As the size of the aerosols increases, the effective vapour pressure decreases and the droplets grow into bulk liquid. It can be easily verified using eq. 2, that H₂O aerosols with a size larger than 25 nm in radius at any temperature above 30°C, the vapour pressure over the curved surface will be equal to a flat surface *i.e.* the effect of surface curvature can be neglected. Therefore, in order to simplify the modelling approach the Kelvin effect is neglected.

7.3 Results and discussion

In this section, some of the main parameters of the absorber section in a PCCC process will be studied as an initial step towards understanding aerosols based emission. Starting from the base case, the sensitivity of the following parameters on the aerosol-based emissions is evaluated,

- CO₂ concentration in the inlet flue gas
- Lean solvent temperature
- Lean solvent loading (mol CO₂/mol MEA)

By studying the impact of the above mentioned parameters on the supersaturation profile an insight into the mechanism of aerosol-based emission can be obtained.

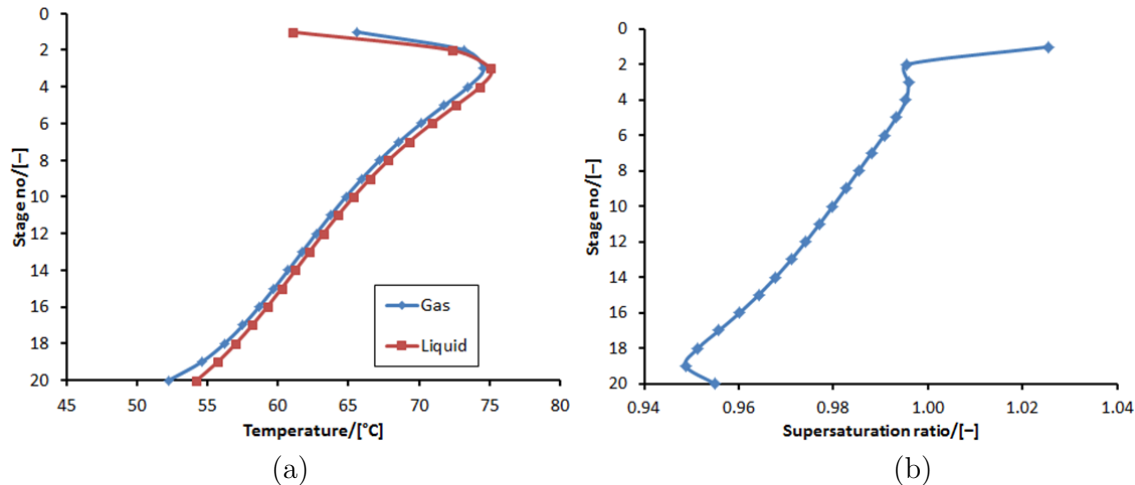


Figure 7.2. (a) Temperature profile, and (b) Supersaturation profile along the absorber column for the case with no aerosols in the flue gas.

7.3.1 Base case

For the base case, the entire absorber column without discretizing into sections and no aerosols is simulated. The degree of supersaturation of the flue gas is calculated using Eq. 1. Figure 7.2 shows the temperature and supersaturation profile across the absorber column. The temperature of the gas increases as the gas moves up the column due to the exothermic reaction between CO₂ and MEA. The temperature of the flue gas reaches its peak (*i.e.* hot zone), typically at 2/3 of the column for the chosen liquid to gas ratio. The increase in temperature along the column leads to increase in the partial pressure of volatile components such as water and MEA. This increase in partial pressure of the volatile components leads to an increase in the supersaturation ratio, however, remains below 1 until stage 2. Above the hot zone, the flue gas temperature decreases by the incoming relatively colder lean solvent. This results in a drastic decrease of the gas temperature forming a temperature bulge inside the absorber column. The temperature bulge can be defined as difference between maximum (hot zone) and top temperature of the flue gas in the absorption column. The drastic temperature decrease leads to a crossover of the gas and liquid temperatures, with the gas being hotter than the liquid in stage 1 and 2. This leads to a significant increase in the supersaturation ratio and reaches a maximum of ca. 1.03 at the top of the column. Therefore, there is a potential for heterogeneous nucleation in the zone where $S>1$ resulting in the growth of aerosols by condensation of water and MEA. It can be inferred that reducing the difference between the gas and liquid temperatures, reduces the supersaturation ratio and thereby, lowering the potential for aerosol formation.

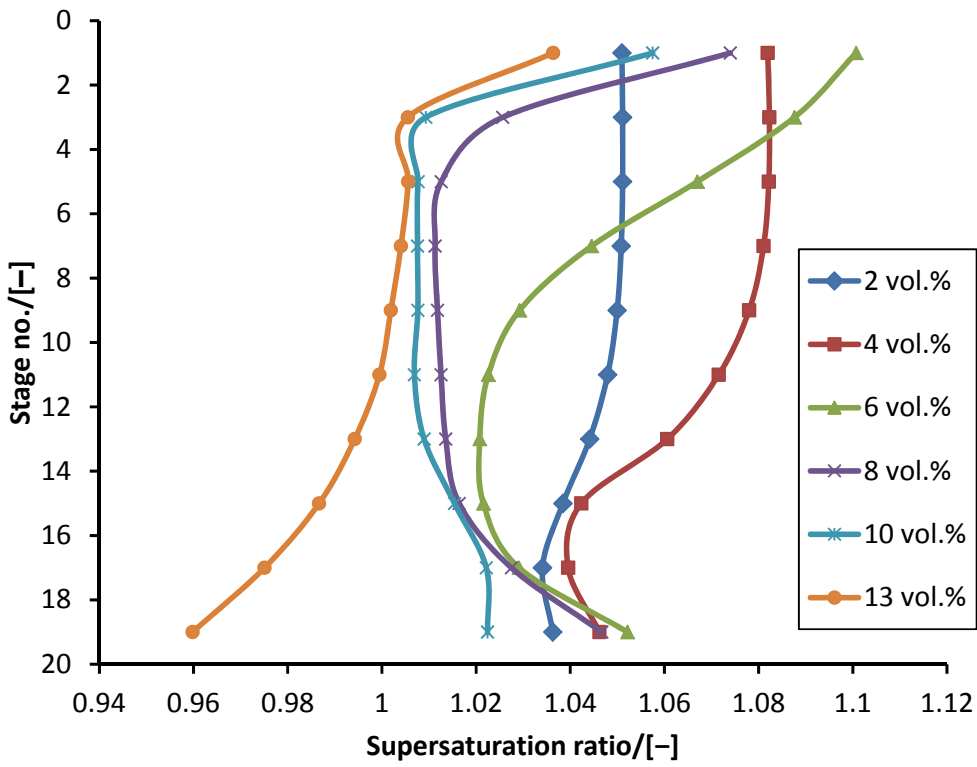


Figure 7.3. Supersaturation ratio along the absorber column at different concentration of CO_2 . The aerosols in the inlet flue gas were maintained at a constant liquid to gas ratio.

7.3.2 Effect of the change in inlet flue gas CO_2 concentration

The flue gas composition in terms of CO_2 and O_2 content of the power plant depends on factors like the composition of the fuel being burned, load variation, combustion conditions, etc. Moreover, studying the effect of different CO_2 concentration in the flue gas gives an insight into the mechanism of aerosol-based emissions.

The CO_2 concentration in the flue gas is varied from 13% to 2%, while the N_2 concentration is adjusted to maintain a constant flow rate. The liquid to gas ratio is kept constant by maintaining the same liquid flow rate. From Figure 7.3, it can be observed that the supersaturation ratio along the column increases as the CO_2 content is reduced. Moreover, at lower CO_2 content the supersaturation ratio is greater than 1, even in the lower stages of the column. The supersaturation ratio has a maximum of 1.1 at 6 vol.% CO_2 in the flue gas. Subsequently, the supersaturation ratio decreases on further decrease in inlet CO_2 content to 1.05 at 2 vol.% CO_2 , but is still higher than the supersaturation ratio at 13 vol.% CO_2 .

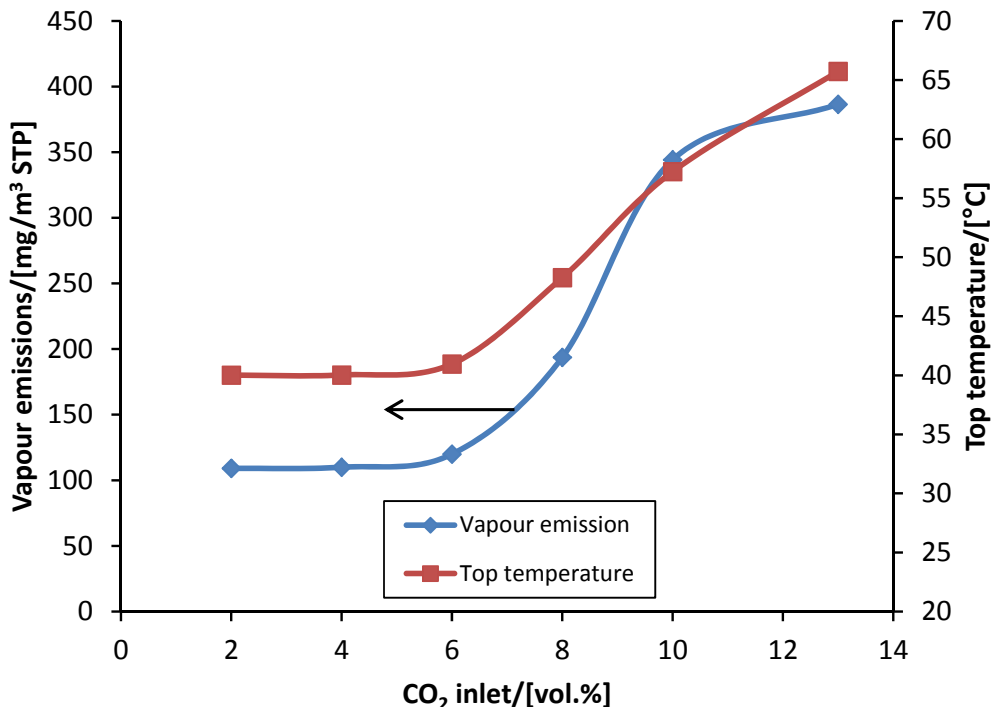


Figure 7.4. Temperature at the top of the absorber column and the corresponding vapour based emissions of MEA at varying inlet CO₂ content.

As seen in Figure 7.4, the temperature of the top stage in the absorber increases at higher CO₂ content because of the larger amount of higher amount of CO₂ transferred to the liquid phase, thereby increasing the total amount of heat released. This temperature increase causes the MEA content in the vapour stream leaving the absorber section to increase to a maximum of 386 mg/m³ STP at 66°C. The increase in vapour based emissions is in accordance with the corresponding increase in temperature and the expected change in activity of MEA in the solvent.

The supersaturation ratio at the top of the absorber column is maximum at 6 vol.% as seen in Figure 7.5. The aerosol-based emissions are seen to increase from 80 mg/m³ STP to ca. 200 mg/m³ STP at 10 vol.% and reduces to 120 mg/m³ STP at 13 vol.% CO₂. The aerosol-based emissions show a maximum at 10 vol.% CO₂, unlike the maximum of supersaturation ratio at 6 vol.% CO₂. The aerosol-based emission depends not only on the supersaturation ratio, but also on the absolute temperature at which the supersaturation occurs. The aerosol-based emissions are expected to be higher if the concentration of volatile components in the gas phase available for transferring to the aerosol phase is higher at the same supersaturation ratio. This could be the possible cause of increase in aerosol-based emissions from 6 to 10 vol.% CO₂. Moreover, the activity of the amine is an important parameter in determining the extent of volatile components present in the aerosol phase. As the activity of the MEA in the solvent reduces when the CO₂ content in the flue gas is increased, the aerosol-based emissions reduces from 10 to 13 vol.% CO₂. As two competing effects; (i) increase in the volatile emissions and (ii) lowering of the amine activity, occur when the inlet CO₂ flue gas

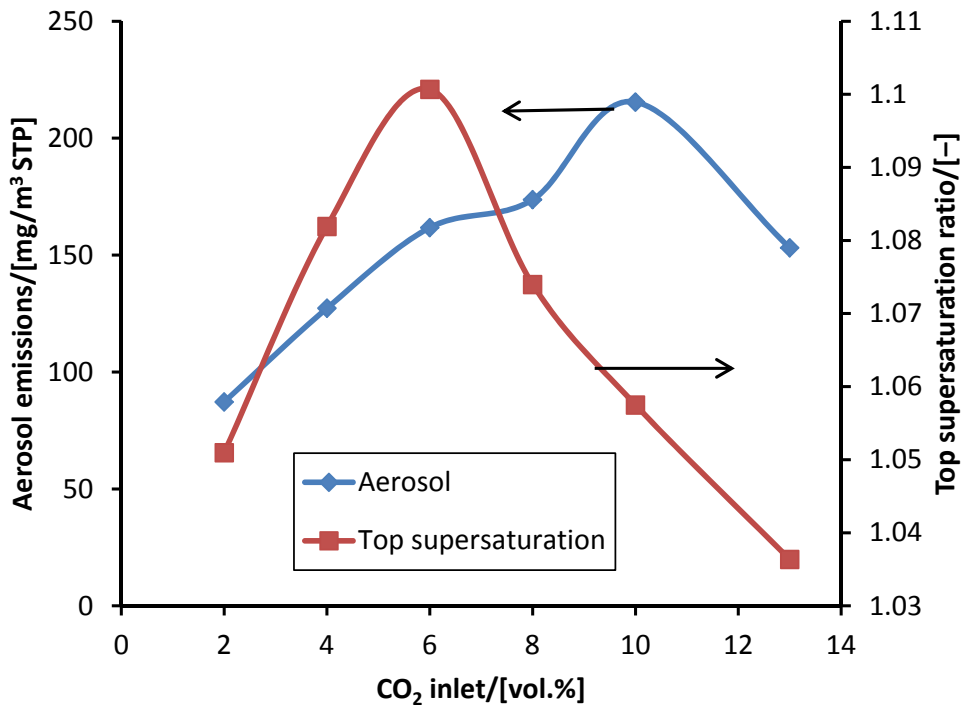


Figure 7.5. Supersaturation ratio at the top of the absorber column and the corresponding aerosol-based emissions of MEA at varying inlet CO₂ content.

content is increased, the modelling methodology shows a mismatch between the top supersaturation ratio and corresponding aerosol-based emissions.

7.3.3 Effect of the lean solvent temperature

In this case, the lean solvent temperature is varied from 30°C to 50°C, while keeping the remaining process parameters constant. On increasing the lean solvent temperature, the flue gas temperature after the hot zone increases. Therefore, the temperature bulge decreases. The decrease in the temperature bulge decreases the top supersaturation ratio too, as shown in Figure 7.6.

The increase in the top supersaturation ratio results in higher aerosol-based emission as shown in Figure 7.7. The top supersaturation ratio increases from 1.02 at 50°C to 1.09 at 30°C, while the corresponding aerosol-based emission increases from 105 to 181 mg/m³ STP. However, the top temperature increase results in a higher vapour emission of MEA as shown in Figure 7.8. Therefore, the total emission increases on increasing the lean solvent temperature however, the aerosol-based emission decreases. The high vapour emission can be more easily removed by a conventional wash section and therefore, increasing the lean solvent temperature can be a short-term solution for reducing aerosol-based emissions.

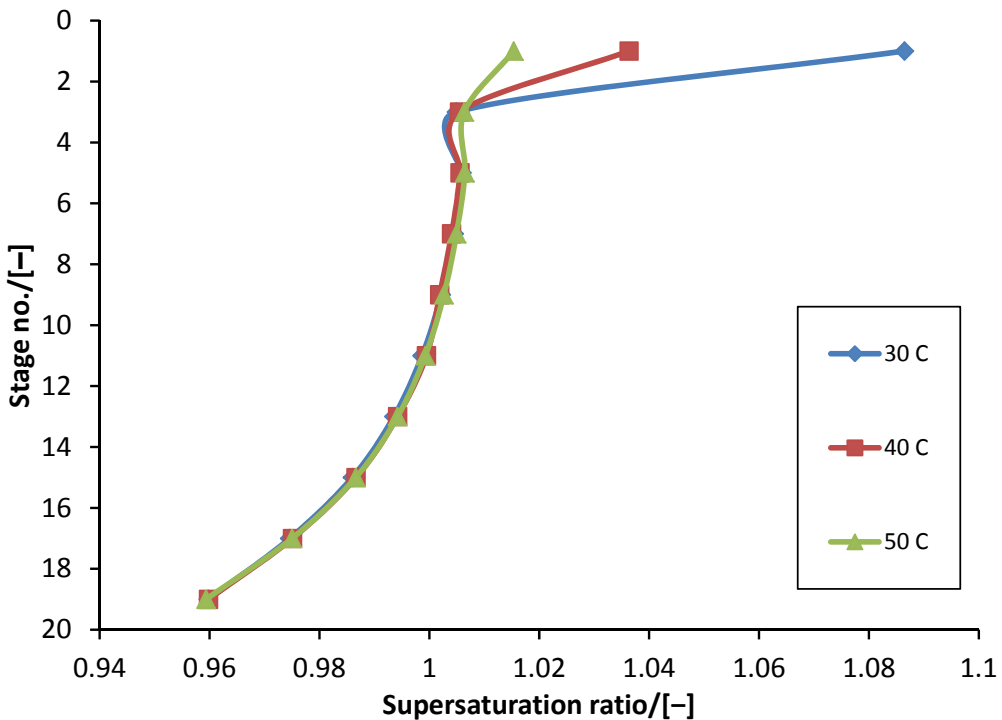


Figure 7.6. Supersaturation profile along the column at different temperatures (30°C , 40°C , and 50°C) of the lean solvent to the absorber.

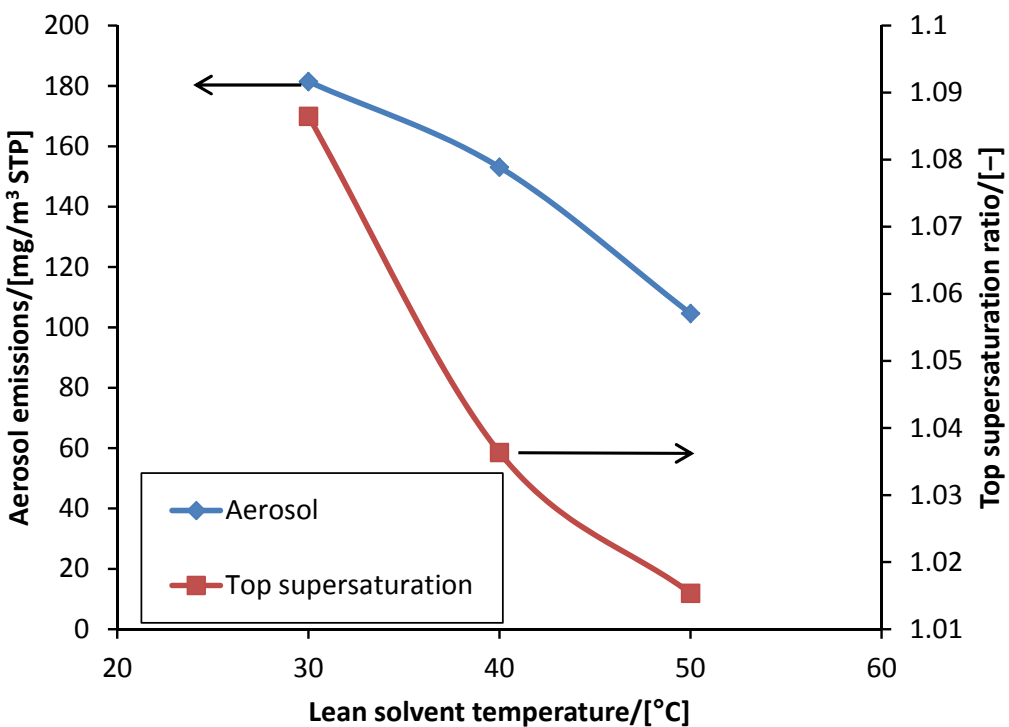


Figure 7.7. Aerosol-based emission of MEA and top supersaturation ratio at varying temperature of the lean solvent to the absorber column.

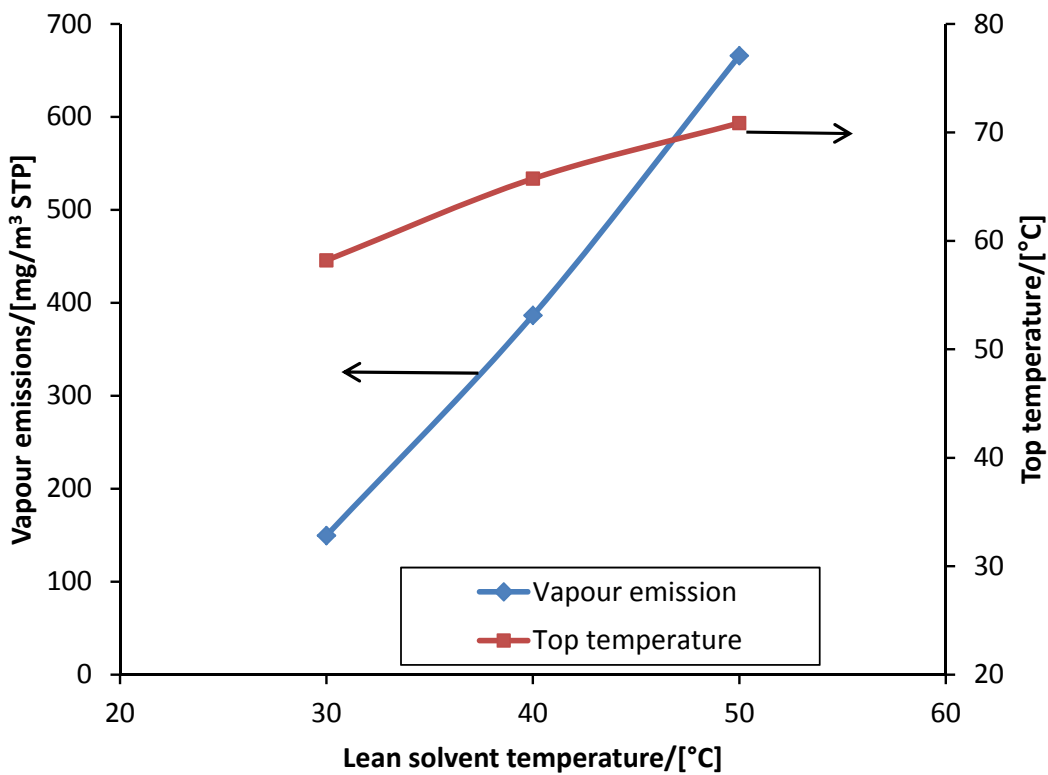


Figure 7.8. Vapour emissions of MEA and the top temperature at varying temperatures of the lean solvent to the absorber column.

7.3.4 Effect of the lean solvent loading

The lean solvent loading represents the degree of regeneration in the stripper. The lean loading of the solvent is varied from 0.13 to 0.30 mol CO₂/mol MEA at a constant liquid to gas ratio. Therefore, the CO₂ capture percentage decreases as the CO₂ loading of the lean solvent increases. As shown in Figure 7.9, the supersaturation profile increases, especially at the top of the column as the lean loading decreases. Up to a lean loading of 0.23, the supersaturation ratio at the bottom of the column is below 1, and increases throughout the column reaching a maximum at the top. However, as the lean loading decreases further, an additional zone of high supersaturation ratio is formed in the lower section of the column. As the lean loading of the solvent increases, the transfer of CO₂ to the solvent shifts lower in the column. Therefore, majority of the corresponding heat is also released in the lower sections of the column resulting in an increase in the supersaturation ratio in the lower section of the column. Moreover, the activity of the volatile components, MEA and water, also increases as the lean loading of the solvent is reduced.

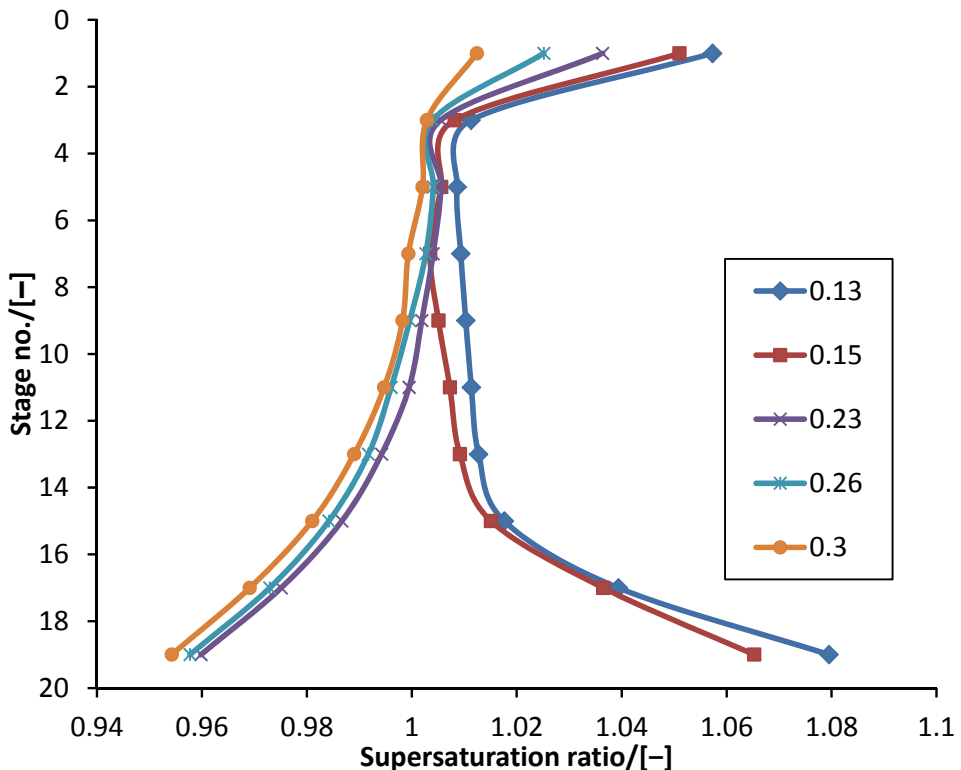


Figure 7.9. Supersaturation profile along the column at varying CO_2 loading (0.13-0.3 mol CO_2 /mol MEA) of the lean solvent.

The corresponding aerosol-based emissions also reduce as the CO_2 loading of the lean solvent is increased as shown in Figure 7.10. The lower supersaturation ratio at the top of the absorber column is a result of the lower activity of the volatile components at higher CO_2 loading of the lean solvent.

The top temperature in the absorber column increases as the lean loading is reduced from 0.3 to 0.23. The corresponding vapour based emissions of MEA are also seen to increase as shown in Figure 7.11. On further decrease of the lean loading, most of the CO_2 is transferred at the bottom sections of the column causing more cooling in the top section of the column and a lower top temperature. This is confirmed by the supersaturation profile change as shown in Figure 7.9. However, the corresponding MEA vapour emission is seen to increase as a result of its higher activity in the solvent and reduces, only at the lean loading of 0.13. Therefore, increasing the lean loading of the solvent decreases the aerosol-based as well as total emissions.

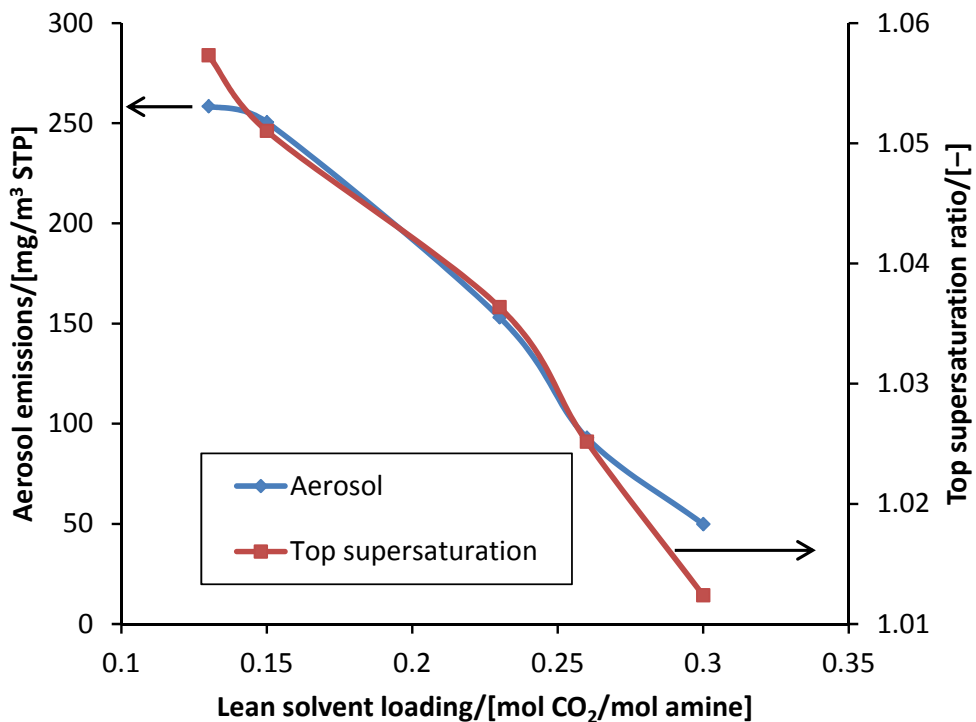


Figure 7.10. Aerosol-based emission of MEA and the top supersaturation ratio in the absorber column for varying CO₂ loading of the lean solvent.

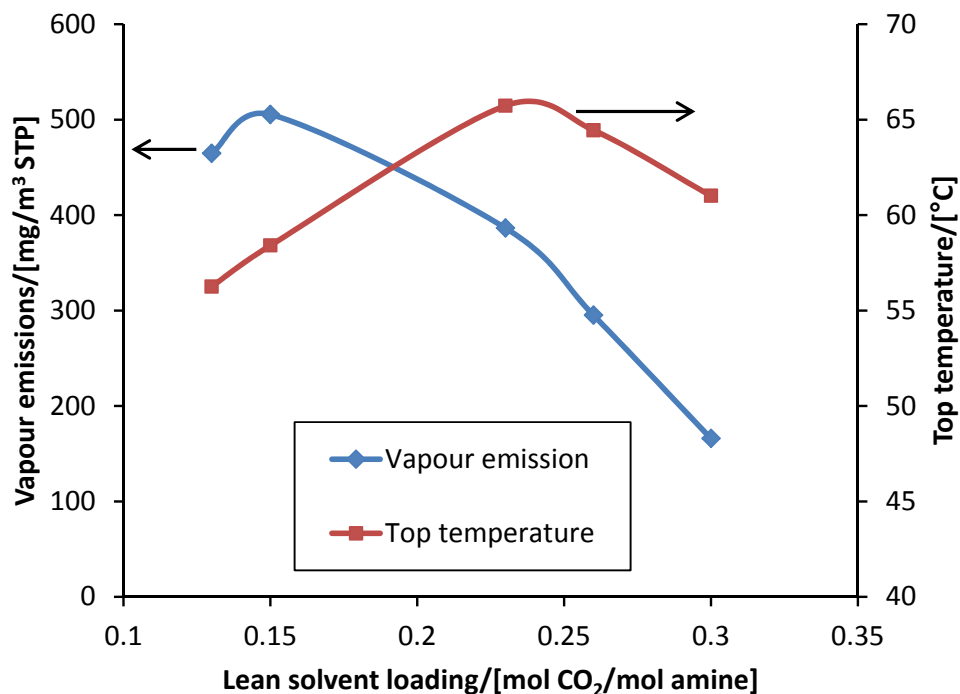


Figure 7.11. Vapour emissions of MEA at the corresponding top temperature in the absorber column for varying CO₂ loading of the lean solvent.

7.4 Conclusions

Aerosol-based emissions of solvent and its components from a PCCC plant need to be understood in detail from both an experimental and theoretical perspective. In this study, a simplified methodology has been presented for understanding aerosol-based emissions from a CO₂ capture absorber column in a PCCC process. The degree of supersaturation was found to be an important parameter in predicting the extent of the aerosol-based emissions. The impact of various process parameters such as the inlet flue gas CO₂ concentration, the temperature of the lean solvent and the CO₂ loading of the lean solvent, on supersaturation profile along the column was investigated. Increasing the lean solvent temperature and the lean solvent loading resulted in lowering of the aerosol-based emissions. A maximum in the supersaturation ratio was observed at 6 vol.% CO₂ and the maximum in aerosol-based emissions was observed at 10 vol.% CO₂. The mismatch in the maximum of aerosol-based emissions and top supersaturation ratio is possibly due to the methodology being not suited for two competing mechanisms. In general, the aerosol-based emissions followed the trend of the supersaturation ratio at the top of the absorber column. The methodology presented in this study can be used for predicting aerosol-based emissions with solvents other than MEA and in reactive absorption processes. Future research on this topic is directed towards comparing the model results with experiments and thereby, validate the model.

Appendix

Supporting information for Chapter 3.

Table S1. Specifications of the column to cool the flue gas (DCC) and reduce SO₂ levels (SO₂ polisher) of the PCCC pilot plant at Maasvlakte, the Netherlands.

Packing height	3 m (1 bed)
Diameter	0.70 m
	Random packing
Packing type	IMTP50 (SS 304L)

Table S2. Specifications of the CO₂ capture absorber tower of the PCCC pilot plant at Maasvlakte, the Netherlands.

Packing height	2.1 m (4 beds)
Diameter	0.65 m
Total height*	23 m
Packing type	Random packing IMTP 50 (SS 304L)
Column material	SS 304L

* includes sump and washing section but excludes acid wash.

Table S3. Specifications of the water wash column mounted above the packed beds for CO₂ capture of the PCCC pilot plant at Maasvlakte, the Netherlands.

Packing height	2 m (1 bed)
Diameter	0.65 m
Packing type	Structured packing Mellapak 252Y (SS 316L)
Column material	SS 304L

Table S4. Specifications of the acid wash column for reducing ammonia emissions downstream of the water wash column of the PCCC pilot plant at Maasvlakte, the Netherlands.

Packing height	1.26 m (1 bed)
Diameter	0.65 m
Total height	4.7 m
Packing type	Structured packing Mellapak 250Y (SS 316L)
Column material	SS 304L

Table S5. Specifications of the stripper tower for the regeneration of the rich solvent of the PCCC pilot plant at Maasvlakte, the Netherlands .

Packing height	4.1 m (2 beds)
Diameter	0.45 m
Total height	16.5 m
Packing type	Random packing IMTP 50 (SS 304L)
Column material	SS 304L

Table S6. Components measured by FTIR for gas phase composition.

Component	Unit
Water vapour	vol.%
Carbon dioxide	vol.%
Ammonia NH ₃	mg/m ³ STP
Ethanolamine C ₂ H ₇ NO (MEA)	mg/m ³ STP
Oxygen	vol. %

Table S7. Composition of the flue gas to the acid wash column used for the modelling the acid wash column for ammonia capture.

Component	Without spiking	Spiking
H ₂ O	6.69 vol.%	6.71 vol.%
CO ₂	0.98 vol.%	0.95 vol.%
MEA	1.53 mg/m ³ STP	6.1 mg/m ³ STP
N ₂	85.26 vol.%	86.21 vol.%
O ₂	7.7 vol.%	6.1 vol.%
NH ₃	9.37 mg/m ³ STP	150 mg/m ³ STP

Table S8. Composition of the acid liquid o the acid wash column as an input to the model. The sulphuric acid concentration was kept constant at 0.5 mmol/l.

pH	NH ₃ (mmol/l)
2.86	-
3.26	0.4
4.04	0.9
5.04	0.99
6.85	1.01
7.84	1.1
8.54	1.5
9.12	3.0

Table S9. Pilot plant settings during the pilot plant campaign to test the acid wash at the PCCC plant, Maasvlakte, the Netherlands.

	Average
Flue gas temperature before absorber [°C]	39.8
Gas flow [m ³ STP/h]	832
Gas velocity in absorber (m/s)	0.7
Lean solvent temperature [°C]	40
Liquid flow [kg/h]	3200
L/G [kg/m ³ STP]	3.8
Average CO ₂ capture rate [%]	94
Wash section flow [l/m]	51.6
Wash water temperature * [°C]	39.2 (average)
Average absorber off-gas temperature [°C]	38.9
Stripper pressure [bar]	1.9
Stripper temperature [°C]	119.9
Average CO ₂ out temperature [°C]	19.7

* This temperature changes to achieve desired absorber off-gas temperature.

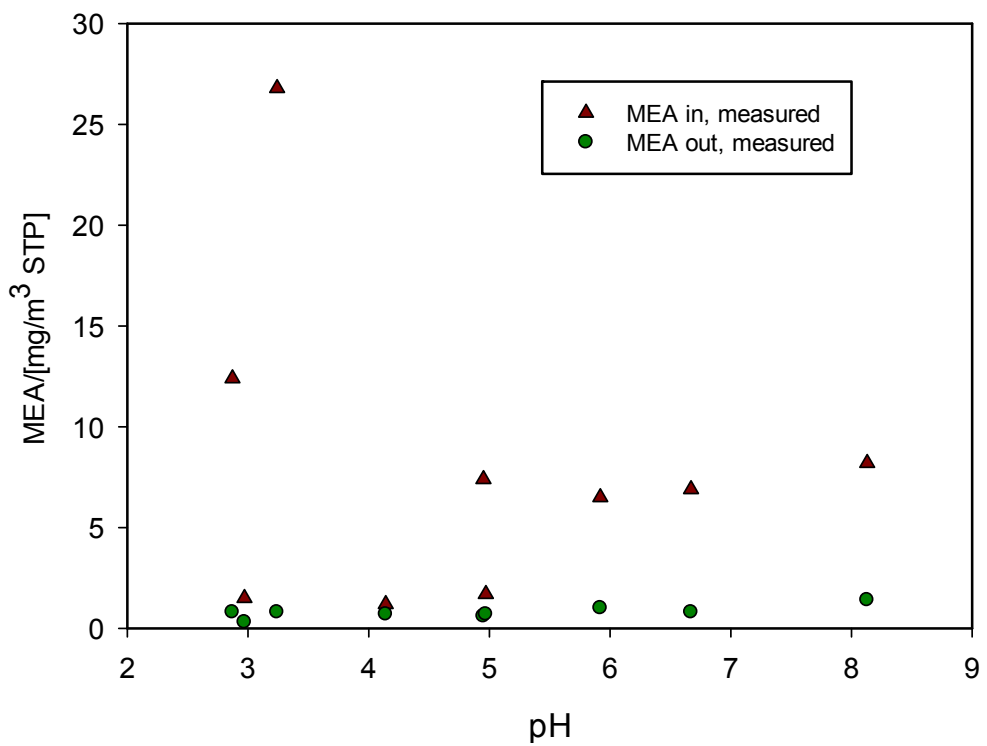


Figure S1. MEA emission across the acid wash as a function of changing pH of acid liquid.

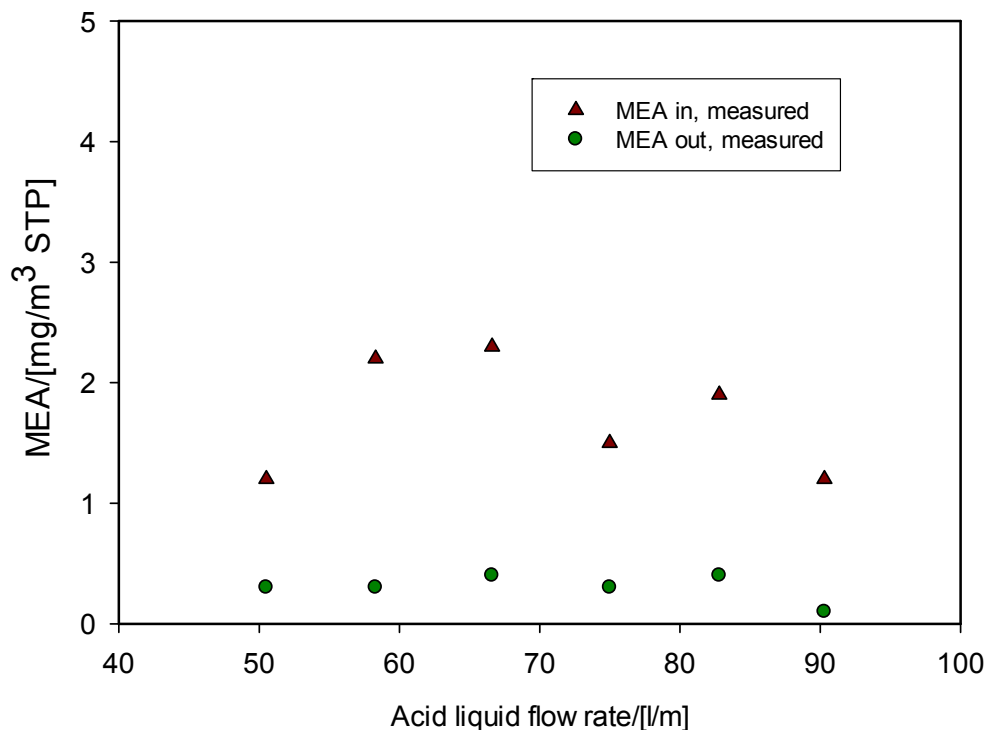


Figure S2. MEA emission across acid wash as a function of changing acid liquid flow rate.

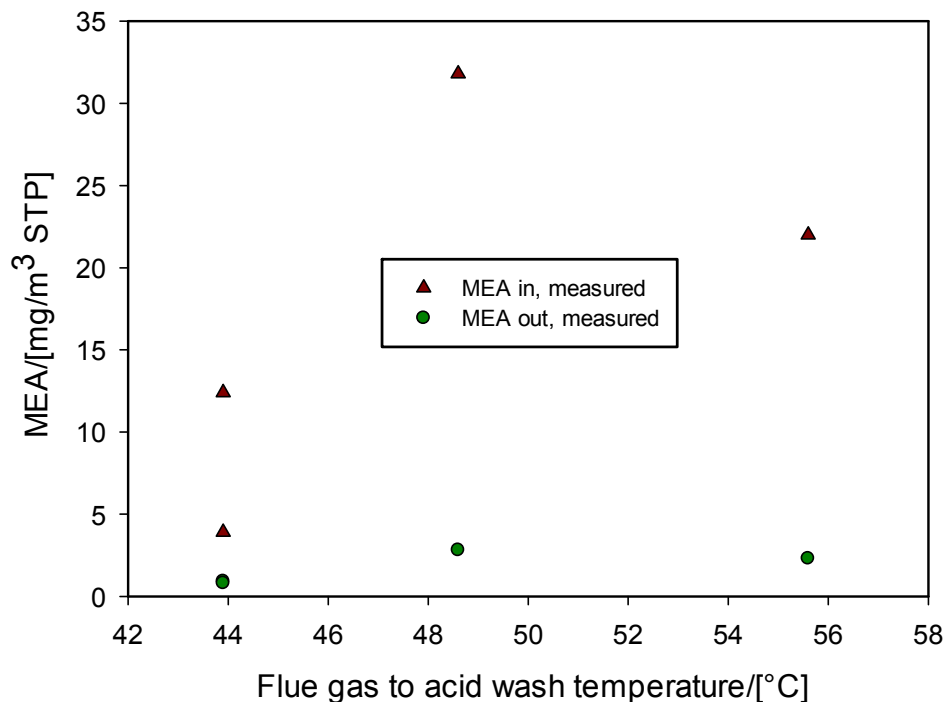


Figure S3. MEA emission across acid wash as a function of varying flue gas temperature to acid wash.

References

- [1] Intergovernmental Panel on Climate Change (IPCC), Climate Change 2013: The Physical Science Basis, Contribution of Working Group I to the Fifth Assessment Report of the Intergovernmental Panel on Climate Change, Cambridge, UK, 2013.
http://www.ipcc.ch/publications_and_data/publications_and_data_reports.shtml#.Uq3XBeLWvAk
- [2] IEA, Key World Energy Statistics, 2013.
<http://www.iea.org/publications/freepublications/publication/key-world-energy-statistics-2013.html>
- [3] IEA, CO₂ emissions from fuel combustion - HIGHLIGHTS, 2013.
<http://www.iea.org/publications/freepublications/publication/co2-emissions-from-fuel-combustion-highlights-2013-.html>
- [4] Campbell, P., Concept for a competitive coal fired integrated gasification combined cycle power plant, *Fuel*, 79, 1031–1040, 2000.
- [5] Hendriks, C., der Waart, A.S., Byers, C., Phylipsen, D., Voogt, M., Hofman, Y., Building the Cost Curves for CO₂ Storage, Part 1, sources of CO₂, IEA Greenhouse Gas R&D Program, 4, 9–20, 2002.
- [6] Intergovernmental Panel on Climate Change (IPCC), Special report on carbon dioxide capture and storage, Cambridge, UK, 2005.
http://www.ipcc.ch/publications_and_data/_reports_carbon_dioxide.htm
- [7] Figueroa, J.D., Fout, T., Plasynski, S., McIlvried, H., Srivastava, R.D., Advances in CO₂ capture technology—The U.S. Department of Energy’s Carbon Sequestration Program, *Int. J. Greenh. Gas Control*, 2, 9–20, 2008.
- [8] Kanniche, M., Gros-Bonnivard, R., Jaud, P., Valle-Marcos, J., Amann, J.-M., Bouallou, C., Pre-combustion, post-combustion and oxy-combustion in thermal power plant for CO₂ capture, *Appl. Therm. Eng.*, 30, 53–62, 2010.
- [9] GCCSI, CO₂ Capture Technologies- Pre Combustion Capture, 2012.
<http://www.globalccsinstitute.com/publications/co2-capture-technologies-pre-combustion-capture>
- [10] Rackley, S.A., Carbon capture and storage, Butterworth-Heinemann/Elsevier, Burlington, MA, 2010.
http://librarycatalog.dol.gov/client/en_US/wirtz/search/detailnonmodal;jsessionid=714789DD804D158FC57E24A4B4796965?qu=Air+quality.&d=ent://SD_ILS/142/SD_ILS:142151~ILS~0~260&ic=true&te=ILS&ps=300

- [11] Ishida, M., Jin, H., A new advanced power-generation system using chemical-looping combustion, *Energy*, 19, 415–422, 1994.
- [12] Moghtaderi, B., Review of the Recent Chemical Looping Process Developments for Novel Energy and Fuel Applications, *Energy & Fuels*, 26, 15–40, 2012.
- [13] Hossain, M.M., de Lasa, H.I., Chemical-looping combustion (CLC) for inherent separations—a review, *Chem. Eng. Sci.*, 63, 4433–4451, 2008.
- [14] Adánez, J., de Diego, L.F., García-Labiano, F., Gayán, P., Abad, A., Palacios, J.M., Selection of Oxygen Carriers for Chemical-Looping Combustion, *Energy & Fuels*, 18, 371–377, 2004.
- [15] Bottoms, R.R., Process for separating acidic gases, 1930.
<http://www.google.com/patents/US1783901>
- [16] Danckwerts, P.V., The reaction of CO₂ with ethanolamines, *Chem. Eng. Sci.*, 34, 443–446, 1979.
- [17] Kohl, A.L., Nielsen, R., Gas Purification, Gulf Professional Publishing, Houston, 5th Edition, 1997.
- [18] Yildirim, Ö., Kiss, A.A., Hüser, N., Leßmann, K., Kenig, E.Y., Reactive absorption in chemical process industry: A review on current activities, *Chem. Eng. J.*, 213, 371–391, 2012.
- [19] Sanchez-Fernandez, E., Heffernan, K., van der Ham, L., Linders, M.J.G., Brilman, D.W.F., Goetheer, E.L. V., Vlugt, T.J.H., Analysis of Process Configurations for CO₂ Capture by Precipitating Amino Acid Solvents, *Ind. Eng. Chem. Res.*, 53, 2348–2361, 2014.
- [20] Lin, Y.-J., Madan, T., Rochelle, G.T., Regeneration with Rich Bypass of Aqueous Piperazine and Monoethanolamine for CO₂ Capture, *Ind. Eng. Chem. Res.*, 53, 4067–4074, 2014.
- [21] Cousins, A., Wardhaugh, L.T., Feron, P.H.M., A survey of process flow sheet modifications for energy efficient CO₂ capture from flue gases using chemical absorption, *Int. J. Greenh. Gas Control*, 5, 605–619, 2011.
- [22] Teng, T.T., Mather, A.E., Solubility of acid gases in chemical and mixed solvents, *Gas Sep. Purif.*, 5, 29–34, 1991.
- [23] Rayer, A. V., Henni, A., Tontiwachwuthikul, P., High pressure physical solubility of carbon dioxide (CO₂) in mixed polyethylene glycol dimethyl ethers (Genosorb 1753), *Can. J. Chem. Eng.*, 90, 576–583, 2012.

- [24] Hoff, K.A., Silva, E.F. da, Kim, I., Grimstvedt, A., Ma'mun, S., Solvent development in post combustion CO₂ capture-Selection criteria and optimization of solvent performance, cost and environmental impact, *Energy Procedia*, 37, 292–299, 2013.
- [25] Mathias, P.M., Reddy, S., Smith, A., Afshar, K., A Guide to Evaluate Solvents and Processes for Post-Combustion CO₂ Capture, *Energy Procedia*, 37, 1863–1870, 2013.
- [26] Sexton, A.J., Rochelle, G.T., Catalysts and inhibitors for oxidative degradation of monoethanolamine, *Int. J. Greenh. Gas Control*, 3, 704–711, 2009.
- [27] Kittel, J., Fleury, E., Vuillemin, B., Gonzalez, S., Ropital, F., Oltra, R., Corrosion in alkanolamine used for acid gas removal: From natural gas processing to CO₂ capture, *Mater. Corros.*, 63, 223–230, 2012.
- [28] Ma'mun, S., Kim, I., Selection and characterization of phase-change solvent for carbon dioxide capture: precipitating system, *Energy Procedia*, 37, 331–339, 2013.
- [29] Raynal, L., Alix, P., Bouillon, P.-A., Gomez, A., de Nailly, M. le F., Jacquin, M., Kittel, J., di Lella, A., Mougin, P., Trapy, J., The DMX™ process: An original solution for lowering the cost of post-combustion carbon capture, *Energy Procedia*, 4, 779–786, 2011.
- [30] Pinto, D.D.D., Zaidy, S.A.H., Hartono, A., Svendsen, H.F., Evaluation of a phase change solvent for CO₂ capture: Absorption and desorption tests, *Int. J. Greenh. Gas Control*, 28, 318–327, 2014.
- [31] Smit, B., Reimer, J.R., Oldenburg, C.M., Bourg, I.C., The Berkley Lectures on Energy-Vol.1: Introduction to Carbon Capture and Sequestration, Imperial College Press, London.
- [32] D'Alessandro, D.M., Smit, B., Long, J.R., Carbon dioxide capture: prospects for new materials., *Angew. Chem. Int. Ed. Engl.*, 49, 6058–82, 2010.
- [33] Wang, Q., Luo, J., Zhong, Z., Borgna, A., CO₂ capture by solid adsorbents and their applications: current status and new trends, *Energy Environ. Sci.*, 4, 42, 2011.
- [34] Banerjee, R., Phan, A., Wang, B., Knobler, C., Furukawa, H., O'Keeffe, M., Yaghi, O.M., High-throughput synthesis of zeolitic imidazolate frameworks and application to CO₂ capture., *Science*, 319, 939–43, 2008.
- [35] Zhang, Z., Zhao, Y., Gong, Q., Li, Z., Li, J., MOFs for CO₂ capture and separation from flue gas mixtures: the effect of multifunctional sites on their adsorption capacity and selectivity., *Chem. Commun. (Camb.)*, 49, 653–61, 2013.
- [36] Ramdin, M., de Loos, T.W., Vlugt, T.J.H., State-of-the-Art of CO₂ Capture with Ionic Liquids, *Ind. Eng. Chem. Res.*, 51, 8149–8177, 2012.

- [37] Reynolds, A.J., Verheyen, T.V., Adelaju, S.B., Meuleman, E., Feron, P., Towards commercial scale postcombustion capture of CO₂ with monoethanolamine solvent: key considerations for solvent management and environmental impacts., *Environ. Sci. Technol.*, 46, 3643–54, 2012.
- [38] Strazisar, B.R., Anderson, R.R., White, C.M., Degradation Pathways for Monoethanolamine in a CO₂ Capture Facility, *Energy & Fuels*, 17, 1034–1039, 2003.
- [39] Gouedard, C., Picq, D., Launay, F., Carrette, P., Amine degradation in CO₂ capture. I. A review, *Int. J. Greenh. Gas Control*, 10, 244–270, 2012.
- [40] Da Silva, E.F., Lepaumier, H., Grimstvedt, A., Vevelstad, S.J., Einbu, A., Vernstad, K., Svendsen, H.F., Zahlsen, K., Understanding 2-Ethanolamine Degradation in Postcombustion CO₂ Capture, *Ind. Eng. Chem. Res.*, 51, 13329–13338, 2012.
- [41] Lepaumier, H., da Silva, E.F., Einbu, A., Grimstvedt, A., Knudsen, J.N., Zahlsen, K., Svendsen, H.F., Comparison of MEA degradation in pilot-scale with lab-scale experiments, *Energy Procedia*, 4, 1652–1659, 2011.
- [42] Sanchez Fernandez, E., Goetheer, E.L.V., Juzwicka, M., van Harmelen, T., van Horssen, A., Emissions of Substances other than CO₂ from Power plants with CCS, 2012. http://ieaghg.org/docs/General_Docs/Reports/2012-03.pdf
- [43] Zhou, S., Wang, S., Chen, C., Thermal Degradation of Monoethanolamine in CO₂ Capture with Acidic Impurities in Flue Gas, *Ind. Eng. Chem. Res.*, 51, 2539–2547, 2012.
- [44] Gao, J., Wang, S., Zhao, B., Qi, G., Chen, C., Pilot-Scale Experimental Study on the CO₂ Capture Process with Existing of SO₂: Degradation, Reaction Rate, and Mass Transfer, *Energy & Fuels*, 25, 5802–5809, 2011.
- [45] Uyanga, I.J., Idem, R.O., Studies of SO₂ and O₂ Induced Degradation of Aqueous MEA during CO₂ Capture from Power Plant Flue Gas Streams, *Ind. Eng. Chem. Res.*, 46, 2558–2566, 2007.
- [46] Supap, T., Idem, R., Tontiwachwuthikul, P., Saiwan, C., Kinetics of sulfur dioxide- and oxygen-induced degradation of aqueous monoethanolamine solution during CO₂ absorption from power plant flue gas streams, *Int. J. Greenh. Gas Control*, 3, 133–142, 2009.
- [47] Sun, C., Wang, S., Zhou, S., Chen, C., SO₂ effect on monoethanolamine oxidative degradation in CO₂ capture process, *Int. J. Greenh. Gas Control*, 23, 98–104, 2014.
- [48] Williams, L.H., N-Nitrosation, 77–112, Cambridge University Press, Cambridge, UK, 1988.

- [49] Fostås, B., Gangstad, A., Nenseter, B., Pedersen, S., Sjøvoll, M., Sørensen, A.L., Effects of NO_x in the flue gas degradation of MEA, *Energy Procedia*, 4, 1566–1573, 2011.
- [50] Challis, B.C., Kyrtopoulos, S.A., The chemistry of nitroso-compounds. Part 11. Nitrosation of amines by the two-phase interaction of amines in solution with gaseous oxides of nitrogen, *J. Chem. Soc. Perkin Trans. 1*, 299–304, 1979.
<http://pubs.rsc.org/en/content/articlelanding/1979/p1/p19790000299>
- [51] Cooney, R.V., Hatch-Pigott, V., Ross, P.D., Ramseyer, J., Carcinogenic N-nitrosamine formation: A requirement for nitric oxide, *J. Environ. Sci. Heal. . Part A Environ. Sci. Eng. Toxicol.*, 27, 789–801, 1992.
- [52] Dai, N., Shah, A.D., Hu, L., Plewa, M.J., McKague, B., Mitch, W.A., Measurement of Nitrosamine and Nitramine Formation from NO_x Reactions with Amines during Amine-Based Carbon Dioxide Capture for Postcombustion Carbon Sequestration, *Environ. Sci. Technol.*, 46, 9793–9801, 2012.
- [53] De Koeijer, G., Talstad, V.R., Nepstad, S., Tønnessen, D., Falk-Pedersen, O., Maree, Y., Nielsen, C., Health risk analysis for emissions to air from CO₂ Technology Centre Mongstad, *Int. J. Greenh. Gas Control*, 18, 200–207, 2013.
- [54] Dai, N., Mitch, W.A., Effects of flue gas compositions on nitrosamine and nitramine formation in postcombustion CO₂ capture systems., *Environ. Sci. Technol.*, 48, 7519–26, 2014.
- [55] Mercader, F. de M., Voice, A.K., Trap, H., Goetheer, E.L.V., Nitrosamine degradation by UV light in post-combustion CO₂ capture: Effect of solvent matrix, *Energy Procedia*, 37, 701–716, 2013.
- [56] Chandan, P., Richburg, L., Bhatnagar, S., Remias, J.E., Liu, K., Impact of fly ash on monoethanolamine degradation during CO₂ capture, *Int. J. Greenh. Gas Control*, 25, 102–108, 2014.
- [57] Huang, Q., Thompson, J., Bhatnagar, S., Chandan, P., Remias, J.E., Selegue, J.P., Liu, K., Impact of Flue Gas Contaminants on Monoethanolamine Thermal Degradation, *Ind. Eng. Chem. Res.*, 53, 553–563, 2014.
- [58] Nielsen, R.B., Lewis, K.R., McCullough, J.G., Hansen, D.A., Controlling corrosion in amine treating plants, Proceedings of the Laurence Reid Gas Conditioning Conference, Norman, Oklahoma, 1995.
- [59] M.S. Du Part, T.R. Bacon, D.J.E., Understanding corrosion in alkanolamine gas treating plants Part 1&2, Hydrocarbon Processing, 1993.

- [60] Kittel, J., Gonzalez, S., Corrosion in CO₂ Post-Combustion Capture with Alkanolamines — A Review, *Oil Gas Sci. Technol. – Rev. d'IFP Energies Nouv.*, 2013.
<http://dx.doi.org/10.2516/ogst/2013161>
- [61] De Vroey, S., Huynh, H., Lepaumier, H., Absil, P., Thielens, M.-L., Corrosion Investigations In 2-ethanolamine Based Post- Combustion CO₂ Capture Pilot Plants, *Energy Procedia*, 37, 2047–2057, 2013.
- [62] Azzi, M., Angove, D., Dave, N., Day, S., Do, T., Feron, P., Sharma, S., Attalla, M., Zahra, M.A., Emissions to the Atmosphere from Amine-Based Post Combustion CO₂ Capture Plant – Regulatory Aspects, *Oil Gas Sci. Technol. – Rev. d'IFP Energies Nouv.*, 2014. DOI:10.2516/ogst/2013159
- [63] Schreiber, A., Zapp, P., Kuckshinrichs, W., Environmental assessment of German electricity generation from coal-fired power plants with amine-based carbon capture, *Int. J. Life Cycle Assess.*, 14, 547–559, 2009.
- [64] Veltman, K., Singh, B., Hertwich, E.G., Human and environmental impact assessment of postcombustion CO₂ capture focusing on emissions from amine-based scrubbing solvents to air, *Environ. Sci. Technol.*, 44, 1496–502, 2010.
- [65] Sanchez Fernandez, E., Novel Process Designs To Improve The Efficiency Of Post Combustion Carbon Dioxide Capture, Delft University, 2013.
- [66] Nguyen, T., Hilliard, M., Rochelle, G.T., Amine volatility in CO₂ capture, *Int. J. Greenh. Gas Control*, 4, 707–715, 2010.
- [67] Da Silva, E.F., Hoff, K.A., Booth, A., Emissions from CO₂ capture plants; an overview, *Energy Procedia*, 37, 784–790, 2013.
- [68] Fujita, K., Muraoka, D., Ogawa, T., Kitamura, H., Suzuki, K., Saito, S., Evaluation of amine emissions from the post-combustion CO₂ capture pilot plant, *Energy Procedia*, 37, 727–734, 2013.
- [69] Mertens, J., Knudsen, J., Thielens, M., Andersen, J., On-line monitoring and controlling emissions in amine post combustion carbon capture: A field test, *Int. J. Greenh. Gas Control*, 6, 2–11, 2012.
- [70] Bedell, S.A., Oxidative degradation mechanisms for amines in flue gas capture, *Energy Procedia*, 1, 771–778, 2009.
- [71] De Koeijer, G., Enge, Y., Sanden, K., Graff, O.F., Falk-Pedersen, O., Amundsen, T., Overå, S., CO₂ Technology Centre Mongstad—Design, functionality and emissions of the amine plant, *Energy Procedia*, 4, 1207–1213, 2011.

- [72] Mertens, J., Lepaumier, H., Desagher, D., Thielens, M., Understanding ethanolamine (MEA) and ammonia emissions from amine based post combustion carbon capture: Lessons learned from field tests, *Int. J. Greenh. Gas Control*, 13, 72–77, 2013.
- [73] Mej dell, T., Haugen, G., Tobiesen, A., Khakharia, P., WP 2 in the project: CCM TQP amine 6 – Validation of simulation models, Trondheim, Norway, 2012.
- [74] Kamijo, T., Kajiya, Y., Endo, T., Nagayasu, H., Tanaka, H., Hirata, T., Yonekawa, T., Tsujiuchi, T., SO₃ Impact on Amine Emission and Emission Reduction Technology, *Energy Procedia*, 37, 1793–1796, 2013.
- [75] Nielsen, C.J., D'Anna, B., Dye, C., Graus, M., Karl, M., King, S., Maguto, M.M., Müller, M., Schmidbauer, N., Stenstrøm, Y., Wisthaler, A., Pedersen, S., Atmospheric chemistry of 2-aminoethanol (MEA), *Energy Procedia*, 4, 2245–2252, 2011.
- [76] CO₂ Capture | Project Road 2020, <http://road2020.nl/en/ccs-technologie/co2-afvang/>
- [77] Boundary Dam CCS project, <http://www.saskpowerccs.com/ccs-projects/boundary-dam-carbon-capture-project/carbon-capture-project/>
- [78] Aspen Plus, <http://www.aspentechnology.com/products/engineering/aspen-plus/>
- [79] Ahn, H., Luberti, M., Liu, Z., Brandani, S., Process configuration studies of the amine capture process for coal-fired power plants, *Int. J. Greenh. Gas Control*, 16, 29–40, 2013.
- [80] Abu-Zahra, M.R.M., Schneiders, L.H.J., Niederer, J.P.M., Feron, P.H.M., Versteeg, G.F., CO₂ capture from power plants, *Int. J. Greenh. Gas Control*, 1, 37–46, 2007.
- [81] Bulger, J., Grgis, M., Polvi, T., Corrosion Due to Process Instability in a Hot Lean Amine System, Corrosion, 05386, NACE International, Houston, 2005.
<https://www.onepetro.org/conference-paper/NACE-05386>
- [82] Gui, F., Sridhar, N., Thodla, R., Brossia, C.S., Corrosion of Carbon Steel in Ethanolamine, 17th International Corrosion Congress on Corrosion Control in the Service of Society, 207–215, NACE International, Las Vegas, 2008.
- [83] Kittel, J., Idem, R., Gelowitz, D., Tontiwachwuthikul, P., Parrain, G., Bonneau, A., Corrosion in MEA units for CO₂ capture: Pilot plant studies, *Energy Procedia*, 1, 791–797, 2009.
- [84] B. Geukens, Vroey, S. De, Corrosion tests results, 2011.
- [85] Wattanaphan, P., Sema, T., Idem, R., Liang, Z., Tontiwachwuthikul, P., Effects of flue gas composition on carbon steel (1020) corrosion in MEA-based CO₂ capture process, *Int. J. Greenh. Gas Control*, 19, 340–349, 2013.

- [86] Goff, G.S., Rochelle, G.T., Monoethanolamine degradation: O₂ mass transfer effects under CO₂ capture conditions, *Ind. Eng. Chem. Res.*, 43, 6400–6408, 2004.
- [87] Voice, A.K., Rochelle, G.T., Products and process variables in oxidation of monoethanolamine for CO₂ capture, *Int. J. Greenh. Gas Control*, 12, 472–477, 2013.
- [88] Freeman, S.A., Davis, J., Rochelle, G.T., Degradation of aqueous piperazine in carbon dioxide capture, *Int. J. Greenh. Gas Control*, 4, 756–761, 2010.
- [89] Chi, S., Rochelle, G.T., Oxidative Degradation of Monoethanolamine, *Ind. Eng. Chem. Res.*, 41, 4178–4186, 2002.
- [90] Davis, J., Rochelle, G., Thermal degradation of monoethanolamine at stripper conditions, *Energy Procedia*, 1, 327–333, 2009.
- [91] Lepaumier, H., Grimstvedt, A., Vernstad, K., Zahlsen, K., Svendsen, H.F., Degradation of MMEA at absorber and stripper conditions, *Chem. Eng. Sci.*, 66, 3491–3498, 2011.
- [92] Schallert, B., Neuhaus, S., Satterley, C.J., Do we underestimate the impact of particles in coal-derived flue gas on amine-based CO₂ capture processes?, *Energy Procedia*, 37, 817–825, 2013.
- [93] Thompson, J.G., Heat Stable Salt Accumulation and Solvent Degradation in a Pilot-Scale CO₂ Capture Process Using Coal Combustion Flue Gas, *Aerosol Air Qual. Res.*, 14, 550–558, 2014.
- [94] Lepaumier, H., Picq, D., Carrette, P.-L., New Amines for CO₂ Capture. II. Oxidative Degradation Mechanisms, *Ind. Eng. Chem. Res.*, 48, 9068–9075, 2009.
- [95] Khakharia, P., Huizinga, A., Jurado Lopez, C., Sanchez Sanchez, C., de Miguel Mercader, F., Vlugt, T.J.H., Goetheer, E., Acid Wash Scrubbing as a Countermeasure for Ammonia Emissions from a Postcombustion CO₂ Capture Plant, *Ind. Eng. Chem. Res.*, 53, 13195–13204, 2014.
- [96] Khakharia, P., Kvamsdal, H.M., da Silva, E.F., Vlugt, T.J.H., Goetheer, E., da Silva, E.F., Field study of a Brownian Demister Unit to reduce aerosol based emission from a Post Combustion CO₂ Capture plant, *Int. J. Greenh. Gas Control*, 28, 57–64, 2014.
- [97] Tanthapanichakoon, W., Veawab, A., McGarvey, B., Electrochemical Investigation on the Effect of Heat-stable Salts on Corrosion in CO₂ Capture Plants Using Aqueous Solution of MEA, *Ind. Eng. Chem. Res.*, 45, 2586–2593, 2006.
- [98] Veawab, A., Tontiwachwuthikul, P., Chakma, A., Corrosion Behavior of Carbon Steel in the CO₂ Absorption Process Using Aqueous Amine Solutions, *Ind. Eng. Chem. Res.*, 38, 3917–3924, 1999.

- [99] Soosaiprakasam, I.R., Veawab, A., Corrosion and polarization behavior of carbon steel in MEA-based CO₂ capture process, *Int. J. Greenh. Gas Control*, 2, 553–562, 2008.
- [100] Lawal, A.O., Idem, R.O., Kinetics of the Oxidative Degradation of CO₂ Loaded and Concentrated Aqueous MEA-MDEA Blends during CO₂ Absorption from Flue Gas Streams, *Ind. Eng. Chem. Res.*, 45, 2601–2607, 2006.
- [101] Moser, P., Schmidt, S., Uerlings, R., Sieder, G., Titz, J.-T., Hahn, A., Stoffregen, T., Material testing for future commercial post-combustion capture plants—Results of the testing programme conducted at the Niederaussem pilot plant, *Energy Procedia*, 4, 1317–1322, 2011.
- [102] Knudsen, J.N., Jensen, J.N., Vilhelmsen, P.-J., Biede, O., Experience with CO₂ capture from coal flue gas in pilot-scale: Testing of different amine solvents, *Energy Procedia*, 1, 783–790, 2009.
- [103] Reid, S.A., Reid, D.A., Assessment of Corrosion, 2001.
<http://www.google.com/patents/US6264824>
- [104] Eden, D.C., Cayard, M.S., Kintz, J.D., Kramer, E., Schrecengost, R.A., Breen, B.P., Making Credible Corrosion Measurements - Real Corrosion, Real Time, Corrosion, 03376, NACE International, San Diego, 2003. <https://www.onepetro.org/conference-paper/NACE-03376>
- [105] Fontana, M.G., Corrosion Engineering, Tata McGraw-Hill Education, Singapore, 3rd Edition, 2005.
- [106] Khakharia, P., Brachert, L., Mertens, J., Huizinga, A., Schallert, B., Schaber, K., Vlugt, T.J.H., Goetheer, E., Investigation of aerosol based emission of MEA due to sulphuric acid aerosol and soot in a Post Combustion CO₂ Capture process, *Int. J. Greenh. Gas Control*, 19, 138–144, 2013.
- [107] Mertens, J., Brachert, L., Desagher, D., Thielens, M.L., Khakharia, P., Goetheer, E., Schaber, K., ELPI+ measurements of aerosol growth in an amine absorption column, *Int. J. Greenh. Gas Control*, 23, 44–50, 2014.
- [108] Lepaumier, H., Picq, D., Carrette, P.-L., New Amines for CO₂ Capture. I. Mechanisms of Amine Degradation in the Presence of CO₂, *Ind. Eng. Chem. Res.*, 48, 9061–9067, 2009.
- [109] Ryer-Powder, J.E., Health effects of ammonia, *Plant/Operations Prog.*, 10, 228–232, 1991.
- [110] Agency for Toxic Substances and Disease Registry (ATSDR), Toxicological profile for Ammonia, 2004. <http://www.atsdr.cdc.gov/phs/phs.asp?id=9&tid=2>

- [111] Norwegian Climate and Pollution Agency (Klif), Permit for activities pursuant to the Pollution Control Act for CO₂ Technology Centre Mongstad DA, 2011.
http://www.tcmda.com/Global/Dokumenter/Klif_TCM_Discharge_permit.pdf
- [112] Os, R. van, Milieueffectrapportage CCS Maasvlakte (ROAD project) Deelrapport Afvang, 2011. http://www.rvo.nl/sites/default/files/sn_bijlagen/bep/70-Opslagprojecten/ROAD-project/Fase1/2_MER/MER-deelrapport-afvang-incl-bijlagen-1-353749.pdf
- [113] Koornneef, J., van Keulen, T., Faaij, A., Turkenburg, W., Life cycle assessment of a pulverized coal power plant with post-combustion capture, transport and storage of CO₂, *Int. J. Greenh. Gas Control*, 2, 448–467, 2008.
- [114] Erisman, J., Schaap, M., The need for ammonia abatement with respect to secondary PM reductions in Europe, *Environ. Pollut.*, 129, 159–163, 2004.
- [115] Busca, G., Pistarino, C., Abatement of ammonia and amines from waste gases: a summary, *J. Loss Prev. Process Ind.*, 16, 157–163, 2003.
- [116] Bade, Otto, M., Gorset, O., Graff, Oscar, F., Woodhouse, S., Method and plant for amine emission control, 2010. <http://patentscope.wipo.int/search/en/WO2010102877>
- [117] Bradie, J.K., Dickson, A.N., Removal of Entrained Liquid Droplets by Wire-Mesh Demisters, *Proc. Inst. Mech. Eng. Conf.*, 184, 195–203, 1969.
- [118] El-Dessouky, H.T., Alatiqi, I.M., Ettouney, H.M., Al-Deffeeri, N.S., Performance of wire mesh mist eliminator, *Chem. Eng. Process. Process Intensif.*, 39, 129–139, 2000.
- [119] Zhang, Y., Chen, H., Chen, C.-C., Plaza, J.M., Dugas, R., Rochelle, G.T., Rate-Based Process Modeling Study of CO₂ Capture with Aqueous Monoethanolamine Solution, *Ind. Eng. Chem. Res.*, 48, 9233–9246, 2009.
- [120] De Brito, M.H., von Stockar, U., Bangerter, A.M., Bomio, P., Laso, M., Effective Mass-Transfer Area in a Pilot Plant Column Equipped with Structured Packings and with Ceramic Rings, *Ind. Eng. Chem. Res.*, 33, 647–656, 1994.
- [121] Bravo, J.L., Fair, J.R., Generalized correlation for mass transfer in packed distillation columns, *Ind. Eng. Chem. Process Des. Dev.*, 21, 162–170, 1982.
- [122] Edwards, T.J., Maurer, G., Newman, J., Prausnitz, J.M., Vapor-liquid equilibria in multicomponent aqueous solutions of volatile weak electrolytes, *AIChE J.*, 24, 966–976, 1978.
- [123] Kawazuishi, K., Prausnitz, J.M., Correlation of vapor-liquid equilibria for the system ammonia-carbon dioxide-water, *Ind. Eng. Chem. Res.*, 26, 1482–1485, 1987.

- [124] Biard, P.-F., Couvert, A., Overview of mass transfer enhancement factor determination for acidic and basic compounds absorption in water, *Chem. Eng. J.*, 222, 444–453, 2013.
- [125] Cesar, D2.4.3 European Best Practice Guidelines for Assessment of CO₂ Capture Technologies, 2011. [http://www.co2cesar.eu/downloadables/Deliverables/Public/CESAR-D2.4.3-APPROVED-European Best Practice Guidelines for CO₂ Capture Technologies - EBTF - 2011.03.08.pdf](http://www.co2cesar.eu/downloadables/Deliverables/Public/CESAR-D2.4.3-APPROVED-European%20Best%20Practice%20Guidelines%20for%20CO2%20Capture%20Technologies%20-%20EBTF%20-%202011.03.08.pdf)
- [126] Abu-Zahra, M.R.M., Schneiders, L.H.J., Niederer, J.P.M., Feron, P.H.M., Versteeg, G.F., CO₂ capture from power plants: Part I. A parametric study of the technical performance based on monoethanolamine, *Int. J. Greenh. Gas Control*, 1, 37–46, 2007.
- [127] Puxty, G., Rowland, R., Allport, A., Yang, Q., Bown, M., Burns, R., Maeder, M., Attalla, M., Carbon Dioxide Postcombustion Capture: A Novel Screening Study of the Carbon Dioxide Absorption Performance of 76 Amines, *Environ. Sci. Technol.*, 43, 6427–6433, 2009.
- [128] DOE, NETL, Carbon Dioxide Capture and Storage RD&D Roadmap, 2010.
- [129] IEAGHG, Environmental impacts of amine emissions during post combustion capture Workshop, Oslo, 2010. <http://ieaghg.org/publications/blog/47-networks/environmental-impacts-of-post-combustion-capture>
- [130] DIPPR, Thermophysical Property Database for Pure Chemical Compounds, 2010.
- [131] Hilliard, M.D., A Predictive Thermodynamic Model for an Aqueous Blend of Potassium Carbonate, Piperazine, and Monoethanolamine for Carbon Dioxide Capture from Flue Gas, The University of Texas at Austin, 2008.
[http://www.che.utexas.edu/rochelle_group/Pubs/Hilliard_Dissertation\(2008\).pdf](http://www.che.utexas.edu/rochelle_group/Pubs/Hilliard_Dissertation(2008).pdf)
- [132] Kim, I., Svendsen, H.F., Børresen, E., Ebulliometric Determination of Vapor–Liquid Equilibria for Pure Water, Monoethanolamine, N-Methyldiethanolamine, 3-(Methylamino)-propylamine, and Their Binary and Ternary Solutions, *J. Chem. Eng. Data*, 53, 2521–2531, 2008.
- [133] Lenard, J.-L., Rousseau, R.W., Teja, A.S., Vapor-Liquid Equilibria for Mixtures of 2-aminoethanol+ water, 86, 1–5, 1990.
- [134] Kvamsdal, H., Ehlers, S., Khakharia, P., Fosbol, P., Liebenthahl, U., Sanchez, C., Haugen, G., Chikukwa, A., Robinson, L., Booth, N., Gomez, A., Chopin, F., A New Reference Case for Benchmarking in the OCTAVIUS project, Bergen, Norway, 2013.
<http://ieaghg.org/conferences/pccc/52-conferences/pccc/346-pccc2-technical-programme>

- [135] Kolderup, H., Hjarbo, K.W., Huizinga, A., Tuinman, I., Zahlsen, K., Vernstad, K., Hyldbakk, A., Holten, T., Kvamsdal, H.M., van Os, P., da Silva, E.F., Goetheer, E., Khakharia, P., WP 1 and 3 in the project: CCM TQP amine 6 - Emission Quantification and Reduction, 2012.
http://www.gassnova.no/no/Documents/EmissionquantificationandreductionWP1and3_Sintef.pdf
- [136] Srivastava, R.K., Miller, C.A., Erickson, C., Jambhekar, R., Emissions of Sulfur Trioxide from Coal-Fired Power Plants, *J. Air Waste Manage. Assoc.*, 54, 750–762, 2004.
- [137] Gretscher, H., Schaber, K., Aerosol formation by heterogeneous nucleation in wet scrubbing processes, *Chem. Eng. Process. Process Intensif.*, 38, 541–548, 1999.
- [138] Wix, A., Schaber, K., Ofenloch, O., Ehrig, R., Deuflhard, P., Simulation of Aerosol Formation in Gas-Liquid Contact Devices, *Chem. Eng. Commun.*, 194, 565–577, 2007.
- [139] Pfeifer, P., Zscherpe, T., Haas-Santo, K., Dittmeyer, R., Investigations on a Pt/TiO₂ catalyst coating for oxidation of SO₂ in a microstructured reactor for operation with forced decreasing temperature profile, *Appl. Catal. A Gen.*, 391, 289–296, 2011.
- [140] Perry, R.H., Green, D.W., Perry's chemical engineers' handbook, McGraw-Hill, New York, 8th Edition, 2008.
- [141] Brachert, L., Kochenburger, T., Schaber, K., Facing the Sulfuric Acid Aerosol Problem in Flue Gas Cleaning: Pilot Plant Experiments and Simulation, *Aerosol Sci. Technol.*, 47, 1083–1091, 2013.
- [142] Wix, A., Brachert, L., Sinanis, S., Schaber, K., A simulation tool for aerosol formation during sulphuric acid absorption in a gas cleaning process, *J. Aerosol Sci.*, 41, 1066–1079, 2010.
- [143] Notz, R., Asprion, N., Clausen, I., Hasse, H., Selection and Pilot Plant Tests of New Absorbents for Post-Combustion Carbon Dioxide Capture, *Chem. Eng. Res. Des.*, 85, 510–515, 2007.
- [144] Cheng, Y.-S., Aerosol Measurement: Principles, Techniques, and Applications, (eds. Kulkarni, P., Baron, P. A. & Willeke, K.), 381–392, John Wiley & Sons, Inc., Hoboken, NJ, USA, 3rd Edition, 2011.
<http://onlinelibrary.wiley.com/doi/10.1002/9781118001684.ch17/summary>
- [145] Cao, Y., Zhou, H., Jiang, W., Chen, C.-W., Pan, W.-P., Studies of the fate of sulfur trioxide in coal-fired utility boilers based on modified selected condensation methods., *Environ. Sci. Technol.*, 44, 3429–34, 2010.
- [146] Schaber, K., Aerosol formation in absorption processes, *Chem. Eng. Sci.*, 50, 1347–1360, 1995.

- [147] Vaidya, P.D., Kenig, E.Y., CO₂-Alkanolamine Reaction Kinetics: A Review of Recent Studies, *Chem. Eng. Technol.*, 30, 1467–1474, 2007.
- [148] Alper, E., Reaction mechanism and kinetics of aqueous solutions of 2-amino-2-methyl-1-propanol and carbon dioxide, *Ind. Eng. Chem. Res.*, 29, 1725–1728, 1990.
- [149] Rinker, E.B., Ashour, S.S., Sandall, O.C., Absorption of Carbon Dioxide into Aqueous Blends of Diethanolamine and Methyldiethanolamine, *Ind. Eng. Chem. Res.*, 39, 4346–4356, 2000.
- [150] Dash, S.K., Samanta, A., Nath Samanta, A., Bandyopadhyay, S.S., Absorption of carbon dioxide in piperazine activated concentrated aqueous 2-amino-2-methyl-1-propanol solvent, *Chem. Eng. Sci.*, 66, 3223–3233, 2011.
- [151] Bishnoi, S., Rochelle, G.T., Absorption of carbon dioxide into aqueous piperazine: reaction kinetics, mass transfer and solubility, *Chem. Eng. Sci.*, 55, 5531–5543, 2000.
- [152] Bishnoi, S., Rochelle, G.T., Absorption of carbon dioxide in aqueous piperazine/methyldiethanolamine, *AICHE J.*, 48, 2788–2799, 2002.
- [153] Wei, C.-C., Puxty, G., Feron, P., Amino acid salts for CO₂ capture at flue gas temperatures, *Chem. Eng. Sci.*, 107, 218–226, 2014.
- [154] Portugal, A.F., Sousa, J.M., Magalhães, F.D., Mendes, A., Solubility of carbon dioxide in aqueous solutions of amino acid salts, *Chem. Eng. Sci.*, 64, 1993–2002, 2009.
- [155] Kumar, P.S., Hogendoorn, J.A., Feron, P.H.M., Versteeg, G.F., Equilibrium Solubility of CO₂ in Aqueous Potassium Taurate Solutions: Part 1. Crystallization in Carbon Dioxide Loaded Aqueous Salt Solutions of Amino Acids, *Ind. Eng. Chem. Res.*, 42, 2832–2840, 2003.
- [156] Vaidya, P.D., Konduru, P., Vaidyanathan, M., Kenig, E.Y., Kinetics of Carbon Dioxide Removal by Aqueous Alkaline Amino Acid Salts, *Ind. Eng. Chem. Res.*, 49, 11067–11072, 2010.
- [157] Tong, D., Trusler, J.P.M., Maitland, G.C., Gibbins, J., Fennell, P.S., Solubility of carbon dioxide in aqueous solution of monoethanolamine or 2-amino-2-methyl-1-propanol: Experimental measurements and modelling, *Int. J. Greenh. Gas Control*, 6, 37–47, 2012.
- [158] Samanta, A., Bandyopadhyay, S.S., Absorption of carbon dioxide into aqueous solutions of piperazine activated 2-amino-2-methyl-1-propanol, *Chem. Eng. Sci.*, 64, 1185–1194, 2009.
- [159] Li, H., Li, L., Nguyen, T., Rochelle, G.T., Chen, J., Characterization of Piperazine/2-Aminomethylpropanol for Carbon Dioxide Capture, *Energy Procedia*, 37, 340–352, 2013.

- [160] Knudsen, J.N., Andersen, J., Jensen, J.N., Biede, O., Results from test campaigns at the 1 t/h CO₂ post-combustion capture pilot-plant in Esbjerg under the EU FP7 CESAR project, 1st Post Combustion Capture Conference, Abu Dhabi, 2011.
http://www.ieaghg.org/docs/General_Docs/PCCC1/Abstracts_Final/pccc1Abstract00010.pdf
- [161] Artanto, Y., Jansen, J., Pearson, P., Puxty, G., Cottrell, A., Meuleman, E., Feron, P., Pilot-scale evaluation of AMP/PZ to capture CO₂ from flue gas of an Australian brown coal-fired power station, *Int. J. Greenh. Gas Control*, 20, 189–195, 2014.
- [162] Ehrig, R., Ofenloch, O., Schaber, K., Deuflhard, P., Modelling and simulation of aerosol formation by heterogeneous nucleation in gas–liquid contact devices, *Chem. Eng. Sci.*, 57, 1151–1163, 2002.
- [163] Vehkamäki, H., Riipinen, I., Thermodynamics and kinetics of atmospheric aerosol particle formation and growth., *Chem. Soc. Rev.*, 41, 5160–73, 2012.
- [164] Khakharia, P., Goetheer, E.L.V., Degradation and emissions modelling and comparison with pilot plant for MEA, Emissions Workshop, Heilbronn, 2014. <http://www.octavius-co2.eu/>
- [165] Brachert, L., Mertens, J., Khakharia, P., Schaber, K., The challenge of measuring sulfuric acid aerosols: Number concentration and size evaluation using a condensation particle counter (CPC) and an electrical low pressure impactor (ELPI+), *J. Aerosol Sci.*, 67, 21–27, 2014.
- [166] Kim, Y.E., Lim, J.A., Jeong, S.K., Yoon, Y. Il, Bae, S.T., Nam, S.C., Comparison of Carbon Dioxide Absorption in Aqueous MEA, DEA, TEA, and AMP Solutions, *Bull. Korean Chem. Soc.*, 34, 783–787, 2013.
- [167] Zahlsen, K., Vernstad, K., Holten, T., Brunsvik, A., Aslak, E., Bernd Wittgens, Per Oscar Wiig, Establish sampling and analytical procedures for potentially harmful components post combustion amine based CO₂ capture, Subtask 5: Establish analytical procedure, Trondheim, Norway, 2011.
http://www.gassnova.no/gassnova2/frontend/files/CONTENT/Rapporter/Establishanalyticalprocedures_Sintef.pdf
- [168] Aas, N., da Silva, E.F., Emission measurements at Dong's pilot plant for CO₂ capture in Esbjerg- EU project Cesar, Environmental impacts of amine emissions during post combustion capture Workshop, Oslo, 2010. <http://ieaghg.org/publications/blog/47-networks/environmental-impacts-of-post-combustion-capture>
- [169] Graff, O.F., Emission Measurement and Analysis from Mobile Carbon Capture Test Facility, Environmental impacts of amine emissions during post combustion capture Workshop, Oslo, 2010. http://ieaghg.org/docs/General_Docs/Env_Impacts/13-Emissionmeasurement_ACC_Graff.pdf

- [170] Dahlina, R.S., Landham, E.C., Kelinske, M.L., Wheeldon, J.M., Love, D.H., Amine Losses and Formation of Degradation Products in Post-Combustion CO₂ Capture, 38th International Technical Conference on Clean Coal & Fuel Systems 2013: The Clearwater Clean Coal Conference, 651, Coal Technologies Associates, Clearwater, Florida, 2013. <http://toc.proceedings.com/18656webtoc.pdf>
- [171] Shah, A.D., Dai, N., Mitch, W.A., Application of ultraviolet, ozone, and advanced oxidation treatments to washwaters to destroy nitrosamines, nitramines, amines, and aldehydes formed during amine-based carbon capture., *Environ. Sci. Technol.*, 47, 2799–808, 2013.
- [172] Sanchez Fernandez, E., Bergsma, E.J., de Miguel Mercader, F., Goetheer, E.L.V., Vlugt, T.J.H., Optimisation of lean vapour compression (LVC) as an option for post-combustion CO₂ capture: Net present value maximisation, *Int. J. Greenh. Gas Control*, 11, S114–S121, 2012.
- [173] Da Silva, E.F., Kolderup, H., Goetheer, E., Hjarbo, K.W., Huizinga, A., Khakharia, P., Tuinman, I., Mej dell, T., Zahlsen, K., Vernstad, K., Hyldbakk, A., Holten, T., Kvamsdal, H.M., van Os, P., Einbu, A., Emission studies from a CO₂ capture pilot plant, *Energy Procedia*, 37, 778–783, 2013.
- [174] Nguyen, T., Hilliard, M., Rochelle, G., Volatility of aqueous amines in CO₂ capture, *Energy Procedia*, 4, 1624–1630, 2011.
- [175] Trollebø, A.A., Saeed, M., Hartono, A., Kim, I., Svendsen, H.F., Vapour-Liquid Equilibrium for Novel Solvents for CO₂ Post Combustion Capture, *Energy Procedia*, 37, 2066–2075, 2013.
- [176] Levenspiel, O., Chemical Reaction Engineering, *Ind. Eng. Chem. Res.*, 38, 4140–4143, 1999.
- [177] Hinds, W.C., Aerosol Technology: Properties, Behavior, and Measurement of Airborne Particles, John Wiley & Sons Inc., USA, 2nd Edition, 1999.

Summary

Global greenhouse gas emissions, especially of CO₂, have been increasing tremendously over the past century. This is known to cause not only an increase of temperature, but also a change in our climate. Along with a shift to renewable sources of energy, Carbon Capture and Storage is necessary to mitigate climate change. Power plants are the largest point source of CO₂ emissions and therefore, capture of CO₂ from such sources is a must. Post Combustion CO₂ Capture (PCCC), and specifically absorption-desorption based technology is the preferred choice of technology for CO₂ capture from flue gases. It has been extensively used in the oil and gas industry for gas treatment. Its application for CO₂ capture from flue gases is not straightforward, mainly due to different flue gas composition and operating conditions. Other aspects such as solvent degradation, solvent emissions and corrosion become even more critical. In Chapter 1, the state-of-the-art in PCCC is explained with further details on the current knowledge and understanding of these aspects.

In Chapter 2, the aspect of solvent ageing is studied over two test campaigns in a CO₂ capture pilot plant using 30 wt.% MEA. Solvent degradation occurs via thermal and oxidative routes, with the latter being more prominent. Ammonia is known to be a major oxidative degradation product, while the remaining degradation products are known to be corrosive. Therefore, solvent degradation is expected to have a significant impact on the corrosion in the plant and the resulting emissions of ammonia. The link between these three parameters was confirmed using online monitoring probes. Moreover, an autocatalytic behaviour was observed resulting in a rapid increase of the solvent metal content and ammonia emissions. The solvent iron content was above 500 mg/kg, while the ammonia emissions exceeded 150 mg/m³ STP (STP; 0°C and 101.325 kPa). By correlating the process conditions to the underlying degradation and corrosion mechanisms, online monitoring tools can be used to assess and manage the lifetime of the solvent.

Even if the state of the solvent is kept in check by reclaiming methods, there could be instances where ammonia emissions could increase. Therefore, it is necessary to have an end of pipe countermeasure for such emissions. Chapter 3 presents the results from a test using an acid wash scrubber for ammonia emissions in a pilot plant test campaign. Several parametric tests were conducted in order to test the efficiency of the acid wash. Moreover, the ammonia concentration in the gas inlet to the acid wash was increased artificially (~150 mg/m³ STP). The acid wash scrubber reduced ammonia emission to very low levels, below 5 mg/m³ STP and mostly below 1 mg/m³ STP. Moreover, the MEA content was also reduced to mostly below 1 mg/m³ STP. A comparison between a model made in Aspen Plus and the experimental results showed good agreement, with deviations only at pH above 5 to 6.

Aerosol-based emissions are known to be a concern in PCCC. In Chapter 4, the impact of flue gas particles such as soot and sulphuric acid aerosol droplets on solvent

emissions was studied in a mobile CO₂ capture plant. These tests confirmed that solvent emissions can be in the order of grams per m³ STP, which is several orders of magnitude higher than volatile emissions. The number concentration of these particles had a direct relation to the extent of emissions. Particle number concentrations in the range of 10⁷-10⁸ per cm³ led to emissions of MEA in the range of 600-1200 mg/m³ STP.

In Chapter 5, further tests were performed on the same setup in order to assess the impact of operating conditions of the CO₂ capture plant on aerosol-based emissions. Increasing the temperature of the lean solvent resulted in lowering of the aerosol-based emissions. However, the total solvent emission increased as a result of increased volatile emissions. Aerosol-based emissions were observed also for AMP-Pz as the capture solvent. The pH of the lean solvent was decreased by lowering the stripper temperature and thereby, changing the CO₂ loading of the solvent. This resulted in an increase in the aerosol-based emissions as the activity of the amine increased in the solvent. As the CO₂ content in the flue gas was reduced from 12.7 vol.% to 0.7 vol.%, a maximum in the emissions was observed between 6 and 4 vol.%. When a mixture of a slow reacting volatile amine, AMP, with a fast reacting non-volatile, taurate, was used, no aerosol-based emissions were observed. This led to the important conclusion that in reactive absorption, along with supersaturation and particle number concentration, the reactivity of the amine plays an important role in aerosol-based emissions.

A Brownian Demister Unit (BDU), consisting of multiple polypropylene fibre elements, can be potentially used as a countermeasure for aerosol-based emissions. This was tested in a pilot plant campaign using MEA and is discussed in Chapter 6. The BDU reduced emissions from about 85-180 mg/m³ STP to about 1-4 mg/m³ STP. A water wash was found to be effective against vapour based emissions, while the BDU was effective against aerosol-based emissions. A BDU is not effective against ammonia emissions, as they are present in the vapour form. From the measured nitrosamines, NDELA was found to be in the solvent in the order of 2000 ng/ml, while in the water wash it was ca. 1 ng/ml. Gas phase nitrosamine concentrations were in the range of tens of ng/m³ STP. The BDU results in a significant additional pressure drop of ca. 50 mbar, for the configuration and type of BDU used here. This translated to an additional consumption of electricity by the blower in the range 26-52%.

A system containing three distinct phases, gas, liquid and aerosol droplets, are complex to understand and model. In Chapter 7, a methodology is presented with which such a complicated system can be modelled in commercially available software such as Aspen Plus. The mass and energy exchanges are split into two distinct interactions, gas-liquid and gas-aerosol. Aerosol droplets are considered to be as bulk liquid without any direct interaction with the solvent. The different parameters that were varied were the CO₂ concentration in the flue gas, temperature of the lean solvent and CO₂ loading of the lean solvent. The resulting trends were in good agreement with the experimental results presented in Chapter 5. The model did not predict a maximum in the emissions as the CO₂ content in the flue gas was varied.

Although absorption-desorption based process for CO₂ capture is well-known, several operating issues needs to be addressed for its application in PCCC, as evident in this thesis. It is important to monitor the degradation of the solvent and deploy appropriate methods at the right time, to minimize its detrimental effect on the corrosion of the plant and avoid high emissions of ammonia. Aerosol-based emissions in a PCCC process is a serious issue. The experimental results, proposed mechanism and modelling methodology will enable the design of appropriate counter-measures against aerosol based emissions. It is recommended to devise appropriate strategy and innovative solutions based on the understanding of the various operational aspects of absorption-desorption based PCCC as presented in this thesis. This will increase the confidence level in the technology and lead to its successful deployment for mitigating climate change in the short term.

Samenvatting

In de afgelopen eeuw is de wereldwijde uitstoot van broeikasgassen, en in het bijzonder van CO₂, enorm toegenomen. Het is bekend dat dit niet alleen een temperatuurtoename veroorzaakt, maar ook een verandering van ons klimaat. Naast een toename van het gebruik van hernieuwbare energiebronnen, is het afvangen en opslaan van CO₂ noodzakelijk om deze klimaatveranderingen te reduceren. Aangezien energiecentrales de grootste stationaire bronnen van CO₂-uitstoot zijn, is het belangrijk om juist hier CO₂ af te vangen. De voorkeurstchnologie voor het afvangen van CO₂ na de verbranding is de zogenaamd Post Combustion CO₂ Capture, PCCC. Meer specifiek gaat het hierbij om afvang met behulp van reactive absorptie-desorptie. Deze technologie wordt al veelvuldig toegepast voor gasbehandeling in de olie- en gasindustrie.

Niet tegenstaande de basisprincipes zeer goed bekend zijn, kan deze technologie niet rechtstreeks geïmplementeerd worden voor het afvangen van CO₂. De belangrijkste redenen hiervoor zijn de verschillen in rookgassamenstelling en procescondities waardoor andere aspecten zoals corrosie, oplosmiddel degradatie en emissie nog belangrijker worden. In hoofdstuk 1 wordt de huidige stand van de PCCC-technologie uitgelegd alsmede de kennis rondom de hierboven genoemde andere aspecten beschreven.

In hoofdstuk 2 wordt het verouderingsproces van het oplosmiddel bestudeerd tijdens twee testcampagnes in een proeffabriek voor CO₂-afvang. Deze proeffabriek maakt gebruik van 30 wt% mono-ethanolamine (MEA) als oplosmiddel. Het oplosmiddel degradeert via thermische en oxidatieve mechanismen, waarbij de laatste overheersen. Een belangrijk product van oxidatieve degradatie is ammonia. Van andere degradatieproducten is het bekend dat ze corrosief zijn. Het ligt daarom in de lijn der verwachtingen dat oplosmiddeldegradatie een significant effect heeft op de resulterende ammonia-emissies en corrosie in een fabriek. De samenhang tussen deze drie parameters is bevestigd door middel van continue metingen met sondes in de processtromen. Bovendien is ook auto-katalytisch gedrag waargenomen, wat resulteerde in een snelle stijging van de ammonia-emissies en metaalconcentratie in het oplosmiddel. De ijzerconcentratie in het oplosmiddel was hoger dan 500 mg/kg, terwijl de ammonia-emissies de 150 mg/m³ STP (STP; 0°C en 101.325 kPa) overstegen. Door het correleren van procescondities aan de onderliggende degradatie- en corrosiemechanismen kunnen continue meetmethodes in de processtromen gebruikt worden om de levensduur van het oplosmiddel te bepalen en waar nodig bij te sturen.

Echter, zelfs wanneer de kwaliteit van het oplosmiddel geregeld wordt met behulp van terugwinningsmethodes, kunnen er zich nog steeds omstandigheden voordoen waarbij de ammonia-emissies stijgen. Het is daarom noodzakelijk om een tegenmaatregel beschikbaar te hebben die aan het eind van het proces toegepast kan worden. Hoofdstuk 3 beschrijft de resultaten van een test met een zure gaswasser om de ammonia-emissies in de proeffabriek te verminderen. Verschillende parametertests zijn

uitgevoerd om de efficiëntie van de zure wasstap te onderzoeken. Bovendien is de ammonia concentratie in het voedingsgas in de stroom naar de zure gaswasser kunstmatig verhoogd naar ongeveer 150 mg/m³ STP. Het bleek dat een zure gaswasser de ammonia-emissies bijzonder ver terugbracht naar waarden lager dan 5 mg/m³ STP en meestal zelfs lager dan 1 mg/m³ STP. Ook werd de MEA-emissie teruggebracht naar waarden die over het algemeen waarden lager lagen dan 1 mg/m³ STP. De experimentele resultaten komen goed overeen met de waarden afkomstig van een model gemaakt in Aspen Plus. Slechts bij een pH hoger dan 5 à 6 waren er afwijkingen.

Een andere bron van zorg in PCCC is aerosol-gerelateerde emissie van oplosmiddel. In hoofdstuk 4 wordt het effect van rookgasdeeltjes, zoals roet en zwavelzuur aerosoldrappeltjes, op de oplosmiddelemissie in een mobiele CO₂-afvangsproeffabriek bestudeerd. Deze tests bevestigen dat de oplosmiddelemissies in de orde van grammen per m³ STP kunnen zijn. Dat is enkele ordegroottes hoger dan de emissies via oplosmiddeldamp. De mate van emissie bleek recht evenredig met het aantal deeltjes per rookgasvolume. Deeltjesconcentraties in de orde van 10⁷-10⁸ per cm³ leidden tot MEA-emissies tussen de 600 en 1200 mg/m³ STP.

Hoofdstuk 5 beschrijft verdere tests die zijn uitgevoerd met behulp van dezelfde proefopstelling om het effect van de procescondities op de aerosol-gerelateerde emissies te bepalen. Het verhogen van de temperatuur van het CO₂-arme oplosmiddel resulterde in lagere aerosol-gerelateerde emissies. Echter, de totale emissies werden hoger vanwege de verhoogde dampdruk van het oplosmiddel. Aerosol-gerelateerde emissies zijn ook waargenomen tijdens het gebruik van AMP-Pz (een mengsel van 2-amino-2-methylpropanol en piperazine in water) als oplosmiddel. De pH van het oplosmiddel is gevarieerd door de desorber condities aan te passen en daarmee de belading van het CO₂-arme oplosmiddel. Hierdoor nam de activiteit van het amine in het oplosmiddel toe wat een stijging van de aerosol-gerelateerde emissies veroorzaakte. Verlaging van de CO₂-concentratie in het rookgas van 12.7 naar 0.7 vol.%, resulterde in een maximum emissie tussen 4 en 6 vol.%.

Echter, bij het gebruik van een mengsel van een langzaam reagerende en vluchte amine (AMP) met een snel reagerende en niet-vluchte amine (taurine) werden geen aerosol-gerelateerde emissies waargenomen. Hieruit kan de belangrijke conclusie getrokken worden dat in reactieve absorptie, naast oververzadiging en deeltjesconcentratie, reactiviteit van het amine een bepalende rol speelt voor aerosol-gerelateerde emissies.

Een *Brownian Demister Unit* (BDU) bestaande uit meerdere polypropyleen vezelelementen kan mogelijk gebruikt worden als tegenmaatregel tegen aerosol-gerelateerde emissies. In hoofdstuk 6 worden de testen die met een BDU uitgevoerd zijn in een proeffabriek met MEA als oplosmiddel bediscussieerd. Hieruit blijkt dat een wasstap met behulp van water effectief is tegen damp-gerelateerde emissies, terwijl de BDU effectief is tegen aerosol-gerelateerde emissies. De BDU verminderde de emissies van ongeveer 85-180 mg/m³ STP naar ongeveer 1-4 mg/m³ STP. Omdat ammonia

aanwezig is als damp, is een BDU niet effectief tegen ammonia-emissies. Van de gemeten nitrosamines bleek de concentratie van NDELA (N-nitrosodiethanolamine) in het oplosmiddel ongeveer 2000 ng/ml te zijn, terwijl die in het water van de waterwasstap slechts rond de 1 ng/ml lag. Gasfase concentraties van nitrosamine waren in de orde van tientallen ng/m³ STP. Een BDU veroorzaakt een significante extra drukval in het systeem. Voor de configuratie en het type BDU gebruikt in dit onderzoek was dat rond de 50 mbar. Dit kan vertaald worden naar een extra elektriciteitsconsumptie van de ventilator van ongeveer 26-52%.

Door de aanwezigheid van drie verschillende fases, gas, vloeistof, en aerosoldrappeltjes, is dit een complex systeem om te begrijpen en modelleren. In hoofdstuk 7 wordt een methode beschreven waarmee een dergelijk ingewikkeld systeem gemodelleerd kan worden met het commercieel beschikbare computerprogramma Aspen Plus. In de methode zijn de massa- en warmteoverdracht opgesplitst in twee afzonderlijke interacties: gas-vloeistof en gas-aerosol. De aerosoldrappeltjes worden beschouwd als bulk vloeistoffase zonder enige directe interactie met de oplosmiddelfase. De CO₂-concentratie in het rookgas, en de temperatuur en CO₂-concentratie van het CO₂-arme oplosmiddel zijn gevarieerd. De verkregen resultaten komen goed overeen met de experimentele resultaten beschreven in hoofdstuk 5. Echter, het model voorspelt geen maximum in de emissies als functie van de CO₂-concentratie in het rookgas.

Uit dit proefschrift blijkt dat, alhoewel absorptie-desorptie gebaseerde processen voor CO₂-afvang bekende technologie is, er nog verschillende operationele problemen zijn die geadresseerd moeten worden voordat het kan worden toegepast in PCCC. Het is belangrijk om de degradatie van het oplosmiddel continu in de gaten te houden en geschikte methodes op het juiste moment toe te passen. Dit minimaliseert de schadelijke effecten op corrosie van de fabriek en voorkomt hoge ammonia-emissies.

Aerosol-gerelateerde emissies zijn een serieus probleem in een PCCC proces. De experimentele resultaten, de voorgestelde mechanismen, en de modelleermethode maken het mogelijk een geschikt ontwerp te maken van tegenmaatregelen. Het is aan te bevelen het begrip over de verschillende operationele aspecten van, op absorptie-desorptie gebaseerde, PCCC beschreven in dit proefschrift te gebruiken om geschikte strategische en innovatieve oplossingen te ontwikkelen. Dit zal het vertrouwen in deze technologie vergroten en leiden tot de succesvolle implementatie ervan, om zo klimaatveranderingen op korte termijn te verminderen.

Curriculum Vitae

Purvil Khakharia was born in Mumbai, India, on the 7th of February, 1988. He obtained his bachelors education, B.Tech, in Pharmaceutical Chemistry and Technology, at the Institute of Chemical Technology (also known as UDCT), Mumbai in 2009. Later, he moved to Netherlands, to pursue MSc. in Chemical Engineering at the Delft University of Technology. He worked on the topic of “Anaerobic bioregeneration of powdered activated carbon” at Imperial College, London for this dissertation. After graduating in 2011, he started working as a Research Scientist, at the department of Gas Treatment (now Process and Instrumentation Development) at TNO. In 2012, he started working towards a PhD, on the topic of “Aerosol-based emissions, solvent degradation, and corrosion in Post Combustion CO₂ Capture” based on the research activity carried out in national and European projects such as CATO-2 and OCTAVIUS. Currently, he is working in TNO as a technical lead on several projects related to process development, solvent management, solvent development, reactive absorption, etc.

Publications

Khakharia, P., Brachert, L., Mertens, J., Huizinga, A., Schallert, B., Schaber, K., Vlugt, T.J.H., Goetheer, E., Investigation of aerosol based emission of MEA due to sulphuric acid aerosol and soot in a Post Combustion CO₂ Capture process, *Int. J. Greenh. Gas Control*, 19, 138–144, 2013.

Khakharia, P., Huizinga, A., Jurado Lopez, C., Sanchez Sanchez, C., de Miguel Mercader, F., Vlugt, T.J.H., Goetheer, E., Acid Wash Scrubbing as a Countermeasure for Ammonia Emissions from a Postcombustion CO₂ Capture Plant, *Ind. Eng. Chem. Res.*, 53, 13195–13204, 2014.

Khakharia, P., Kvamsdal, H.M., da Silva, E.F., Vlugt, T.J.H., Goetheer, E., da Silva, E.F., Field study of a Brownian Demister Unit to reduce aerosol based emission from a Post Combustion CO₂ Capture plant, *Int. J. Greenh. Gas Control*, 28, 57–64, 2014.

Khakharia, P., Mertens, J., Vlugt, T.J.H., Goetheer, E., Predicting Aerosol Based Emissions in a Post Combustion CO₂ Capture Process Using an Aspen Plus Model, *Energy Procedia*, 63, 911–925, 2014.

Khakharia, P., Brachert, L., Mertens, J., Anderlohr, C., Huizinga, A., Fernandez, E.S., Schallert, B., Schaber, K., Vlugt, T.J.H., Goetheer, E., Understanding aerosol based emissions in a Post Combustion CO₂ Capture process: Parameter testing and mechanisms, *Int. J. Greenh. Gas Control*, 34, 63–74, 2015.

Brachert, L., Mertens, J., Khakharia, P., Schaber, K., The challenge of measuring sulfuric acid aerosols: Number concentration and size evaluation using a condensation particle counter (CPC) and an electrical low pressure impactor (ELPI+), *J. Aerosol Sci.*, 67, 21–27, 2014.

Mertens, J., Brachert, L., Desagher, D., Thielens, M.L., Khakharia, P., Goetheer, E., Schaber, K., ELPI+ measurements of aerosol growth in an amine absorption column, *Int. J. Greenh. Gas Control*, 23, 44–50, 2014.

Mertens, J., Anderlohr, C., Rogiers, P., Brachert, L., Khakharia, P., Goetheer, E., Schaber, K., A wet electrostatic precipitator (WESP) as countermeasure to mist formation in amine based carbon capture, *Int. J. Greenh. Gas Control*, 31, 175–181, 2014.

Presentations at conferences, symposia and workshops

Khakharia, P., Mertens, J., Vlugt, T. J. H., Goetheer, E., Predicting aerosol-based emissions in a post combustion CO₂ capture process using an Aspen Plus model, GHGT-12, Austin, USA, 2014. <http://www.sciencedirect.com/science/journal/18766102>

van der Ham, L.V., van Eckeveld, A.C., Khakharia, P., Goetheer, E.L.V., Online monitoring of dissolved CO₂ and MEA concentrations: Effect of solvent degradation on predictive accuracy, GHGT-12, Austin, USA, 2014.

<http://www.sciencedirect.com/science/journal/18766102>

Khakharia, P., et. al., Understanding the impact of aerosols in CO₂ capture absorber, Emissions Workshop, Heilbronn, Germany, 2014. <http://www.octavius-co2.eu/>

Khakharia, P., Goetheer, E.L.V., Degradation and emissions modelling and comparison with pilot plant for MEA, Emissions Workshop, Heilbronn, 2014. <http://www.octavius-co2.eu/>

Khakharia, P., et. al., Emission counter-measures in post combustion CO₂ capture: Acid wash demonstration at a pilot plant scale, PCCC-2, Bergen, Norway, 2013.

<http://ieaghg.org/conferences/pccc/52-conferences/pccc/346-pccc2-technical-programme>

Khakharia, P., et. al., Effect of number concentration of soot and H₂SO₄ on aerosol based emissions from a post combustion CO₂ capture plant, PCCC-2, Bergen, Norway, 2013.

<http://ieaghg.org/conferences/pccc/52-conferences/pccc/346-pccc2-technical-programme>

Khakharia, P., et. al., Power plant and CO₂ capture plant integration: Holistic evaluation of different process configurations, 9th European Congress of Chemical Engineering, The Hague, the Netherlands, 2013.

Khakharia, P., Goetheer, E., Carbon Capture: from dream to realization, PAC symposium, Amsterdam, the Netherlands, 2013.

Acknowledgements

In order to contribute towards the development of science and technology in society, the help from organisations and individuals is an absolute necessity. Moreover, several people have been instrumental in my personal ambition of a PhD degree. Hereby, my sincere acknowledgements to all of them.

Firstly, I would like to thank TNO, for giving me the opportunity to embark on such an exciting journey. Specifically, the resources allotted from the department of Gas Treatment, and projects such as CATO-2 and Octavius, allowed me complete freedom in pursuing high quality research. Moreover, the dynamic nature of such activities meant that there was never a dull moment.

I am extremely grateful to Thijs Vlugt (Professor at TU Delft), for being the promotor for my PhD. He has been an excellent guide on how to pursue research at the highest level. He has been instrumental in disseminating the, sometimes chaotic, research activities in a scientific and concise manner. His speed in correcting manuscripts, without losing attention to details is truly commendable. His prompt responses, high availability, and non-adherence to redundant formalities has been key in completing this journey in relatively short period of time.

I would like to thank, Earl Goetheer (principal scientist at TNO), firstly for bringing up the idea and giving me the opportunity to pursue a PhD. He has been the guiding force in all the research activities carried out here. His ability to use fundamental knowledge for applied research and development is truly unparalleled. I have learnt from him to see opportunities in challenges and eventually develop innovative solutions for it. His pragmatic approach helped make a lot of the research work, directly usable for operators, engineers, scientists and decision makers, alike. Several of the chapters in the thesis have been a collaborative effort. His knack for inspiring collaborators to pursue a common goal, has led the research work to have a multi-disciplinary perspective. Finally, his passion for science (and sweets) is truly encouraging.

In my opinion the research work presented here is interesting due to the use of representative conditions of a CO₂ capture system. Specifically, the pilot plant at Maasvlakte and the mini-capture plant have been used for the tests. These are the ‘toys’ of Arjen Huizinga, my colleague at TNO. I sincerely acknowledge his effort for performing long pilot plant campaigns, in sometimes challenging weather conditions, and in operation of the ‘mobile’ mini-capture plant. His ability to look at the practical side, was an absolute must in converting ideas to working setups.

Jan Mertens, from Laborelec, has been an extremely valuable partner on this topic. His experience on the topic of emissions and specifically, aerosols, which has made this research work, truly pioneering. Moreover, I thank him for his company during the long days of experiments and pursuit of finding the best curry at Indian restaurants. I would also like to thank colleagues at Laborelec/GDF-Suez, Marie-Laure Thielens, Dominique Desagher, Pieter Rogers and Kristine for their help.

E.ON has been a great partner in CATO-2 and specifically, on the several research topics presented here. I would like to thank Bernd Schallert, Nick Booth, Chris Satterley, and colleagues for the interesting discussions. The impact and usefulness of the research work, has been clearly stated by Andy Read, from ROAD, which makes such a work, satisfying.

Several of the chapters are based on aerosol emission. Any scientific understanding on this interesting and acute problem, wouldn't have been possible without the collaboration with KIT. The experimental setup and immense experience at the group of Prof. Schaber was a gateway to understanding this phenomena. I thank him for hosting us for several weeks over the past few years. My sincere thanks to Leonie Brachert for not only her scientific contributions but also being a great host to the invasion by the Dutch, Belgian, and Indian with their large setups. Her keen interest in applying the group's expertise on a problem for CO₂ capture, helped devise several interesting experiments. I also would like to thank all the group members and technicians at KIT.

Firstly, I would like to thank Sven van der Gijp (ex-research manager at Gas Treatment) for providing time for the PhD work and Ronald van den Berg, (current research manager at now, PID) to continue the same. They both have made it a point to make this a priority and a target for the department. I would like to thank my long term 'roomie', Annemieke van de Runstraat, for all the PhD related talks, do's and don't's, and above all, a jovial atmosphere in the room. My sincere thanks to Peter Petiet for the dutch translation, keen interest in my progress, his encouragement, and interesting conversations on tennis and music! Thanks to Leen van der Ham, for being the dutch guru with the translation and his attempt to teach the language. I would like to thank all my colleagues in GT, LWS and other groups at TNO, for their keen interest on my progress. Moreover, I would like to thank several ex-colleagues, from whom I have learnt a lot and have been a great company. I have enjoyed several educational trips as part of the CATO-2 PhD group, made possible by the organizational team.

I am extremely grateful to also have wonderful roommates, Rajat (Babaji), Sumit (the Professor), Lalit (the Kalakar), Trinath (Shehzada), Krishna (the GOD), Bhaskar, Sriram, and Ramavtar, who are like family. Also thanks to Rupali (recent entry as RB2 and completing the Mahabharat team). All the fun outings and celebrations, have made this journey really smooth. The same is true for all the other friends in the Netherlands. Special thanks to Krishna, Venkatesh and Sumit for the tips on thesis formatting, party place, etc.

The pursuit of good grades when young can be very challenging. I thank all my teachers in school, high school and tuitions for their passion in education. Special thanks to the professors at ICT, where excellence is a norm, for imparting knowledge and their guidance for higher education. Several friends have made the 4 years at ICT, extremely fun.

Finally, my entire family is greatly appreciated for their support. My father, has always been a role model for me. His pursuit for excellence and strong interpersonal skills have had a great influence on me. I owe this, and other academic achievements to him. One of the most important aspect in pursuing a PhD, is patience. Thanks to my mother, I was equipped with it. Her infinite love and nurture is sorely missed during my stay away from home.

Purvil Khakharia

January 2015.

